Biochemical characterization

of GAS2L3,

a target gene of the

DREAM complex

Dissertation zur Erlangung des

naturwissenschaftlichen Doktorgrades

der Bayerischen Julius-Maximilians-Universität Würzburg

vorgelegt von

Marc Fackler

aus

Memmingen

Würzburg, 2014

Eingereicht am:

_____

Mitglieder der Promotionskommission:

Vorsitzender:

1. Gutachter: Prof. Dr. Stefan Gaubatz

2. Gutachter: Prof. Dr. Manfred Alsheimer

Tag des Promotionskolloquiums:

_____

Doktorurkunde ausgehändigt am:

_____

Table of contents

III

Parts of this thesis were first published in:

Wolter, P., Schmitt, K., Fackler, M., Kremling, H., Probst, L., Hauser, S., Gruss, O.J., and Gaubatz, S. (2012). GAS2L3, a target gene of the DREAM complex, is required for proper cytokinesis and genomic stability. J. Cell Sci. *125*, 2393–2406.

Fackler, M., Wolter, P., and Gaubatz, S. (2014). The GAR domain of GAS2L3 mediates binding to the chromosomal passenger complex and is required for localization of GAS2L3 to the constriction zone during abscission. FEBS J. *281*, 2123–2135.

1. Introduction

1.1. Mammalian cell cycle and its regulation

The mammalian cell cycle is a highly conserved, complex physiological process. It is essential for proliferation, development and survival. During cell cycle, which is precisely regulated, one maternal cell doubles its genetic information and divides into two genetically equal daughter cells. The cell cycle can be subdivided into four different phases: Gap 1 (G1) phase, synthesis (S) phase, gap 2 (G2) phase and mitosis (M) phase (fig 1.1) (Alberts et al., 2008; Pollard et al., 2007). During the G1 phase, cells enlarge their size and synthesize all cellular components needed for physiological activity. A growth stimulus delivered through different growth factors (e.g. PDGF, EGF, FGF, IGF-I and –II) leads to progression into S phase, in which the parental chromosomes are duplicated by the process of DNA replication. During G2 phase, cells are synthesizing proteins which are necessary for the subsequent cell cycle stage and integrity of the duplicated chromosomes is controlled. In M phase the duplicated chromosomes are separated. This phase can be further subdivided into prophase, prometaphase, metaphase, anaphase and telophase (fig 1.1). In prophase the chromosomes condense and the duplicated centrosomes migrate to the cell poles to form the mitotic spindle. In prometaphase, the nuclear membrane breaks down while in metaphase all the chromosomes align in the equatorial plate and microtubules of the mitotic spindle attach to the kinetochores, multi-protein complexes located at the centromeric region of the chromosomes. In anaphase the sister chromatides are separated and pulled to the opposite spindle poles. In telophase all chromatids are concentrated at the spindle poles, the chromosomes decondense and the nuclear membrane is re-formed (Alberts et al., 2008; Pollard et al., 2007). In cytokinesis, the last step of cell division, the maternal cell is finally divided into two daughter cells. This process is mediated by a contractile ring, consisting of myosin and actin filaments, which forms a cleavage furrow between the proto-daughter cells. The cleavage furrow ingresses until the cytoplasmic connection between the proto-daughter cells is closed and the cells are only connected by the so called midbody, a thin microtubule rich structure which contains a large number of regulatory proteins (Skop et al., 2004). Cytokinesis is completed by abscission of the midbody, which leads to physical separation of the two daughter cells (Glotzer, 2003; Skop et al., 2004). In absence of growth stimuli cells are also able to leave G1 phase and enter a quiescent cell cycle stage, called G0 phase. In this stage, cells do not proliferate anymore and are able to survive for longer time periods. Most of the differentiated, non-proliferating cells in the mammalian body have entered G0 phase (Alberts et al., 2008; Coller, 2007; Pollard et al., 2007; Shackelford et al., 1999). For maintenance of genomic integrity, progression of cell cycle is strictly controlled at two major

cell cycle checkpoints, the G1/S checkpoint before entering S phase and the G2/M checkpoint after DNA replication (Hartwell and Weinert, 1989). DNA damage leads to activation of the checkpoints and a delay in cell cycle progression. This mechanism gives cells enough time to repair the damaged DNA before cell cycle transition. In case the damage is too severe cells undergo apoptosis or senescence to prevent further genomic instability (Kastan and Bartek, 2004; Kuilman et al., 2010; Shackelford et al., 1999).

Cell cycle progression is mainly controlled by heterodimeric protein complexes, the so called cyclin dependent kinase (CDK) / cyclin complexes (Sánchez and Dynlacht, 2005). CDKs belong to the family of serine/threonine kinases and are bound by cyclins, which act as regulatory proteins. Protein levels of the CDKs remain constant during cell cycle, while cyclins are expressed in a cell cycle specific manner (Dorée and Galas, 1994; Morgan, 1997; Tyers and Jorgensen, 2000). In mammalian cells activity of CDK2, CDK4 and CDK6 is specific for the G1/S phase of the cell cycle, while CDK1 activity is specific for G2 phase (Morgan, 2006; Pollard et al., 2007). CDK/cyclin complexes regulate cell cycle progression by phosphorylation of substrates which are necessary for DNA replication and mitosis (Lees, 1995; Morgan, 2006, 1997; Murray, 2004; Pollard et al., 2007). Different growth factors lead to G1/S transition by inducing expression of cyclin D which binds to and activates the G1/S specific CDKs, CDK4 and CDK6 (Hunter and Pines, 1994). The tumor suppressor protein Retinoblastoma-associated protein (pRB), which acts as negative regulator of proliferation by binding to and inhibiting E2F1, E2F2 and E2F3 (E2F1-3) transcription factors in the unphosphorylated state (Nevins, 1992; Sherr, 1996; Stevaux and Dyson, 2002), becomes phosphorylated by the CDK4/cyclin D and CDK6/cyclin D complexes (Sherr, 1996). Phosphorylation of pRB releases E2F1-3 proteins from inhibition (Nevins, 1992; Stevaux and Dyson, 2002) and leads to G1/S transition independent of external growth stimuli (Planas-Silva and Weinberg, 1997). The protein pRB forms together with p107 and p130 the family of the so called pocket proteins, which share a highly conserved protein domain (pocket domain) (Lipinski and Jacks, 1999), necessary for binding of E2F family members and other regulatory proteins (Felsani et al., 2006; Giacinti and Giordano, 2006). While the above mentioned E2F1-3 proteins are activators of transcription, the other five members of the E2F family (E2F4-8) act as transcriptional repressors. E2F4 and E2F5 preferentially bind to p107 and p130 (Beijersbergen et al., 1994; Ginsberg et al., 1994; Hijmans et al., 1995; Moberg et al., 1996), while E2F6, E2F7 and E2F8 are not interacting with pocket proteins (de Bruin et al., 2003; Cartwright et al., 1998; Christensen et al., 2005; Gaubatz et al., 1998; Di Stefano et al., 2003; Trimarchi et al., 1998). For DNA binding E2F1-6 proteins form heterodimers with dimerization partner (DP) proteins (Buck et al., 1995; Cartwright et al., 1998; Ginsberg et al., 1994; Wu et al., 1995). E2F7 and E2F8 are interacting with DNA by a tandem DNA binding motif independent of DP proteins (Logan et al., 2004, 2005; Maiti et al., 2005).

E2F1-3 proteins induce transcription of the cyclins A and E and other genes important for S phase entry (Dyson, 1998; Humbert et al., 2000; Trimarchi and Lees, 2002). Cyclin E specifically binds to and activates CDK2 which mainly regulates G1/S transition (Ohtsubo et al., 1995) while binding of cyclin A to CDK2 is important for control of DNA replication in S phase before onset of G2 phase (Girard et al., 1991). Cyclin A also binds to CDK1 to facilitate entry into M phase (Walker and Maller, 1991). At the end of S phase cyclin B is expressed. It accumulates first in the cytosol, than translocates into the nucleus and finally binds to and activates CDK1 (Porter and Donoghue, 2003). Active CDK1/cyclin B complex coordinates entry into mitosis (Gavet and Pines, 2010). Polyubiquitination of cyclin B in late mitosis by the E3 ubiquitin ligase anaphase promoting complex / cyclosome (APC/C) and subsequent proteasomal degradation leads to mitotic exit and re-entering of G1 phase (King et al., 1994; Kramer et al., 2000; Peters, 2006; Zachariae and Nasmyth, 1999). The following figure gives a schematic illustration of the mammalian cell cycle (fig 1.1).
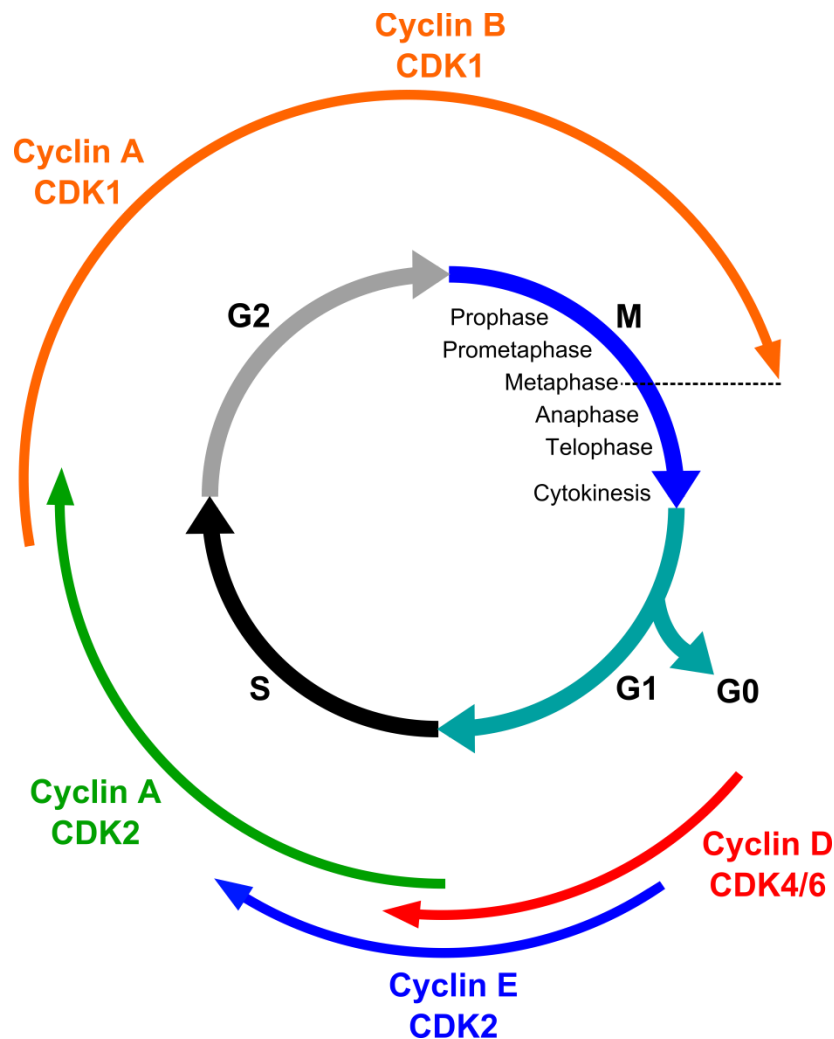
Figure 1.1: Schematic illustration of the mammalian cell cycle. The cell cycle can be subdivided into four different phases called Gap 1 (G1), synthesis (S), gap 2 (G2) and mitosis (M) phase. The M phase can be further subdivided into Prophase, Prometaphase, Metaphase, Anaphase and Telophase. Cell cycle progression is controlled by different cyclin dependent kinase (CDK) / cyclin complexes. A detailed description of the cell cycle is given in the main text. The different cell cycle phases are not shown to scale. G0: Quiescent cell cycle stage

Activity of CDKs is strictly controlled on cellular level by different CDK inhibitors, which either bind monomeric CDK kinases directly or associate with CDK/cyclin heterodimers (Pavletich, 1999). The CDK inhibitor p16 for example binds directly to CDK4 and CDK6. This prevents binding of cyclin D what in turn inhibits G1/S transition (Lees, 1995; Morgan, 2006; Pollard et al., 2007). Other CDK inhibitors like p21, p27 or p57 bind to and inhibit CDK/cyclin complexes, what in turn inhibits CDK kinase activity and finally leads to cell cycle arrest (Carnero and Hannon, 1998; Harper et al., 1995; Lee et al., 1995; Sherr and Roberts, 1999; Vidal and Koff, 2000).

1.2. DREAM complex

In 2004, the first native pocket-protein complex was identifed in *D. melanogaster*. This complex was named Myb-MuvB (MMB) (Lewis et al., 2004) or Drosophila RBF, dE2F2 and dMyb interacting proteins (dREAM) (Korenjak et al., 2004). It consists of the proteins RBF1, RBF2, dE2F2, dimerization partner (Dp), dMyb, three dMyb interacting proteins (Mip) (Mip40, Mip120 and Mip130), chromatin assembly factor 1 (Caf1) and dLin52 (Korenjak et al., 2004; Lewis et al., 2004). A similar complex was later identified in *C. elegans* where it was named DRM (DP, RB and MuvB) (Harrison et al., 2006). In 2007 it could be shown by different groups that the complex is also present in mammalian cells (Litovchick et al., 2007; Pilkinton et al., 2007; Schmit et al., 2007). It was named LINC (LIN complex) (Schmit et al., 2007) or DREAM (DP, RB-like, E2F, and MuvB) (Litovchick et al., 2007) complex and is composed of the five core subunits LIN37, LIN54, LIN9, LIN52 and RbAp48 and the associated proteins B-MYB, p130, E2F4 and DP1 (Litovchick et al., 2007; Pilkinton et al., 2007; Schmit et al., 2007). All proteins are well conserved between different organsims, except BMyb which is absent in *C. elegans* (Harrison et al., 2006). Biochemical assays showed that the composition of the mammalian DREAM complex switches in a cell cycle dependent manner (fig 1.2). The core complex interacts with p130, E2F4 and DP1 in quiescent cells and acts there as a transcriptional repressor (Litovchick et al., 2007; Pilkinton et al., 2007). During S phase p130, E2F4 and DP1 are released and the core complex dissociates from G1/S promoters (Knight et al., 2009; Litovchick et al., 2007; Pilkinton et al., 2007; Sadasivam et al., 2012; Schmit et al., 2007). The core complex then binds to the transcription factor BMyb during S phase (Pilkinton et al., 2007; Schmit et al., 2007) and FoxM1 during G2 phase (Sadasivam et al., 2012). The newly formed complex associates with promoters of G2/M specific genes and activates their transcription (Pilkinton et al., 2007; Sadasivam et al., 2012; Schmit et al., 2007). Re-assembly of the DREAM repressor complex contributes to entering quiescence. Lin52 is phosphorylated at serine 28 by dual specificity tyrosine-phosphorylation-regulated kinase 1A (DYRK1A), which in turn leads to association of p130, E2F4 and DP1 with the core complex and formation of the repressor complex (Litovchick et al., 2011).

4

The importance of the DREAM complex in transcriptional regulation of the G2/M phase was reported recently by using a Lin9 knockout mouse model (Reichert et al., 2010). During embryogenesis, loss of Lin9 leads to early embryonic lethality shortly after implantation (Reichert et al., 2010) possibly due to loss of transcriptional activation of G2/M specific genes important for embryonic development (Howman et al., 2000; Lee et al., 2006; Lu et al., 2008). Conditional deletion of Lin9 in adult mice results in complete atrophy of the small intestine and finally death within seven days (Reichert et al., 2010). Histological analysis of the intestine tissues revealed also evidence of failure in mitosis and cytokinesis (Reichert et al., 2010). Upon Lin9 deletion, mouse embryonic fibroblasts (MEFs) show severe defects in mitosis and cytokinesis like binucleation, centrosome amplification, tetraploidization, formation of multipolar spindles and abnormally shaped nuclei (Reichert et al., 2010). A high rate of premature senescence is also observable in those MEFs (Reichert et al., 2010). Chromatin immunoprecipitation (ChIP) and microarray experiments in human and mouse cells showed that Lin9 is required to activate genes which are involved in different phases of mitosis and cytokinesis, such as mitotic entry, mitotic spindle assembly, chromosome segregation, mitotic exit and cytokinesis (fig 1.2) (Osterloh et al., 2007; Reichert et al., 2010).
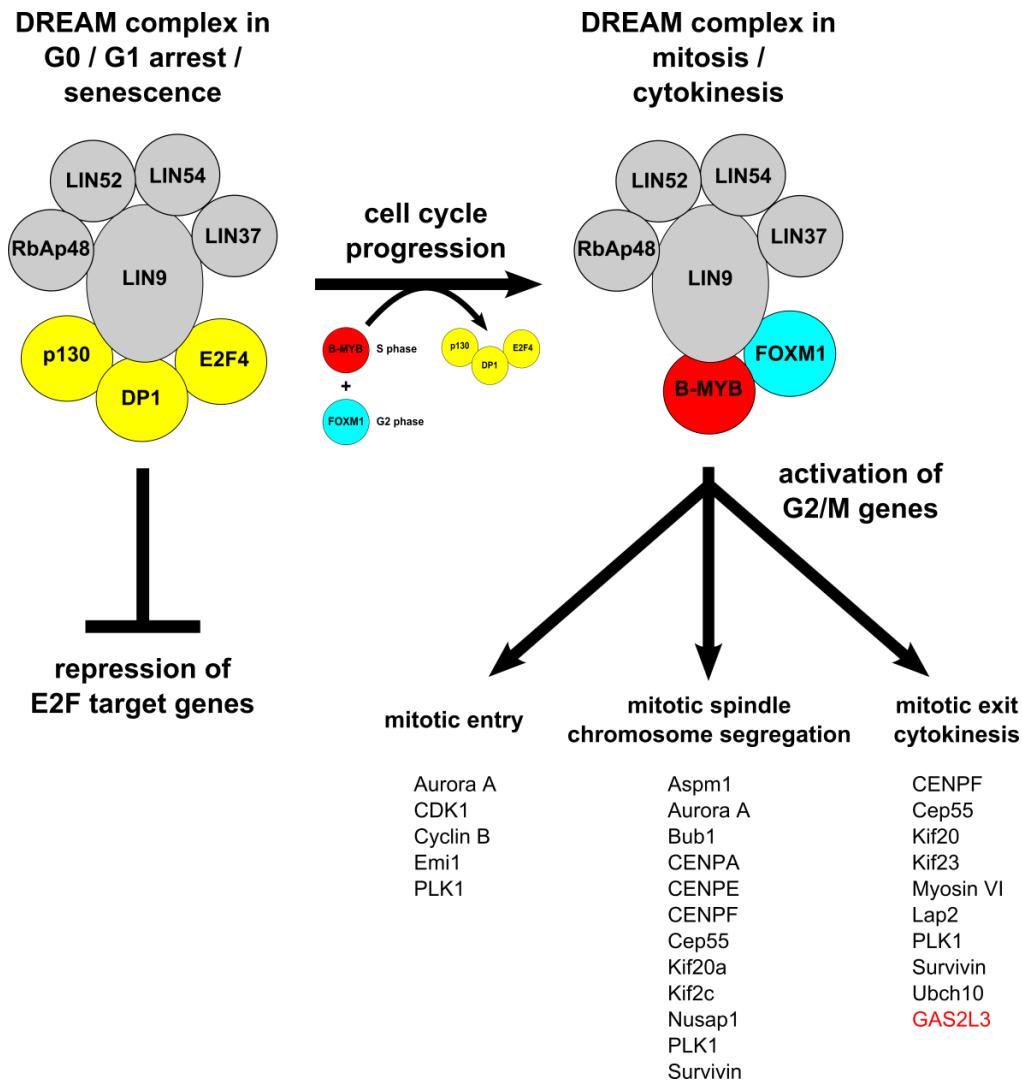
Figure 1.2: Composition and function of the DREAM complex in mammalian cells. The composition of the DREAM complex switches in a cell cycle dependent manner. In non-proliferating cells p130, E2F4 and DP1 bind to the DREAM core complex and lead to repression of E2F target genes. Entry into S phase leads to release of p130, E2F4 and DP1 and binding of B-MYB and FOXM1 to the DREAM core complex. This switch activates many G2/M specific genes important for mitotic entry, mitotic spindle formation, chromosome segregation, mitotic exit and cytokinesis. G2/M specific target genes were identified by microarray analysis of Lin9 knockout MEFs (Reichert et al., 2010).

One gene which was strongly downregulated after Lin9 deletion was growth arrest specific 2 like 3 (GAS2L3).

1.3. Growth arrest specific 2 protein family

The Growth arrest specific 2 (GAS2) protein family consists of the four members GAS2, GAS2 like 1 (GAS2L1), GAS2 like 2 (GAS2L2) and GAS2 like 3 (GAS2L3). The protein family is well conserved throughout vertebrates, but absent in primitive eukaryotes like yeast. In *D. melanogaster* only one paralog protein called Pigs (pickled eggs) is present which is important for maintenance of muscle integrity and proper differentiation of follicle cell (Pines et al., 2010). All family members have two conserved domains in common the so called

calponin homology (CH) and the growth arrest specific (GAS2/GAR) domain. The CH domain is described as an actin binding domain mainly found in cytoskeleton but also in signal transduction associated proteins (Castresana and Saraste, 1995). It comprises around 100 amino acids and is composed of four alpha helices (Korenbaum and Rivero, 2002). It was originally identified in the protein Calponin (Vancompernolle et al., 1990) but meanwhile a plethora of proteins harboring this domain were discovered (Hartwig, 1995). CH domain containing proteins can be further subdivided according to the number of domains present. Proteins belonging to the so called calponin-type group only harbor one CH domain while the actinin-type proteins have either two or four CH domains (Korenbaum and Rivero, 2002; Stradal et al., 1998). Interestingly it was shown that the CH domain of Calponin is neither necessary nor sufficient for actin filament binding (Gimona and Mital, 1998). The GAS2 or GAR domain is a small protein domain harboring between 60 and 80 amino acids. It was originally identified in the GAS2 protein (Brancolini et al., 1992). Apart from the GAS2 family, only the spectraplakins microtubule-actin cross-linking factor 1 (MACF1) and Dystonin contain a GAR domain in the human proteome. Both proteins are giant cytoskeleton cross-linkers which are necessary for maintenance of cellular integrity by binding and stabilizing intermediate filaments as well as microtubule and actin cytoskeleton (Röper et al., 2002; Suozzi et al., 2012). The GAR domain was originally described as a microtubule binding domain (Goriounov et al., 2003; Sun et al., 2001), although this finding could not be verified for all proteins harboring this domain (Stroud et al., 2011; Wolter et al., 2012). Figure 1.3 gives an overview of the GAS2 protein family.
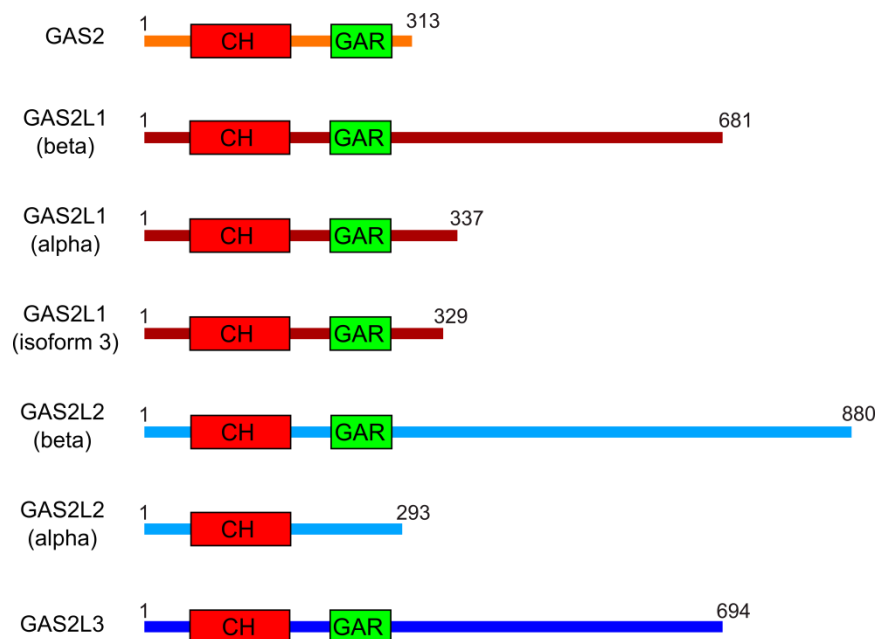
Figure 1.3: Overview of the Growth arrest specific 2 (GAS2) protein family. The GAS2 protein family consists of the four members GAS2, GAS2L1, GAS2L2 and GAS2L3. All known isoforms of the family members are shown. See main text (section 1.3.1 to 1.3.4) for further description of the proteins. Parts of the figure were first published in Wolter et al., 2012.

1.3.1. GAS2

The GAS2 gene is located on chromosome 11p14.3 and codes for the GAS2 protein which is 313 amino acids in length. It was first described as a protein solely expressed in growth arrested mammalian fibroblasts (Schneider et al., 1988). Later it was shown that it is a component of the microfilament network by interacting with F-actin and that it becomes hyperphosphorylated in quiescent cells upon serum stimulation (Brancolini et al., 1992). During transition from G0 to G1 phase, the phosphorylation of GAS2 is coupled to reorganization of the actin cytoskeleton (Brancolini and Schneider, 1994). It has also been shown that GAS2 is a substrate of the interleukin-1 beta converting enzymes caspase-3 and caspase-7 and is involved in regulation of coordinated actin cytoskeleton dependent cell shape changes during apoptosis (Brancolini et al., 1995; Sgorbissa et al., 1999). Furthermore GAS2 is involved in regulation of apoptosis and chondrogenesis in the developing mouse limb (Lee et al., 1999) and it increases susceptibility to p53 dependent apoptosis by binding to m-calpain and thereby increasing p53 stability (Benetti et al., 2001, 2005). Recently it was reported that GAS2 inhibits cell division in *X. laevis* embryos (Zhang et al., 2011) and that it is up-regulated in chronic myeloid leukemia (CML) and required for growth of CML cells (Zhou et al., 2014).

1.3.2. GAS2L1

The GAS2L1 gene, also known as GAR22, is located on chromosome 22q12.2 (Zucman-Rossi et al., 1996). In the UniProt protein knowledgebase three different isoforms of the GAS2L1 protein are annotated which are generated by alternative splicing of the GAS2L1 mRNA. Isoform 1, also called beta isoform is 681 amino acids in length. The other two isoforms, isoform 2 (also called alpha isoform) and isoform 3 are C-terminally truncated versions of the full length protein. They are 337 and 329 amino acids in length (Zucman-Rossi et al., 1996). GAS2L1 gene expression was confirmed in many different mouse and human tissues by northern blotting but on protein level it was only detected in testis and brain (Goriounov et al., 2003). Interestingly, only the beta and not the alpha isoform is detectable, what might be explained by posttranscriptional inhibition of gene expression or a high rate of degradation of the GAS2L1 alpha protein (Goriounov et al., 2003). Furthermore it was shown that overexpressed GAS2L1 beta can act as a cytoskeleton cross-linker by binding to actinfilaments and microtubules (Goriounov et al., 2003). Recently it was reported that GAS2L1 is a target gene of thyroid hormone receptors and that ectopic expression lengthens cell cycle and causes growth inhibition in human erythroid cells (Gamper et al., 2009). It was also shown that GAS2L1 influences microtubule dynamics, stability and guidance along actin stress fibers by interacting with end binding proteins (Stroud et al., 2014).

1.3.3. GAS2L2

The GAS2L2 gene, also known as GAR17, is located on chromosome 17q12. GAS2L2 mRNA encodes for two different splice variants of the protein. The two isoforms harbor 880 and 293 amino acids and are called beta and alpha isoform respectively (Goriounov et al., 2003). Northern blotting experiments showed that expression of GAS2L2 is limited to skeletal muscle and that the beta isoform transcript is more frequently found in this tissue than the one coding for the alpha isoform (Goriounov et al., 2003). Biochemical experiments revealed, that overexpressed GAS2L2 beta is able to act as a cytoskeleton cross-linker by interacting with actin filaments and microtubules (Goriounov et al., 2003). Very recently it was reported that GAS2L2 influences microtubule stability, dynamics and guidance along actin stress fibers by interacting with end binding proteins (Stroud et al., 2014).

1.3.4. GAS2L3

GAS2L3 gene is located on chromosome 12q23.1. It codes for the GAS2L3 protein which is 694 amino acids in length. As described above GAS2L3 was identified as a DREAM complex target gene in a microarray screen (Reichert et al., 2010). While we investigated the function of GAS2L3 it was reported that GAS2L3 is a cytoskeleton associated protein, which is ubiquitously expressed in human tissues (Stroud et al., 2011). Furthermore it was shown that GAS2L3 is able to bind to F-actin and microtubules *in vitro* and that the binding strength to the cytoskeleton is modulated by the GAR domain (Stroud et al., 2011). In 2012 Asai and colleagues reported, that the response of hematopoietic stem cells to genotoxic stress is mediated by Necdin in a GAS2L3 dependent manner (Asai et al., 2012). One year later it was shown that GAS2L3 is a constriction site associated protein which is phosphorylated by CDK1 in mitosis and targeted for ubiquitin mediated proteolysis by the APC/C^{Cdh1} but not by APC/C^{Cdc20} complex (Pe'er et al., 2013). Recently it was reported that GAS2L3 interacts with end binding proteins via its C-terminus (Stroud et al., 2014). Work in our laboratory revealed that GAS2L3 shows a dynamic localization pattern during mitosis and cytokinesis. Specifically, in metaphase and anaphase the protein is located at the mitotic spindle. It then moves to the spindle midzone in telophase and finally localizes to the midbody in cytokinesis (Wolter et al., 2012). During interphase GAS2L3 co-localizes with the microtubule cytoskeleton (Wolter et al., 2012), although this localization is only detectable after GAS2L3 overexpression. We also reported that GAS2L3 is required for genomic stability and proper cytokinesis (Wolter et al., 2012).

1.4. Chromosomal passenger complex (CPC)

The chromosomal passenger complex (CPC) is an important protein complex which regulates many crucial steps during mitosis and cytokinesis. The CPC is highly conserved in eukaryotes and consists in mammals of the three regulatory proteins inner centromere

protein (Incenp), Borealin, Survivin and the kinase Aurora B (Carmena et al., 2009, 2012; van der Waal et al., 2012). The four CPC members show an interdependent relationship. In case one of the four proteins is lost, mislocalized on cellular level or functionally perturbed sever defects in cell division occur (Adams et al., 2001; Carvalho et al., 2003; Gassmann et al., 2004; Honda et al., 2003; Vader et al., 2006; Wheatley et al., 2001).

1.4.1. Borealin

Borealin was discovered in 2004 as a mitotic chromosome associated protein in two different studies (Gassmann et al., 2004; Sampath et al., 2004). It is 280 amino acids in length and harbors a helical formed stretch at the N-terminus. Together with Survivin and the N-terminal part of Incenp the N-terminus of Borealin forms the triple helix bundle, which is necessary for localization of the CPC to centromeres, spindle midzone and midbody (Ainsztein et al., 1998; Gassmann et al., 2004; Jeyaprakash et al., 2007; Klein et al., 2006; Vader et al., 2006). In mitotic cells all Survivin molecules are bound to Borealin (Gassmann et al., 2004) by forming a soluble complex in a 1:1 ratio (Bourhis et al., 2007; Jeyaprakash et al., 2007). Borealin interacts via its central region with the charged multivesicular body protein 4C (CHMP4C) subunit of the endosomal complex required for transport III (ESCRT-III) (Capalbo et al., 2012; Carlton et al., 2012), a multi-protein complex important for regulation of abscission (Dukes et al., 2008; Elia et al., 2011; Guizetti et al., 2011; Schiel et al., 2013). On posttranslational level Borealin is strongly modified. It becomes sumoylated in early mitosis in a Ran-binding protein 2 (RanBP2) dependent manner by a multi subunit SUMO E3 ligase (Klein et al., 2009; Werner et al., 2012) and de-sumoylated at onset of anaphase by sentrin-specific protease 3 (Senp3) (Klein et al., 2009). The physiological function of this sumoylation/de-sumoylation cycle is not yet known. Apart from this Borealin gets phosphorylated by different kinases like Aurora B (Hayama et al., 2007), monopolar spindle protein 1 (Mps1) (Jelluma et al., 2008) and CDK1 (Kaur et al., 2010; Tsukahara et al., 2010) which leads to precise regulation of protein function. Phosphorylation by Mps1 is modulating dimerization of Borealin molecules and it is assumed to be involved in regulating CPC activity in error correction and chromosome alignment (Bourhis et al., 2007; Jelluma et al., 2008). Interestingly the C-terminally located dimerization motif is also involved in regulation of protein stability (Date et al., 2012). Phosphorylation by CDK1 creates a binding platform for the two proteins Shugoshin 1 and 2 which enables proper CPC localization to the centromeres (Tsukahara et al., 2010).

1.4.2. Survivin

Survivin was discovered in 1997 as an inhibitor of apoptosis protein (IAP) (Ambrosini et al., 1997). It was reported that it accumulates in G2 phase of the cell cycle and that it is involved in negative regulation of cell death in mitosis (Ambrosini et al., 1997). Many reports have

been published about the role of Survivin in regulation of apoptosis, but not all showed clear evidence for involvement of Survivin in this process (Uren et al., 1999, 2000; Yue et al., 2008). It was shown that Survivin has an active nuclear export signal (Stauber et al., 2006). Due to this it was postulated that nuclear localized Survivin is incorporated into the CPC and takes part in regulation of mitosis whereas cytoplasmic Survivin is involved in regulation of apoptosis (Connell et al., 2008). Alpha isoform of Survivin harbors 142 amino acids but according to UniProt knowledgebase six other isoforms created by alternative splicing exist. It is composed of an N-terminally located baculoviral inhibitor of apoptosis repeat (BIR) domain and a C-terminally located helical formed stretch of amino acids which forms together with Incenp and Borealin the already described triple helix bundle (section 1.4.1), necessary for proper localization of the CPC during mitosis and cytokinesis (section 1.4.4). The BIR domain is important for proper localization of the CPC to centromeres (Lens et al., 2006; Yue et al., 2008) and it is assumed that it also plays a role for CPC localization during anaphase at least in *D. melanogaster* (Szafer-Glusman et al., 2011). Purified Survivin molecules form homo-dimers in solution (Chantalat et al., 2000; Sun et al., 2005; Verdecia et al., 2000) but dimerization is prevented within the CPC by direct binding of Borealin to the dimerization motif of Survivin (Jeyaprakash et al., 2007, 2011). Like the other CPC members, Survivin is also regulated on posttranslational level. It becomes phosphorylated by CDK1 (O'Connor et al., 2000, 2002), casein kinase 2 (Ck2) (Barrett et al., 2011), Aurora B (Wheatley et al., 2004, 2007) and Plk1 (Chu et al., 2011; Colnaghi and Wheatley, 2010). It was reported that phosphorylation of Survivin on threonine 34 by CDK1 is important for prevention of spontaneous apoptosis (Grossman et al., 2001; Yan et al., 2006) although this function does not seem to be conserved in all organisms (Yue et al., 2008). Additionally it was reported, that phosphorylation by Ck2 on threonine 48 is involved in regulation of the interaction between Borealin and Survivin (Barrett et al., 2011). Despite phosphorylation, Survivin is also modified by ubiquitylation. It was shown that ubiquitylation of Survivin is necessary for association with centromeres while de-ubiquitylation leads to dissociation (Vong et al., 2005). In yeast, the Survivin homologue Bir1 is also regulated by sumoylation (Montpetit et al., 2006) although it was not shown that this modification also occurs in vertebrates.

1.4.3. Aurora B

Aurora B kinase was first discovered in *D. melanogaster* in 1995 (Glover et al., 1995). It forms together with Aurora A and Aurora C a family of Serine/Threonine kinases. Aurora A kinase localizes to the mitotic spindle poles (Glover et al., 1995) and has important functions during mitotic entry, centrosome maturation and bipolar spindle formation (Carmena et al., 2009). Its activity is regulated by a plethora of different interacting proteins like Tpx2, Ajuba, Bora and many more (Bayliss et al., 2003; Eyers et al., 2003; Hirota et al., 2003; Hutterer et

al., 2006; Kufer et al., 2002; Wittmann et al., 2000). Aurora C kinase is biochemically similar to Aurora B and can complement Aurora B function in mitotic cells (Sasai et al., 2004). It is able to interact with the CPC member Incenp (Li et al., 2004) and it might play a role together with the CPC in embryonic development during preimplantation (Avo Santos et al., 2011). Aurora C is highly expressed in testis (Tseng et al., 1998). In concordance with this, it was reported that loss of Aurora C leads to abnormally shaped spermatozoa, male infertility and polyploidy of oocytes what indicates an important role during spermato- and oogenesis (Dieterich et al., 2007; Ben Khelifa et al., 2011, 2012; Yang et al., 2010). Aurora B is the catalytic subunit of the CPC and binds to the IN box of Incenp by its N-terminal region (Adams et al., 2000; Kaitna et al., 2000). The protein is 344 amino acids in length and harbors a C-terminally located kinase domain. Establishment of Aurora B kinase activity is a precisely regulated process. It is assumed that multiple steps are necessary to fully activate Aurora B kinase. First of all, the IN box of Incenp binds to and partially activates Aurora B. Aurora B then phosphorylates a C-terminally located threonine-serine-serine (TSS) motif in Incenp and subsequently a conserved threonine residue in the T-loop of its own kinase domain (Bishop and Schumacher, 2002; Honda et al., 2003). At the moment it is not fully clear if those phosphorylations occur *in trans* for example through another CPC molcecule located in close proximity, although recent studies strengthen this assumption (Kelly et al., 2007; Sessa et al., 2005; Wang et al., 2011). Apart from this it was also shown that presence of microtubules increases activity of Aurora B kinase in a telophase disk protein of 60 kDa (TD60) dependent manner (Fuller et al., 2008; Kelly et al., 2007; Rosasco-Nitcher et al., 2008; Tseng et al., 2010).

Despite phosphorylation, Aurora B activity and localization is also regulated by other posttranslational modifications. It was reported that monoubiquitylation of Aurora B by the E3 ubiquitin ligase Cullin 3 regulates removal of the CPC from chromatin and influences localization of the CPC during anaphase (Sumara et al., 2007). Additionally it was shown that sumoylation of Aurora B within its kinase domain modulates kinase activity and is also necessary for mitotic progression (Ban et al., 2011; Fernández-Miranda et al., 2010). Finally, degradation of Aurora B is mediated by polyubiquitylation via the E3 ubiquitin ligase APC/C and subsequent proteasomal destruction (Nguyen et al., 2005; Stewart and Fang, 2005). Because Aurora kinases are frequently overexpressed in different cancer types, it is believed that they are valuable targets for cancer therapy (Katayama et al., 2003; Vader and Lens, 2008). At the moment there are a number of Aurora specific inhibitors in preclinical or clinical trials (Taylor and Peters, 2008; Yeung et al., 2008).

1.4.4. CPC localization during interphase, mitosis and cytokinesis

The CPC shows a dynamic localization pattern during cell cycle. The complex first localizes to pericentromeric heterochromatin during late stage of S phase (Beardmore et al., 2004; Cooke et al., 1987; Hayashi-Takanaka et al., 2009; Monier et al., 2007; Zeitlin et al., 2001). The localization is mediated by HP1 which binds simultaneously to trimethylated lysine 9 of histone H3 (Fischle et al., 2005) and to Incenp (Ainsztein et al., 1998; Kang et al., 2011; Nozawa et al., 2010). After entering mitosis Aurora B phosphorylates histone H3 on serine 10 (Hsu et al., 2000; Murnion et al., 2001) what in turn leads to dissociation of HP1 together with bound CPC from trimethylated lysine 9 of histone H3 (Hirota et al., 2005). For dissociation pogo transposable element derived protein with zinc finger domain (POGZ) is required (Nozawa et al., 2010). Next, histone H3 is phosphorylated by Haspin kinase at threonine 3 what leads to binding of the CPC via interaction with the BIR domain of Survivin (Du et al., 2012; Jeyaprakash et al., 2011; Niedzialkowska et al., 2012). Additionally histone H2A is phosphorylated by Bub1 kinase at threonine 120 what creates a binding motif for the Shugoshins 1 and 2 which are interacting simultaneously with CDK1 phosphorylated Borealin (Kawashima et al., 2007; Tsukahara et al., 2010). The combination of those interaction events leads to an enrichment of the CPC at the inner centromere, the region where the two histone modifications overlap (Dai and Higgins, 2005; Kawashima et al., 2007; Kelly et al., 2010; Wang et al., 2010; Yamagishi et al., 2010). At onset of anaphase the CPC is removed from inner centromeres and localizes to the spindle midzone and cell cortex (Carmena et al., 2009, 2012). In late mitosis histone H3 is dephosphorylated at threonine 3 what leads to a repression of CPC localization to centromeres (Kelly et al., 2010; Qian et al., 2011; Vagnarelli et al., 2011). Additionally Aurora B becomes ubiquitylated by the E3 ubiquitin ligase complexes Cul3-Kelch-like protein 9 (KLHL9)-KLHL13 and Cul3-KLHL21 (Maerki et al., 2009; Sumara et al., 2007). This leads to active removal of the CPC from inner centromeres by the AAA ATPase cell division control protein 48 (CDC48) and promotes reformation of the nucleus and decondensation of chromosomes (Ramadan et al., 2007). After release from the inner centromeres the CPC is targeted to the mitotic spindle. This process is mediated by an interaction between the microtubule binding protein mitotic kinesin-like protein 2 (Mklp2) and Incenp (Cesario et al., 2006; Gruneberg et al., 2004; Jang et al., 2005). Importantly, this interaction only occurs during anaphase after removal of an inhibitory phosphate residue on threonine 59 of Incenp which blocks Mklp2 binding (Hümmer and Mayer, 2009). The CPC finally localizes to the midbody during telophase and cytokinesis. For this, enzymatic activitiy of DNA topoisomerase II and Aurora B kinase as well as phosphorylation of Incenp on serine 197 by an unknown kinase is needed (Coelho et al., 2008; Xu et al., 2009; Yang et al., 2007).

1.4.5. Functions of the CPC during mitosis and cytokinesis

The CPC fulfills a plethora of different functions during mitosis and cytokinesis. During early mitosis it is involved in maintenance of mitotic chromosome structure, regulation of kinetochore-microtubule attachments (section 1.4.5.1), control of spindle assembly checkpoint and formation as well as stabilization of the mitotic spindle (Carmena et al., 2009, 2012). During late mitosis and cytokinesis it regulates contractile ring formation and function and it also participates in regulation of abscission (section 1.4.5.2) (Carmena et al., 2009, 2012).

1.4.5.1. Regulation of kinetochore-microtubule attachments

The CPC ensures correct segregation of sister chromatids by regulation of kinetochore-microtubule attachments. Kinetochores are multi-protein complexes which are located at the centromeres. They mediate attachment of microtubules to chromosomes and regulate chromosomal segregation (Varma and Salmon, 2012). The kinetochore harbors a microtubule binding platform which consists of the protein complex network KNL1, Mis12 and Ndc80 (KMN network) (Varma and Salmon, 2012). The KMN network captures microtubule tips (Powers et al., 2009) and by this connects kinetochores with spindle poles. In case erroneous kinetochore-microtubule attachments (for example syntelic or monotelic attachments) are established no tension is generated across the kinetochores. Lack of tension is detected by the CPC which acts as a tension sensor (Tanaka et al., 2002). To repair incorrect kinetochore-microtubule attachments the CPC phosphorylates the positively charged N-terminal region of Ndc80 at multiple residues and by this weakens the affinity of the KMN network for the negatively charged C-terminal part of tubulin (Alushin et al., 2010; Cheeseman et al., 2006; Ciferri et al., 2008; DeLuca et al., 2006, 2011; Miller et al., 2008; Tooley et al., 2011; Wei et al., 2007). Subunits of the KNL1 and Mis12 complexes are also phosphorylated by the CPC what further decreases the microtubule binding affinity of the KMN network (Hua et al., 2011; Welburn et al., 2010). Perpetual phosphorylation of the KMN network further weakens the erroneous kinetochore-microtubule attachments until the microtubules are released from the kinetochore (Cheeseman et al., 2006; DeLuca et al., 2006). After achievement of correct bipolar (amphitelic) attachment, tension across kinetochores is generated which leads to a physical separation of the CPC located at the centromeres from the kinetochores. Due to the spatial distance the CPC is no longer able to destabilize the kinetochore-microtubule interactions by phosphorylation (Lampson and Cheeseman, 2010; Maresca and Salmon, 2010; Tanaka et al., 2002). The established kinetochore-microtubule connections are further stabilized by the two protein phosphatases 1 (PP1) and 2A (PP2A) located at the kinetochores which mediate removal of phosphate residues from the KMN network (Espeut et al., 2012; Foley et al., 2011; Kim et al., 2010;

Meadows et al., 2011; Posch et al., 2010; Rosenberg et al., 2011). The model of Aurora B acting as a tension sensor is widely accepted and was further confirmed by another study (Liu et al., 2009). Apart from this, Aurora B also influences microtubule stability directly by regulating the localization and activity of the mitotic centromere associated kinesin (MCAK), which functions as an important microtubule depolymerase at centromeres (Andrews et al., 2004; Lan et al., 2004; Ohi et al., 2004; Tanenbaum et al., 2011) and by inhibiting the activity of the formin mDia3 which acts as a microtubule stabilizer at kinetochores (Cheng et al., 2011). .

1.4.5.2. Regulation of abscission

During abscission which is the last step of cytokinesis the separation of daughter cells is completed by fusion of membranes. The CPC is involved in the so called abscission checkpoint (or "No-Cut" pathway in yeast) (Norden et al., 2006), which detects lagging chromatin in the cleavage furrow and subsequently delays abscission. This mechanism protects cells from DNA damage by chromosome breakage and tetraploidization (Steigemann et al., 2009). The exact mechanism how the CPC regulates this process is not clear in every detail at the moment. It is known that the CPC interacts with the ESCRT-III complex mediated by an interaction between Borealin and CHMP4C (section 1.4.1). An accepted idea is that the binding of Borealin facilitates Aurora B mediated phosphorylation of CHMP4C what in turn inhibits the activity of the protein and leads to a delay in abscission (Capalbo et al., 2012; Carlton et al., 2012).

1.5. Aim of the project

GAS2L3 was identified as a DREAM complex target gene in microarray experiments performed in Lin9 knockout MEFs (Reichert et al., 2010). It was reported that GAS2L3 expression is regulated in a cell cycle dependent manner and that it is important for maintenance of genomic stability (Wolter et al., 2012).

The aim of the project was to further characterize the biochemical properties and physiological function of GAS2L3. By using different *in vitro* assays the cytoskeleton binding properties of GAS2L3 were analyzed biochemically. Novel protein interactors of GAS2L3 were identified by a combination of *in vitro* and *in vivo* protein-protein interaction experiments like GST pulldown assays, co-immunoprecipitation and tandem affinity purification with subsequent mass spectrometrical analysis. Cell biological experiments in combination with RNA interference mediated depletion were used to further investigate the cellular function of GAS2L3 in cells. To analyze the role of GAS2L3 *in vivo*, a conditional and a non-conditional knockout mouse strain was established.

2. Materials and Methods

2.1. Materials

2.1.1. Chemical stocks & reagents

[gamma-P32]-ATP (Hartmann analytic)	10 µCi/µl
4-Hydroxytamoxifen (4-OHT)	10 mg/ml in ethanol
Ammonium Persulfate (APS)	10% in H_2O
AZD1152	20 mM in DMSO
Bovine serum albumin (BSA)	10 mg/ml in H_2O
Bromophenol blue	4 mg/ml in H_2O
Diethylpyrocarbonate (DEPC)	ready to use
Dimethyl sulfoxide (DMSO)	ready to use
dNTPs (dATP, dCTP, dGTP, dTTP)	2 mM
Dithiothreitol (DTT)	1 M in H_2O
Ethidiumbromide	10 mg/ml in H_2O
GTP	100 mM in H_2O (pH 7)
Hoechst 33258	10 mg/ml in H_2O
ImmuMount	ready to use
Isopropyl- β-D-1-thiogalactopyranoside (IPTG)	1 M in H_2O
Luminol	250 mM in DMSO
Nocodazole	1 mg/ml in DMSO
NP-40	ready to use
p-Coumaric acid	90 mM in DMSO
Phenylmethylsulphonylfluoride (PMSF)	100 mM in isopropanol
Polybrene (Hexadimethrine bromide)	4 mg/ml in H_2O

Protease Inhibitor Cocktail (Sigma)	ready to use
ProtoGel 30% (Biozym)	ready to use
Random Primer (Roche)	500 µg/ml in H_2O
Sodium dodecyle sulfate (SDS)	20% in H_2O
Taxol	10 mM in anhydrous DMSO
Temed (99%)	ready to use
Thymidine	200 mM in DMSO
Trifast (Peqlab)	ready to use
Triton X-100	ready to use
Tween-20	ready to use
Xylene	ready to use

All chemicals were purchased from AppliChem, Invitrogen, Roth or Sigma Aldrich unless otherwise noted.

2.1.2. Enzymes

Pfu DNA Polymerase (2.5 U/µl)	Thermo Scientific (Fermentas)
His-Taq DNA Polymerase (15 U/µl)	provided by AG Prof. Dr. Gessler
Absolute QPCR SYBR Green mix	Thermo Scientific
M-MLV-RT Transcriptase (200 U/µl)	Life Technologies
RevertAid Reverse Transcriptase (200 U/µl)	Thermo Scientific
RiboLock RNase Inhibitor (40 U/µl)	Thermo Scientific
Restriction endonucleases (10 U/µl)	Thermo Scientific (Fermentas) & New England Biolabs
T4 DNA Ligase (400 U/µl)	New England Biolabs
RNase A (10 mg/ml)	Sigma Aldrich

2.1.3. Antibiotics

name	stock concentration	final concentration	description
Ampicillin	100 mg/ml	100 µg/ml	selection of *E. coli* cells
Hygromycin	100 mg/ml	400 µg/ml	selection of HeLa cells
Puromycin	10 mg/ml	0.5 to 5 µg/ml	selection of HeLa cells
Tetracycline	10 mg/ml	1.5 to 2.5 µg/ml	induction of protein expression in HeLa cells

2.1.4. Buffers & Solutions

2.1.4.1. General buffers

	1 X
	13.7 mM NaCl
	0.3 mM KCl
Phosphate buffered saline (PBS)	0.64 mM Na_2HPO_4
	0.15 mM KH_2PO_4
	adjust pH to 7.4 with HCl

	1 X
	50 mM Tris/HCl (pH 7.5)
Tris buffered saline (TBS)	150 mM NaCl
	adjust to pH 7.4

	1 X
	40 mM Tris/HCl
TAE buffer	5 mM CH_3COOH
	10 mM EDTA (pH 8.0)

TE buffer	**1 X**
	10 mM Tris/HCl (pH 7.5)
	1 mM EDTA

HEPES buffered saline (HBS)	**2 X**
	280 mM NaCl
	1.5 mM Na_2HPO_4
	50 mM HEPES-KOH (pH 7.05)

Miniprep Solution S1	25 mM Tris/HCl (pH 8.0)
	10 mM EDTA

Miniprep Solution S2	200 mM NaOH
	1% SDS

Miniprep Solution S3	29.44 g KCH_3COO
	11.5 ml CH_3COOH
	28.5 ml H_2O

DNA Loading Buffer	**5 X**
	15% ficoll
	0.05% bromophenol blue
	0.05% xylene cyanol
	0.05 M EDTA
	in 1 X TAE

Luria Bertani (LB) liquid Medium	25 g powder in 1 l H_2O, autoclaved

Luria Bertani (LB) Agar	40 g powder in 1 l H_2O, autoclaved

SB liquid medium	32 g yeast extract
	20 g select pepton
	5 g NaCl
	in 1 l H_2O, autoclaved

Glycerol stock buffer	65 ml glycerol
	0.1 M $MgSO_4$
	25 mM Tris/HCl (pH 8)
	ad 100 ml H_2O, autoclaved

2.1.4.2. Buffers for whole cell lysates

TNN lysis buffer	50 mM Tris/HCl (pH 7.5)
	120 mM HCl
	5 mM EDTA
	0.5% NP-40
	10 mM $Na_4P_2O_7$
	2 mM Na_3VO_4
	100 mM NaF
	ad 500 ml H2O
	Protease Inhibitors (PI) 1:100 (add fresh)
	1 mM DTT (add fresh)

Bradford solution	50 mg Coomassie Brilliant Blue G250
	23.75 ml Ethanol
	50 ml 85% (v/v) H_3PO_4
	ad 500 ml H2O / filter twice

2.1.4.3. Buffers for tandem affinity purification (TAP)

TAP cell lysis buffer	10 mM Tris/HCl (pH 7.6)
	100 mM KCl
	2 mM MgCl$_2$
	0.5% NP-40
	10 mM Na$_4$P$_2$O$_7$
	2 mM Na$_3$VO$_4$
	100 mM NaF
	Protease Inhibitors (PI) 1:100 (add fresh)
	1 mM DTT (add fresh)

TAP elution buffer	2.5 mM desthiobiotine
	in TAP cell lysis buffer

TAP wash buffer	10 mM Tris/HCl (pH 7.6)
	2 mM MgCl$_2$

2.1.4.4. Buffers for immunoblotting

Acrylamide solution	30% (w/v) acrylamide
	0.8% (w/v) N,N´-methylenbisacrylamide

SDS running buffer	**10 X**
	576 g glycine
	120 g Tris base
	40 g SDS
	ad 4 l H2O

Blotting buffer	**1 X**
	0.6 g Tris base
	2.258 g glycine
	150 ml methanol
	ad 1 l H2O

Stripping buffer	15 g glycine
	1 g SDS
	10 ml Tween-20
	ad 1 l H_2O
	adjust pH to 2.2

Separating gel buffer	1.5 M Tris/HCl (pH 8.8)

Stacking gel buffer	0.8 M Tris/HCl (pH 6.8)

Blocking Solution	3 g milk powder in 100 ml TBS-T

Protein sample buffer	**3 X**
	300 mM Tris/HCl (pH 6.8)
	15 mM EDTA
	150 mM DTT
	12% (w/v) SDS
	15% (w/v) glycerol
	0.03% (w/v) bromophenol blue

TBS-T	**1 X**
	0.5 ml Tween-20 in 1 l TBS

Chemiluminescence solution	10 ml 100 mM Tris/HCl (pH 8.5)
	50 µl 250 mM luminol
	22 µl 90 mM p-coumaric acid
	3 µl 30% H_2O_2

2.1.4.5. Buffers for immunofluorescence

Blocking Solutions	5 g BSA in 100 ml PBS
	or
	10 ml FCS ad 100 ml PBS / filtered

| PFA fixative | 4% paraformaldehyde in PBS |

| Permeabilization buffer | 0.5% Triton X-100 in PBS |

2.1.4.6. Buffers for recombinant protein purification

| GST lysis buffer | 1 mM PMSF in TBS |

| GST wash buffer | 1% NP-40 in TBS |

GST elution buffer	20 mM glutathione (reduced)
	in GST wash buffer
	pH adjusted to 8

	1 X
BRB80 buffer	80 mM PIPES (pH 6.8)
	1 mM $MgCl_2$
	1 mM EGTA
	adjust pH to 6.8 with KOH

BRB80 fixing solution	50% glycerol
	8% formaldehyde
	in BRB80 buffer

His-tag lysis buffer	10 mM imidazole
	1 mM PMSF
	in TBS
	adjust pH to 8

His-tag wash buffer	20 mM imidazole
	2% NP-40
	in TBS
	adjust pH to 8

2.1.4.7. Buffers for kinase assays

Kinase assay buffer	50 mM Tris/HCl (pH 7.5)
	10 mM MgCl$_2$
	1 mM DTT
	20 µM ATP

2.1.4.8. Buffers for genomic DNA extraction

Tail buffer I (base buffer)	**1 X**
	25 mM NaOH
	0.2 mM EDTA
	adjust pH to 12.0

| **Tail buffer II (neutralizing buffer)** | **1 X** |
| | 40 mM Tris/HCl (pH 5.0) |

2.1.4.9. Buffers for antibody purification

Borate buffers	1 M borate buffer (pH 8)
	1 M borate buffer (pH 9)
	0.1 M borate buffer (pH 8)
	0.1 M borate buffer (pH 9)
	0.2 M borate buffer (pH 9)

Crosslinking buffer	40 mM dimethylpimelimidate
	in 0.2 M borate buffer (pH 9)
	adjust pH to 9

Stop buffer	50 mM Tris/HCl (pH 8)

Elution buffer	0.2 M glycine/HCl (pH 2.5)

Neutralization buffer	1 M K_2HPO_4

2.1.4.10. Staining solutions

Ponceau S solution	0.1 g Ponceau S
	5 ml CH_3COOH
	ad 100 ml H_2O

Coomassie blue staining solution	1 g Coomassie Brilliant Blue R 250
	125 ml isopropanol
	50 ml CH_3COOH
	ad 500 ml H_2O / filter

Coomassie destaining solution	125 ml isopropanol
	50 ml CH_3COOH
	ad 500 ml H_2O

2.1.5. Plasmids

2.1.5.1. Plasmids for bacterial overexpression

plasmid name	internal #	encoded protein
pGEX4T2	397	GST empty vector
pGEX4T2-GAS2L3	1031	GST-GAS2L3
pGEX4T2-GAS2L3(aa1-310)	1206	GST-GAS2L3(aa1-310)
pGEX4T2-GAS2L3(aa170-310)	1225	GST-GAS2L3(aa170-310)
pGEX4T2-GAS2L3(aa170-535)	1164	GST-GAS2L3(aa170-535)
pGEX4T2-GAS2L3(aa303-375)	1290	GST-GAS2L3(aa303-375)
pGEX4T2-GAS2L3(aa303-455)	1291	GST-GAS2L3(aa303-455)
pGEX4T2-GAS2L3(aa303-535)	1226	GST-GAS2L3(aa303-535)
pGEX4T2-GAS2L3(aa303-694)	1067	GST-GAS2L3(aa303-694)
pGEX4T2-GAS2L3(aa456-694)	1309	GST-GAS2L3(aa456-694)
pGEX4T2-GAS2L3(Δ170-309)	1335	GST-GAS2L3(Δ170-309)
pGEX4T2-mGas2l3(aa305-683)	1435	GST-mGas2l3(aa305-683)
pGEX4T2-Histone H3(aa1-46)	-	GST-Histone H3(aa1-46)
pRSETA	319	His-tag empty vector
pRSETA-Aurora B	1412	His-Aurora B
pRSETA-Borealin	1413	His-Borealin
pRSETA-Borealin(aa1-141)	1416	His-Borealin(aa1-141)
pRSETA-Borealin(aa142-280)	1417	His-Borealin(aa142-280)
pRSETA-Survivin	1415	His-Survivin
pRSETA-Survivin(aa1-89)	1418	His-Survivin(aa1-89)
pRSETA-Survivin(aa90-142)	1419	His-Survivin(aa90-142)
pRSETA-Incenp	1414	His-Incenp

2.1.5.2. Plasmids for transient overexpression in mammalian cells

plasmid name	internal #	encoded protein
pcDNA3_HA-mGas2l3	1019	HA-mGas2l3
pcDNA3_eGFP-GAS2L3	1033	eGFP-GAS2L3
pcDNA3_eGFP-GAS2L3(Δ170-309)	1334	eGFP-GAS2L3(Δ170-309)
pcDNA3_eGFP	170	eGFP
pcDNA3_FLAG-Actinin1	1427	Flag-Actinin1
pcDNA3_FLAG-Actinin4	1428	Flag-Actinin4
pcDNA3_FLAG-Bag2	1429	Flag-Bag2
pcDNA3_FLAG-Bag3	1430	Flag-Bag3
pcDNA3_FLAG-CapZa1	1431	Flag-CapZa1
pcDNA3_FLAG-CapZb	1432	Flag-CapZb
pcDNA3_FLAG-HSC70	1433	Flag-HSC70

2.1.5.3. Plasmids for establishment of stable cell lines

plasmid name	internal #	encoded protein / shRNA
pcDNA5/FRT/To-eGFP-GAS2L3 RNAi resistant	1442	eGFP-GAS2L3 RNAi resistant
pcDNA5/FRT/To-eGFP-GAS2L3(Δ170-309) RNAi resistant	1443	eGFP-GAS2L3(Δ170-309) RNAi resistant
pOG44	1157	Flp recombinase
pSuperior.puro-shGAS2L3	1099	shRNA against GAS2L3 mRNA

2.1.5.4. Plasmids for retroviral infection of MEFs

plasmid name	internal #	encoded protein
pBABE-neo-Large T antigen	923	large T antigen
pBABE-H2B-GFP	746	H2B-GFP

2.1.6. Antibodies

2.1.6.1. Primary antibodies

antigen	company	origin	application & dilution	internal #
Aurora B	Abcam ab2254	rabbit polyclonal	IB 1:5000	194
			IP 1:100	
Borealin	Santa Cruz sc-98869	rabbit polyclonal	IB 1:2500	246
CDK 1	Santa Cruz sc-54	mouse monoclonal	IB 1:1000	44
CDK 2	Santa Cruz sc-163	rabbit polyclonal	IB 1:1000	47
Cyclin B1	Santa Cruz sc-245	mouse monoclonal	IB 1:5000	40
			IP 1:100	
GAS2L3	Abnova H00283431-M01	mouse monoclonal	IP 1:100	195
GAS2L3	Abnova H00283431-M02	mouse monoclonal	IP 1:100	215
GAS2L3	Immunoglobe antigen aff. purified	rabbit polyclonal	IB 1:1000	193
			IP 1:10	
GFP	Santa Cruz sc-9996	mouse monoclonal	IP 1:100	99
GST	Santa Cruz sc-138	mouse monoclonal	IB 1:5000	96
P-CENPA	Cell Signaling #2187	rabbit polyclonal	IB 1:2500	247
P-Histone H3	Millipore (Upstate) 06-570	rabbit polyclonal	IB 1:5000	57
Survivin	Cell Signaling #2808	rabbit monoclonal	IB 1:5000	231
			IP 1:100	
Tubulin	Sigma Aldrich T6074	mouse monoclonal	IB 1:5000	158
			IF 1:200	

2.1.6.2. Secondary antibodies

specificity	company	application & dilution
anti-mouse HRP linked	GE Healthcare	IB 1:5000
anti-Protein A HRP linked	BD Biosciences	IB 1:5000
anti-rabbit HRP linked	Life Technologies	IB 1:5000
anti-mouse Alexa Fluor 594	Life Technologies	IF 1:500

2.1.7. Primer sequences

Primer oligonucleotides were purchased from Metabion or MWG.

2.1.7.1. Primers for cloning

internal #	sequence		gene
SG 1075	GCGGATCCATGCAGCCTGCAATTCAAGTATGGTTTG	fwd	hum. GAS2L3 (aa 1-310)
SG 1402	GGCTCGAGTTATCTGGCAGGCGAATCAGGTACACT	rev	
SG 1106	GCGGATCCAGATACGGGGTTGAGCCACCAG	fwd	hum. GAS2L3 (aa 170-310)
SG 1402	GGCTCGAGTTATCTGGCAGGCGAATCAGGTACACT	rev	
SG 1106	GCGGATCCAGATACGGGGTTGAGCCACCAG	fwd	hum. GAS2L3 (aa 170-535)
SG 1350	GGCTCGAGTTATGTTCCTAGACCCGTGGCTATGGTT	rev	
SG 1107	GCGGATCCAGTGTACCTGATTCGCCTGCCAG	fwd	hum. GAS2L3 (aa 303-375)
SG 1470	GCCTCGAGTTAATTTGGCAATTTAGAACGGACTGACA	rev	
SG 1107	GCGGATCCAGTGTACCTGATTCGCCTGCCAG	fwd	hum. GAS2L3 (aa 303-455)
SG 1469	GCCTCGAGTTACAGATCTGCTGAATTCTGGGCTGGA	rev	

SG 1107	GCGGATCCAGTGTACCTGATTCGCCTGCCAG	fwd	hum. GAS2L3 (aa 303-535)
SG 1350	GGCTCGAGTTATGTTCCTAGACCCGTGGCTATGGTT	rev	
SG 1492	GCGGATCCCCCGAGTCCACACTTTTGCCAAATAA	fwd	hum. GAS2L3 (aa 456-694)
SG 1102	GCCTCGAGGAGTATGTATTTATTTTCTAGGTTTCTTACTTCCAG	rev	
SG 1075	GCGGATCCATGCAGCCTGCAATTCAAGTATGGTTTG	fwd	hum. GAS2L3 (aa 1-169)
SG 1554	GGTCTAGACACAATTCGACCAATTTCAAGAAGACAAAG	rev	
SG 1555	GGTCTAGAACACCTCAGCCTCCTGAAATGAATC	fwd	hum. GAS2L3 (aa 310-694)
SG 1348	GCGCGGCCGCGAGTATGTATTTATTTTCTAGGTTTCTTACTTCCAG	rev	
SG 1590	GCGGATCCAGCGTGCCAGATTCGCCTGCC	fwd	mouse Gas2l3 (aa 305-683)
SG 1053	GCCTCGAGCACCCTGATTTGCTGAAACGATACAAGTG	rev	
SG 1548	GCGGATCCATGGCCCAGAAGGAGAACTCCTAC	fwd	human Aurora B
SG 1549	GGGCGGCCGCTTAGGCGACAGATTGAAGGGCAGAG	rev	
SG 1550	GCGGATCCATGGCTCCTAGGAAGGGCAGTAG	fwd	human Borealin
SG 1551	GCGCGGCCGCTTATTTGTGGGTCCGTATGCTGCTGC	rev	
SG 1623	GCGGATCCATGGCTCCTAGGAAGGGCAGTAG	fwd	hum. Borealin (aa 1-141)
SG 1624	GCGCGGCCGCTTATCTTGCAGTTTGAAGATTCTTACGTTCATTTTC	rev	
SG 1625	GCCTCGAGGTCAAAAGGTGTCCTCCATCCAAGAAG	fwd	hum. Borealin (aa 142-280)
SG 1551	GCGAATTCTTATTTGTGGGTCCGTATGCTGCTGC	rev	
SG 1626	GCGGATCCATGGGTGCCCCGACGTTGCC	fwd	hum. Survivin (aa 1-89)
SG 1627	GCGCGGCCGCTTAGACAGAAAGGAAAGCGCAACCGG	rev	

SG 1628	GCGGATCCAAGAAGCAGTTTGAAGAATTAACCCTTGGTG	fwd	hum. Survivin (aa 90-142)
SG 1629	GCGCGGCCGCTTAATCCATGGCAGCCAGCTGCTCG	rev	
SG 1754	GGTGATCAATGGACCATTATGATTCTCAGCAAACCAAC	fwd	human Actinin1
SG 1755	GGGAATTCTTAGAGGTCACTCTCGCCGTACAG	rev	
SG 1752	GGTGATCAATGGTGGACTACCACGCGGCG	fwd	human Actinin4
SG 1753	GGGAATTCTCACAGGTCGCTCTCGCCATAC	rev	
SG 1756	GGGGATCCATGGCTCAGGCGAAGATCAACGC	fwd	human Bag2
SG 1757	GGGAATTCCCCCTAGCTGAACGTTTGTTTTCCC	rev	
SG 1758	GGGGATCCATGAGCGCCGCCACCCACTC	fwd	human Bag3
SG 1759	GGGAATTCCTACGGTGCTGCTGGGTTACCA	rev	
SG 1750	GGGGATCCATGGCCGACTTCGATGATCGTGTG	fwd	human CapZa1
SG 1751	GGGAATTCGACCACACGTTGAATCCTTGTCTTTCC	rev	
SG 1782	GGGGATCCATGAGTGATCAGCAGCTGGACTGTG	fwd	human CapZb
SG 1749	GGGAATTCGCACGGCGTGTCTGGTTAGCAT	rev	
SG 1760	GGGGATCCATGTCCAAGGGACCTGCAGTTGG	fwd	human HSC70
SG 1761	GGGAATTCTTAATCAACCTCTTCAATGGTGGGCCC	rev	

2.1.7.2. Primers for qPCR

internal #	sequence		gene
SG 783	TCCTCCTCAGACCGCTTTT	fwd	mouse HPRT1
SG 784	CCTGGTTCATCATCGCTAATC	rev	

SG 1034	GCAGCCTGCAATCCAAGT	fwd	mouse Gas2l3
SG 1035	AGGGGACACCTGGGACTTA	rev	
SG 1700	CGAGTGGATAGCCGTGAGAC	fwd	mouse Gas2l3
SG 1701	TCTGCCTTGATGTCAACACCT	rev	
SG 1907	CTCCTCAGACCGCTTTTCC	fwd	rat HPRT1
SG 1908	TCATAACCTGGTTCATCATCACTAA	rev	
SG 1903	GCTTGAAGAGTCCATCAGCA	fwd	rat Gas2l3
SG 1904	TCGGCGATGTGCTTAACAG	rev	
SG 645	GCCCAATACGACCAAATCC	fwd	human GAPDH
SG 646	AGCCACATCGCTCAGACAC	rev	
SG 1058	GCTGTCGGCATGAAGAGC	fwd	human GAS2L3
SG 1059	AATCGATGAGAACAACTACAAGGA	rev	

2.1.7.3. Primers for genotyping

internal #	sequence		allele / product size
SG 1481	CGCGTCGAGAAGTTCCTATT	fwd	targeted / 200 bp
SG 1482	TTAAATACAGGAGGAGAATAACTGG	rev	
SG 1589	ACCCAAACTCAGGACCACAG	fwd	floxed / 370 bp
SG 1482	TTAAATACAGGAGGAGAATAACTGG	rev	wild type / 290 bp
SG 1589	ACCCAAACTCAGGACCACAG	fwd	Δ floxed / 391 bp
SG 1681	TGAGCCTTTGGGAATCTGTC	rev	wild type / 1062 bp
SG 914	CTA GTG CGA AGT AGT GAT CAG G	fwd	Flp / 725 bp
SG 913	CAC TGA TAT TGT AAG TAG TTT GC	rev	

SG 926	GGCATTTCTGGGGATTGC	fwd	Cre / 400 bp
SG 927	CAGACCAGGCCAGGTATCTC	rev	
SG 1113	TGGGATACAGAAGACCAATGC	fwd	CreER^{T2} / 300 bp wild type / 240 bp
SG 1114	ACGGACAGAAGCATTTTCCA	rev	
SG 1115	GTCTCTGCCTCCAGAGTGCT	rev	

2.1.7.4. Primers for long range PCR

internal #	sequence		allele / product size
SG 1530	CATAGCTCCAGCACGGTGGAGCGGAGACAG	fwd	targeted / 7615 bp
SG 1529	CACAACGGGTTCTTCTGTTAGTCC	rev	
SG 1531	GTCCATAGCTCCAGCACGGTGGAGCGGAG	fwd	targeted / 7618 bp
SG 1529	CACAACGGGTTCTTCTGTTAGTCC	rev	
SG 1532	CACACCTCCCCCTGAACCTGAAAC	fwd	targeted / 7440 bp
SG 1533	CATAGGCCTCGTGTTAGCTTCGCCAGGAC	rev	
SG 1532	CACACCTCCCCCTGAACCTGAAAC	fwd	targeted / 7445 bp
SG 1534	GCCTCGTGTTAGCTTCGCCAGGACAG	rev	

2.1.8. siRNA sequences

siRNA oligonucleotides were purchased from Metabion or MWG.

internal #	sequence	targeted mRNA
1	GGGAUACUCUUCAAGGAUUTT	GAS2L3
2	CUAUGUCAGUCCGUUCUAA	GAS2L3
3	CAUUAAAUCCAGUAGGUAAT	GAS2L3
-	UAGCGACUAAACACAUCAA	non targeting ctrl.

2.1.9. Transfection reagents

Lipofectamine 2000	Life Technologies
Lipofectamine RNAiMAX	Life Technologies

2.1.10. Markers

GeneRuler 1 kb DNA ladder	Thermo Scientific (Fermentas)
GeneRuler 100 bp DNA ladder	Thermo Scientific (Fermentas)
PageRuler Prestained Protein Ladder	Thermo Scientific (Fermentas)

2.1.11. Kits

PureLink HiPure Plasmid Midiprep Kit	Life Technologies
PureLink HiPure Plasmid Maxiprep Kit	Life Technologies
QIAquick PCR Purification Kit	Qiagen
Jetstar Gel Extraction Kit	Genomed
GeneJET Gel Extraction Kit	Thermo Scientific
Colloidal Blue Staining Kit	Life Technologies
Expand Long Template PCR System Kit	Roche
Actin Binding Protein Biochem Kit	Cytoskeleton

2.1.12. Beads

Protein G agarose	Millipore
Anti-HA agarose	Sigma Aldrich
Strep-Tactin sepharose	IBA
Glutathione sepharose 4B	GE Healthcare
Ni-NTA agarose	Qiagen

2.1.13. *Escherichia coli* strains

strain	description
DH5α	cloning strain
BL21 (DE3) pLysS	overexpression of recombinant proteins
Rosetta (DE3)	overexpression of recombinant proteins

2.1.14. Reagents for standard cell culture

DMEM (4.5 g Glucose/L-Glutamine)	Life Technologies (Gibco)
OptiMEM	Life Technologies (Gibco)
Penicillin/Streptomycin (10 u/µl each)	Life Technologies (Gibco)
Trypsin/EDTA (200 mg/l)	Life Technologies (Gibco)
TrypLE	Life Technologies (Gibco)
Fetal calf serum (FCS)	Life Technologies (Gibco)

2.1.15. Reagents for SILAC cell culture

DMEM (without L-lysine and L-arginine)	Silantes
Penicillin/Streptomycin (10 u/µl each)	Life Technologies (Gibco)
TrypLE	Life Technologies (Gibco)
Stem Cell Screened Dialyzed FCS	Thermo Scientific (Pierce)
L-glutamine solution (200 mM)	Silantes
$^{13}C_6$ labelled L-lysine (Lys-6)	Silantes
$^{13}C_6$ $^{15}N_4$ labelled L-arginine (Arg-10)	Silantes
L-lysine	Sigma Aldrich
L-arginine	Sigma Aldrich
L-proline	Sigma Aldrich

2.1.16. Cell culture medium & cell lines

standard cell culture medium	500 ml DMEM
	50 ml FCS
	5 ml Penicillin/Streptomycin solution

"light" SILAC medium	500 ml DMEM (without L-lysine/L-arginine)
	50 ml dialyzed FCS
	5 ml Penicillin/Streptomycin solution
	5 ml L-glutamine solution (200 mM)
	100 mg L-lysine (per bottle)
	50 mg L-arginine (per bottle)
	115 mg L-proline (per bottle)

"heavy" SILAC medium	500 ml DMEM (without L-lysine/L-arginine)
	50 ml dialyzed FCS
	5 ml Penicillin/Streptomycin solution
	5 ml L-glutamine solution (200 mM)
	100 mg $^{13}C_6$ L-lysine (per bottle)
	50 mg $^{13}C_6$ $^{15}N_4$ L-arginine (per bottle)
	115 mg L-proline (per bottle)

cell lines	culture condtions & descritption
HeLa Flp-In T-REx / HSS-GAS2L3 RNAi resistant	standard cell culture medium tetracycline inducible expression of HSS-GAS2L3; maternal cell line was a gift from Dr. Stephen Taylor; established by Dr. Stefanie Hauser
HeLa Flp-In T-REx / HSS-GAS2L3	"heavy" and "light" SILAC DMEM tetracycline inducible expression of HSS-GAS2L3; maternal cell line was a gift from Dr. Stephen Taylor, used for SILAC experiments; established by Dr. Stefanie Hauser

HeLa Flp-In T-REx / shGAS2L3	standard cell culture medium tetracycline inducible expression of shRNA directed against GAS2L3 mRNA; maternal cell line was a gift from Dr. Stephen Taylor; Flp-In system was not used for creating cell line
HeLa Flp-In T-REx / eGFP-GAS2L3 RNAi resistant	standard cell culture medium tetracycline inducible expression of eGFP-GAS2L3; maternal cell line was a gift from Prof. Dr. Alexander Buchberger
HeLa Flp-In T-REx / eGFP-GAS2L3(Δ170-309) RNAi resistant	standard cell culture medium tetracycline inducible expression of eGFP-GAS2L3(Δ170-309); maternal cell line was a gift from Prof. Dr. Alexander Buchberger
Platinum-E	standard cell culture medium retrovirus packaging cell line based on HEK 293T cell line
primary Gas2l3$^{fl/fl}$ CreER^{T2} MEFs	standard cell culture medium tamoxifen inducible knockout of Gas2l3 in primary MEFs
Large T immortalized Gas2l3$^{fl/fl}$ CreER^{T2} MEFs	standard cell culture medium tamoxifen inducible knockout of Gas2l3 in large T immortalized MEFs
HEK 293	standard cell culture medium human embryonic kidney cell line; used for transient overexpression experiments

2.1.17. Mouse strains

strain	description
FLPe	mice express Flp recombinase constitutively under control of human ACTB promoter; used for deletion of insertion cassettes between FRT sites (Rodríguez et al., 2000); strain: B6.SJL-Tg(ACTFLPe)9205Dym/J
Zp3cre	mice express Cre recombinase under control of Zp3 promoter; used for germline deletion of floxed alleles (de Vries et al., 2000); strain: B6.Tg(Zp3-cre)93Knw/J
CreER^{T2}	mice express Cre recombinase after tamoxifen induction; used for conditional deletion of floxed alleles (Hameyer et al., 2007); strain: B6.Gt(ROSA)26Sor$^{tm2(cre/ERT2)Brn}$
Gas2l3 ta	mice carrying one targeted Gas2l3 allele including insertion cassette; strain: B6.129-Gas2l3$^{tm1a(EUCOMM)Hmgu}$
Gas2l3 fl	mice carrying floxed Gas2l3 alleles; strain was created by crossing 'Gas2l3 ta' with 'FLPe' strain; strain: B6.129-Gas2l3^{fl}; CreER^{T2}
Gas2l3 fl CreER^{T2}	conditional Gas2l3 knockout mouse strain; Gas2l3 is knocked out after tamoxifen administration; strain was created by crossing 'Gas2l3 fl' with 'CreER^{T2}' strain; strain: B6.129-Gas2l3^{fl}; CreER^{T2}
Gas2l3 Δfl	non-conditional Gas2l3 knockout strain; mice lack functional Gas2l3; strain was created by crossing 'Gas2l3 fl' with 'Zp3cre' strain; strain: B6.129-Gas2l3^{Δfl}

2.2. Methods

2.2.1. Cell biological methods

2.2.1.1. Passaging of cells

All mammalian cells were cultivated in a standard tissue culture incubator at 37 °C with 5% carbon dioxide (CO_2) and 95% air. For passaging, old medium was discarded, cells were washed once with PBS and subsequently incubated for a few minutes in TrypLE Express or Trypsin/EDTA solution at 37 °C. The detached cells were resuspendend in fresh medium and plated into new cell culture dishes in the desired ratio.

2.2.1.2. Freezing and thawing of cells

For freezing, old medium was discarded, cells were washed once with PBS and subsequently incubated for a few minutes in Trypsin/EDTA solution at 37 °C. The detached cells were resuspendend in fresh medium, transferred to a 15 ml tube and centrifuged for 3 min at 180 g (1200 rpm). The cell pellet was resuspended in 1 ml freezing medium and transferred to precooled cryotubes. The cryotubes were stored for short term at -80 °C and for long term in liquid nitrogen.

For thawing, cryotubes were put into a 37 °C water bath for 1 min. The defrosted cell suspension was transferred into a 15 ml tube containing 9 ml fresh medium and centrifuged for 3 min at 180 g (1200 rpm). The cell pellet was resuspended in 10 ml fresh medium and plated into a new cell culture dish.

2.2.1.3. Counting of cells

For cell counting a Neubauer chamber was used. The cells were thoroughly trypsinized, resuspended in fresh medium and number of cells in suspension per 1 ml was calculated by using the following formula:

Cells / 1 ml = (Cells counted per 64 squares / 40) * 10^5

2.2.1.4. Transient transfection

For transient transfection of mammalian cells two different methods were used. Calcium phosphate transfection was performed by mixing 5 to 10 µg of plasmid DNA with 50 µl of 2.5 M $CaCl_2$. The mixture was brought to a final volume of 500 µl with autoclaved H_2O and added dropwise to 500 µl of 2 x HBS solution which was continuously bubbled. The mixture was incubated for 15 min at room temperature and subsequently added dropwise to the cells. Care was taken that the precipitated DNA was evenly distributed among the cell culture dish. After overnight incubation old medium was discarded, cells were washed with PBS and

fresh medium was added. 48 hours after transfection cells were harvested and further processed.

Lipofection of cells with plasmid DNA or siRNA was carried out by using Lipofectamine 2000 or Lipofectamine RNAiMAX according to the manufacturer's instructions. In general, 1 µg plasmid DNA and 2 µl of Lipofectamine 2000 or 1.5 µl siRNA stock solution and 2 µl of Lipofectamine 2000 or RNAiMAX were used per well of a 6 well plate.

2.2.1.5. Generation of stable cell lines

For generation of a stable cell line expressing a tetracycline inducible shRNA against GAS2L3 mRNA, a HeLa cell line stably expressing the Tet-repressor protein was used (section 2.1.16). HeLa cells were plated into 6 well plates and transfected with the pSuperior.puro-shGAS2L3 plasmid. 48 hours after transfection, cells were plated into a 10 cm dish and antibiotic selection was started by adding 0.5 µg/ml puromycin. After one week of antibiotic selection, single cell clones were isolated and further kept in culture until cell number was sufficient for further experiments. To test for tetracycline inducible knockdown of GAS2L3 mRNA, cells were treated for 72 hours with 2.5 µg/ml tetracycline or were left untreated. Total RNA was prepared from cells and the expression level of GAS2L3 mRNA was analyzed by quantitative PCR. Depletion of GAS2L3 was also verified on protein level.

For generation of stable cell lines expressing tetracycline inducible RNAi resistant eGFP-GAS2L3 full length and Δ170-309 mutant protein, the FlpIn T-Rex system from LifeTechnologies was used according to manufacturer's instructions (section 2.1.16). Briefly, FlpIn T-Rex HeLa cells were plated into 6 well plates and co-transfected with pOG44 and the desired pcDNA5/FRT/To plasmids. 48 hours after transfection, cells were plated into a 10 cm dish and antibiotic selection was started by adding 400 µg/ml hygromycin and 5 µg/ml puromycin. After two weeks of antibiotic selection, single cell clones were isolated and further kept in culture until cell number was sufficient for further experiments. To test for tetracycline inducible overexpression of eGFP-GAS2L3 full length and Δ170-309 mutant, cells were treated for 48 hours with 1.5 µg/ml tetracycline or were left untreated. Next, cells were harvested, lysed, the exogenous protein was immunoprecipitated and the expression was analyzed by immunoblotting. Correct localization of eGFP- GAS2L3 full length and Δ170-309 mutant protein was verified in parallel by immunofluorescence analysis.

2.2.1.6. Reconstitution assays

HeLa cells stably expressing tetracycline inducible RNAi resistant eGFP-GAS2L3 full length and Δ170-309 mutant protein were plated onto coverslips in 6 well plates. Cells were treated with 1.5 µg/ml tetracycline for 72 hours or were left untreated. 24 hours after beginning of the treatment, cells were transfected with siRNA directed against human GAS2L3 mRNA. 48

hours after siRNA transfection, cells were fixed for immunofluorescence analysis and percentage of multinucleated cells and cells with abnormally shaped nuclei was quantified.

2.2.1.7. Generation of Mouse Embryonic Fibroblasts (MEFs)

Mouse embryonic fibroblasts (MEFs) were isolated from 14.5 dpc (days post coitus) old embryos from timed pregnancies. Single embryos were put into separate 6 cm dishes and released out of the yolk sac. The blood containing organs and head were removed and discarded and the remaining body was washed once with PBS in a fresh 10 cm dish. Next, PBS was discarded, 2 ml Trypsin/EDTA solution was added and the remaining body was chopped into fine pieces with razorblades. The chopped embryos were incubated at 37 °C for 10 min, subsequently 2 ml Trypsin/EDTA solution was added, cell suspension was pipetted up and down several times and dishes were put back to 37 °C for additional 10 min. After the second incubation, 10 ml fresh DMEM medium was added, the cell suspension was thoroughly resuspended by pipetting up and down, plated to a fresh 10 cm dish and put to the cell culture incubator for overnight incubation. Next day the supernatant containing cell debris and unattached cells was harvested and further used for genotyping of the embryos (section 2.2.2.6). The attached cells (passage 1) were washed twice with PBS, further passaged in a ratio of 1:4 (passage 2) or directly frozen.

2.2.1.8. Production of retrovirus in Plat-E cells

For production of retrovirus Plat-E cells were transiently transfected with the desired plasmid using the calcium phosphate method (section 2.2.1.4). The morning after transfection old medium was discarded, cells were washed carefully with PBS and 8 ml of fresh medium was added. 48 hours after transfection the retroviral supernatant was harvested and filtered through a 0.45 µm filter. Afterwards the supernatant was used for infection or flash frozen in liquid nitrogen and stored at -80 °C.

2.2.1.9. Infection and immortalization of MEFs

For retroviral infection of primary MEFs with SV40 large T antigen a nearly confluent 10 cm dish of MEFs was split in a 1:5 ratio. On the next day, the old medium was discarded and 4 ml of SV40 large T antigen retroviral supernatant containing 8 µg/ml polybrene was added to the dish. After 8 hours 4 ml fresh medium was added and cells were further incubated over night. Next day the retroviral medium was discarded, cells were washed with PBS and fresh medium was added. To select for the successfully immortalized large T antigen transformed cells serial passaging was used. 48 hours after infection cells were passaged in a ratio of 1:4 (high confluency dish as backup) and 1:10 (low confluency dish). After the low confluency dish became nearly confluent, the dish was passaged again in a 1:4 and 1:10 ratio. This

procedure was repeated (five times in total) until only transformed cells were left which reached confluency after a 1:10 splitting ratio in 2 to 3 days.

2.2.1.10. Induction of Cre recombinase by tamoxifen

To induce knockout of floxed alleles on genomic level, expression of Cre recombinase was induced by treating CreER^{T2} positive MEFs with 1µM 4-hydroxytamoxifen (4-OHT). After 48 hours the 4-OHT containing medium was discarded, cells were washed with PBS and fresh medium was added. Cells were processed for further experiments after 1 day recovery.

2.2.1.11. Synchronization of cells

Synchronization of cells in M phase of the cell cycle was achieved by adding 100 ng/ml nocodazole for 15 hours to the cells. Mitotic cells were harvested by mitotic shake off, washed with PBS and further processed. Synchronization of cells in G1 phase was achieved by adding 2.5 mM thymidine for 24 hours. Cells were directly used for further experiments or washed with PBS 3 times and released into fresh medium for 8 hours to achieve synchronization in G2 phase of the cell cycle.

2.2.1.12. Pharmacological inhibition of the CPC

Cells were pretreated with different concentrations of AZD1152 ranging from 0.5 to 5 nM for 9 hours before 100 ng/ml nocodazole was added for additional 15 hours. Afterwards cells were harvested with mitotic shake off and lysed with TNN lysis buffer. Cell extracts were resuspended in SDS protein sample buffer, boiled for 5 min, separated on a SDS-PAGE gel and blotted. Expression level of different proteins was analyzed via immunoblotting.

2.2.1.13. Determination of CPC activity

HeLa cells expressing a tetracycline inducible shGAS2L3 were either treated with tetracycline (2.5 µg/ml) or were left untreated for 72 hours. Nocodazole was added for 15 hours, the cells were harvested with mitotic shake off and lysed with TNN lysis buffer. Cell extracts were resuspended in SDS protein sample buffer, boiled for 5 min, separated on a SDS-PAGE gel and blotted. Expression or phosphorylation level of different proteins was analyzed via immunoblotting and quantified using ImageJ.

2.2.1.14. Immunofluorescence

Cells were plated onto glass coverslips in 6 well plates 2 to 3 days before fixation. For methanol fixation, cells were rinsed with PBS and ice cold methanol was added. Fixation took place for 4 min at -20 °C. For PFA fixation, cells were rinsed with PBS and incubated for 10 min at room temperature with PFA fixative. PFA-fixed cells were permeabilized for 10 min with 0.5% Triton X-100 in PBS. After fixation, cells were rinsed several times with PBS and subsequently incubated for 30 min in blocking solution. Fixed cells were incubated with the

desired primary antibody diluted in PBS for 1 hour in a dark humid chamber. The coverslips were washed gently for 3 times, 5 min each with PBS and incubated in a dark humid chamber with the appropriate secondary antibody diluted in PBS for 30 min. Nuclei were stained by treating the fixed cells with Hoechst 33258 (bisbenzimide) dissolved in PBS (10 µg/ml) for 2 min. Afterwards the coverslips were washed again for 3 times, 5 min each and finally mounted onto standard glass slides for microscopy.

2.2.2. Molecular biological methods

2.2.2.1. RNA extraction

Total RNA was extracted from cultured cells and mouse tissue by using Trifast reagent. For cultured cells, medium was aspirated and 1 ml Trifast reagent was added. After an incubation time of 3 min, Trifast reagent was pipetted to a 1.5 ml tube, 500 µl chloroform was added and the mixture was vortexed thoroughly for 20 sec. Afterwards the sample was centrifuged for 10 min at 13200 g, the clear upper phase containing the RNA was pipetted to a fresh 1.5 ml tube and 1 ml of isopropanol was added to precipitate the RNA. The sample was incubated for 10 min at room temperature, centrifuged for 5 min at 13200 g, the aqueous supernatant was discarded and the RNA pellet was washed with RNase free 75% ethanol. The sample was centrifuged again for 5 min at 13200 g, the ethanol was discarded and the remaining RNA pellet was dried for 5 min. Afterwards the pellet was resuspended in 25 µl RNase free water. For RNA extraction from mouse tissue, 100 mg of tissue was put into a 2 ml tube and flash frozen in liquid nitrogen. Afterwards the tissue piece was put into a glass dounce homogenizer together with 1 ml Trifast reagent. The tissue was mechanically disrupted until the sample was homogenous. Afterwards the homogenate was pipetted to a fresh 2 ml tube, 500 µl chloroform was added and the mixture was vortexed thoroughly for 20 sec. The sample was centrifuged for 10 min at 13200 g, the clear upper phase containing the RNA was pipetted to a fresh 1.5 ml tube and 1 ml of isopropanol was added to precipitate the RNA. The sample was incubated for 10 min at room temperature, centrifuged for 5 min at 13200 g, the aqueous supernatant was discarded and the RNA pellet was washed with RNase free 75% ethanol. The sample was centrifuged again for 5 min at 13200 g, the ethanol was discarded and the remaining RNA pellet was dried for 5 min. Afterwards the pellet was resuspended in 50 µl RNase free water and the RNA was stored at -80 °C.

2.2.2.2. Reverse transcription

For reverse transcription, between 1 and 2.5 µg RNA was mixed with 0.5 µl of random hexamer primers (0.5 µg/µl) and brought to a final volume of 10 µl with RNase free water. The mixture was incubated at 70 °C for 5 min and afterwards cooled down to 4 °C. To the sample 6.25 µl dNTPs (2mM), 0.5 µl Ribolock RNase inhibitor (40 U/µl), 0.5 µl RevertAid

reverse transcriptase (200 U/µl), 5 µl 5 x RevertAid reaction buffer and 2.75 µl RNase free water were added. For cDNA synthesis the mixture was incubated for 1 hour at 42 °C and then inactivated for 15 min at 70 °C.

2.2.2.3. Quantitative PCR

Amounts of specific mRNAs compared to a housekeeping gene were determined by using quantitative real-time PCR. Samples were set up by combining 12.5 µl 2 fold concentrated Absolute QPCR SYBR Green Mix, 10.5 µl DNase free water, 0.5 µl forward primer (10 pmol/µl), 0.5 µl reverse primer (10 pmol/µl) and 1 µl cDNA. Quantitative PCR was performed using the following program:

95 °C	15 min	
95 °C	15 sec	40
60 °C	60 sec	cycles

Relative expression of a specific mRNA compared to a housekeeping gene was calculated by using the following formula:

$$2^{-\Delta\Delta Ct}$$

$$\Delta Ct = Ct\ (gene\ of\ interest) - Ct\ (housekeeping\ gene)$$

$$\Delta\Delta Ct = \Delta Ct\ (sample) - \Delta Ct\ (reference)$$

The standard deviation of ΔΔCt was calculated by using:

$$s = \overline{s_1^2 + s_2^2}$$

s_1 = standard deviation of gene of interest

s_2 = standard deviation of housekeeping gene

The margin of error for $2^{-\Delta\Delta Ct}$ was calculated by using:

$$2^{-\Delta\Delta Ct \pm s}$$

The error used for the error bars was calculated by using:

$$2^{-\Delta\Delta Ct \pm s} - 2^{-\Delta\Delta Ct}$$

2.2.2.4. Small scale preparation of plasmid DNA from bacteria

After transformation of chemically competent *E. coli* cells, single bacterial clones were picked from a LB agar plate and incubated in 3 ml liquid LB medium containing appropriate antibiotics overnight at 37 °C at 160 rpm on a platform shaker. For small scale preparation of plasmid DNA (minipreparation) 1.5 ml of overnight culture was pipetted to a 1.5 ml tube and centrifuged for 3 min at 13200 *g*. The supernatant was discarded and the cell pellet was resuspended in 150 µl S1 buffer supplemented with 0.6 µl RNase A (10 µg/µl). For cell lysis, 150 µl S2 buffer was added and the mixture was incubated for 5 min at room temperature. To precipitate the genomic DNA and proteins, 150 µl S3 buffer was added and the sample was centrifuged at 13200 *g* for 10 min. 400 µl of the cleared supernatant was pipetted to a fresh 1.5 ml tube and 1 ml isopropanol was added to precipitate the plasmid DNA. The sample was incubated for 5 min at room temperature and centrifuged for 10 min at 13200 *g*. The supernatant was discarded and the DNA pellet was washed with 1 ml 70% ethanol. The sample was centrifuged again for 5 min at 13200 *g*, the supernatant was discarded, the plasmid DNA pellet was air dried for 5 min and finally resuspended in 50 µl 10 mM Tris/HCl (pH 8.5). To identify clones harboring the correct plasmid, the prepared plasmid DNA was digested with appropriate restriction endonucleases and analyzed by agarose gel electrophoreses. Plasmid DNA of positive clones was stored at -20 °C.

2.2.2.5. Large scale preparation of plasmid DNA from bacteria

For large scale preparation of plasmid DNA (midi- / maxipreparation) a single bacterial clone was picked from a LB agar plate and incubated in 3 ml liquid LB medium containing appropriate antibiotics for 5 to 6 hours at 37 °C at 160 rpm on a platform shaker. The culture was transferred to 100 ml liquid LB medium containing appropriate antibiotics and incubated overnight at 37 °C at 160 rpm on a platform shaker. After over night incubation the culture was transferred to 50 ml tubes and cells were harvested by centrifugation at 4300 *g* for 10 min. For plasmid DNA preparation the PureLink HiPure Plasmid Midi-/Maxiprep Kit from Life technologies was used according to manufacturer's instructions. The prepared plasmid DNA was set up to a concentration of 1 µg/µl and stored at -20 °C.

2.2.2.6. Extraction of genomic DNA from tissue/cells and genotyping via PCR

For genomic DNA extraction, 75 µl tail buffer I was added to a 1.5 ml tube containing a mouse tail, tissue piece or cell pellet. The tube was boiled at 95 °C for 30 min and afterwards put on ice for 10 min. 75 µl tail buffer II was added and the tube was vortexed briefly. For genotyping, 2 µl supernatant, 2.5 µl dNTPs (2 mM), 2.5 µl 10 fold concentrated ReproFast buffer, 1 µl forward primer (10 µM), 1 µl reverse primer (10 µM), 0.3 µl His-Taq polymerase

(15 U/µl) and 15.7 µl DNase free water were mixed. PCR was performed according to following program:

95 °C	3 min	
95 °C	30 sec	30 cycles
54 – 58 °C	30 sec	
72 °C	60 sec	
72 °C	5 min	

2.2.2.7. Extraction of DNA fragments from agarose gels

The DNA fragments were loaded onto an agarose gel (0.8% to 1.2%) containing ethidiumbromide (0.35 µg/ml) and separated by electrophoresis between 1 and 2 hours at 100 V. The agarose gel was put onto a UV transilluminator and the desired DNA fragments were cut out with a clean scalpel. The DNA was extracted from the agarose gel by using the Jetstar gel extraction kit from Genomed or the GeneJET gel extraction kit from ThermoScientific according to manufacturer's instructions.

2.2.2.8. Purification of PCR fragments via column purification

PCR fragments were purified by using the QIAquick PCR Purification Kit from QIAgen according to manufacturer's instructions.

2.2.2.9. Determination of nucleic acid concentration

Concentration of nucleic acids was determined by using a NanoDrop 2000c spectral photometer from Peqlab according to manufacturer's instructions.

2.2.2.10. Agarose gel electrophoresis

DNA fragments were separated by size using agarose gel electrophoresis. Agarose gels were prepared by adding the desired amount of agarose powder to an appropriate volume of one fold concentrated TAE buffer. The mixture was boiled in a microwave oven until the agarose completely dissolved and ethidiumbromide was added to a final concentration of 0.35 µg/ml. DNA samples were prepared by adding an appropriate amount of 5 fold DNA loading buffer to the DNA samples. 1 kb or 100 bp DNA ladder from Thermo Scientific was used as size marker. Electrophoresis was performed between 1 and 2 hours at 100 V in a standard electrophoresis chamber. DNA bands were visualized by using a UV transilluminator and photographed or excised.

2.2.2.11. Restriction of DNA with restriction endonucleases

For restriction, DNA (plasmid DNA or PCR fragments) was mixed with the desired restriction endonuclease and the recommended buffer and incubated for 1 to 3 hours at 37 °C. As a standard reaction, 5 to 10 units of the desired restriction endonuclease were added to 0.5 to 3 µg DNA and 5 µl of 10 fold concentrated buffer. The mixture was filled up to a final volume of 50 µl with DNase free water and incubated for 3 hours at 37°C. The digested DNA was purified by gel extraction or column purification.

2.2.2.12. Standard cloning procedure

For molecular cloning the vector and insert DNA was digested with appropriate restriction endonucleases and afterwards purified by gel extraction or column purification. DNA concentration was determined and ligation reaction was set up. As standard reaction, 1 µl T4 DNA ligase, 2 µl 10 fold concentrated T4 DNA ligase buffer, 5 ng vector DNA and 50 to 100 ng insert DNA were mixed and brought to a final volume of 20 µl with DNase free water. The reaction was incubated for 30 min at room temperature and afterwards directly used for transformation of chemically competent DH5α *E. coli* cells. After transformation single bacterial clones were picked, plasmid DNA was prepared and analyzed via control restriction.

2.2.2.13. Proofreading PCR using Pfu polymerase

For standard proofreading PCR, 5 µl dNTPs (2 mM), 5 µl 10 fold concentrated Pfu buffer with MgSO$_4$, 2.5 µl forward primer (10 µM), 2.5 µl reverse primer (10 µM), 0.5 µl Pfu polymerase (2.5 U/µl) and 150 to 200 ng template DNA were mixed and filled up with DNase free water to a final volume of 50 µl. PCR was performed according to following program:

95 °C	3 min	
95 °C	30 sec	35 cycles
T$_M$ – 5 °C	30 sec	
72 °C	2 min / kb	
72 °C	10 min	

When cDNA was used as template for proofreading PCR, the following slightly modified program was used:

95 °C	3 min	
95 °C	30 sec	3 cycles
T_M + 2 °C	30 sec	
72 °C	2 min / kb	
95 °C	30 sec	3 cycles
T_M	30 sec	
72 °C	2 min / kb	
95 °C	30 sec	3 cycles
T_M - 2 °C	30 sec	
72 °C	2 min / kb	
95 °C	30 sec	6 cycles
T_M - 4 °C	30 sec	
72 °C	2 min / kb	
95 °C	30 sec	20 cycles
T_M - 5 °C	30 sec	
72 °C	2 min / kb	
72 °C	15 min	

2.2.2.14. Long range PCR

Long range PCR was performed by using the Expand Long Template PCR System from Roche according to manufacturer's instructions.

2.2.3. Biochemical methods

2.2.3.1. Whole cell lysates

For whole cell lysates old medium was discarded and cells were washed once with PBS. The dish was put on ice, 10 ml cold PBS was added and the cells were scraped from the dish with a plastic cell scraper. The cell suspension was transferred to a 15 ml tube and centrifuged for 3 min at 300 *g* at 4 °C. The supernatant was aspirated, the cell pellet was resuspended in an appropriate volume of freshly prepared TNN lysis buffer and transferred to a 1.5 ml tube. After incubation for 45 min on ice, the tube was centrifuged at 20000 *g* for 15 min at 4 °C to precipitate the cell debris. The cleared supernatant was transferred to a fresh 1.5 ml tube and protein concentration was determined. The whole cell lysate was either used directly for further assays or mixed with 3 fold concentrated protein sample buffer, boiled for 5 min at 95 °C and stored at -20 °C.

2.2.3.2. Determination of protein concentration

Protein concentration was determined by using the Bradford method (Bradford, 1976). In brief, 2 µl whole cell lysate was mixed with 1 ml Bradford solution and extinction was measured at a wave length of 595 nm. As reference, a BSA dilution series of known protein concentration was used.

2.2.3.3. Immunoprecipitation

For immunoprecipitation, the desired antibody was added in a ratio of 1:10 to 1:200 to a fresh prepared whole cell lysate containing between 250 µg to 10 mg total protein. The mixture was rotated for 2 to 3 hours at 4 °C before protein G beads were added for 1 hour. Beads were harvested by centrifugation at 1200 *g* for 1 min and the supernatant was discarded. Beads were washed 6 times with 1 ml cold TNN lysis buffer. After washing, supernatant was completely aspirated, beads were resuspended in 3 fold concentrated protein sample buffer, boiled for 5 min at 95 °C and stored at -20 °C.

2.2.3.4. Stable isotope labelling by amino acids in cell culture (SILAC)

For SILAC experiments HeLa cells stably expressing tetracycline inducible HA-/Strep-/Strep-tagged (HSS-) GAS2L3 were grown in "heavy" or "light" SILAC medium. After a sufficient incorporation of labelled amino acids was achieved (about 5 passages), cells were plated to 15 cm dishes and further cultivated in "heavy" or "light" medium until cell number was sufficient for further experiments. Cells growing in "heavy" medium were treated with 1.5 µg/ml tetracycline for 48 hours before start of the experiment to induce expression of HSS-GAS2L3. To trap the cells into mitosis, nocodazole (100 ng/ml) was added for 15 hours. Cells were harvested with mitotic shake off and thoroughly washed with PBS. One third of the cells was snap frozen in liquid nitrogen and stored at -80 °C, the other two thirds were separated into two parts and released into fresh medium for 30 min and 1 hour. After release cells were harvested, washed with PBS, snap frozen in liquid nitrogen and stored at -80 °C. The three different time points were chosen to identify interacting proteins of GAS2L3 in early stage (no release from nocodazole), mid stage (30 min release from nocodazole) and late stage of mitosis (60 min release from nocodazole).

2.2.3.5. Tandem affinity purification of HA-/Strep-/Strep-tagged proteins

Tandem affinity purification was performed according to the protocol described by Wyler and colleagues (Wyler et al., 2011). Cell pellets were lysed in an appropriate volume of TAP cell lysis buffer. The whole cell lysates were cleared by centrifugation at 20000 *g* for 15 min at 4 °C and protein concentration was determined with the Bradford method. Strep-Tactin sepharose beads were added and samples were incubated for 30 min at 4 °C on a rotator. Beads were harvested by centrifugation at 1200 *g* for 1 min and washed 3 times with TAP

cell lysis buffer. Bound proteins were eluted 3 consecutive times with TAP cell lysis buffer supplemented with 2.5 mM desthiobiotine. The single eluates were pooled and HA beads were added. The samples were incubated for 1 hour at 4 °C on a rotator, before the beads were harvested by centrifugation at 1200 *g* for 1 min. Beads were washed 2 times with TAP cell lysis buffer and once with 10 mM Tris/HCl supplemented with 2 mM MgCl$_2$. Proteins were eluted from the beads with SDS protein sample buffer without DTT. The finale eluates were cleared by centrifugation through a Mobicol spin filter column, and DTT was added to a final concentration of 30 mM. The samples were concentrated by using Amicon spin columns, the corresponding "heavy" and "light" samples were mixed in equal ratios and separated by Nupage Bis-Tris gel electrophoresis. The protein bands were stained with colloidal coomassie and the gel was sent to the Max-Planck-Institute for Biophysical Chemistry, Göttingen for further mass spectrometrical analysis.

2.2.3.6. Sodium dodecyl sulfate polyacrylamide gel electrophoresis

For standard SDS-PAGE, the MiniProtean III system from Biorad in combination with the discontinuous method described by Laemmli (Laemmli, 1970) was used. First a separating gel of the desired concentration (8 to 15%) was prepared. After polymerization of the separating gel, a stacking gel (5%) was poured on top. For preparation of a 1.5 mm gel the following recipe was used:

separating gel	8%	10%	12.5%	15%
H$_2$O ultrapure [µl]	3894	3344	2656	1969
separating gel buffer [µl]	2035	2035	2035	2035
20% SDS [µl]	60.5	60.5	60.5	60.5
10% APS [µl]	55	55	55	55
30% acrylamide [µl]	2200	2750	3438	4125
TEMED [µl]	5.5	5.5	5.5	5.5

stacking gel	5%
H$_2$O ultrapure [µl]	990
bromophenol blue [µl]	60
stacking gel buffer [µl]	1000
20% SDS [µl]	60
10% APS [µl]	40
30% acrylamide [µl]	500
TEMED [µl]	4

Gels were run at 70 V unless protein samples migrated through the stacking gel. Afterwards voltage was increased to 150 V for approximately 1 hour for separation of the protein sample.

2.2.3.7. Nupage Bis-tris gel electrophoresis

For mass spectrometrical analysis, proteins were separated by using precast 4-12% gradient Bis-Tris gels together with the Novex Nupage SDS PAGE Gel System from Life Technologies according to manufacturer's instructions.

2.2.3.8. Coomassie blue staining of polyacrylamide gels

After SDS-PAGE, the polyacrylamide gel was rinsed briefly with ultrapure H_2O and placed in Coomassie blue staining solution for 1 hour at room temperature under constant shaking. Afterwards, gel was rinsed a couple of times with ultrapure H_2O to wash away excess Coomassie blue stain and placed into Coomassie destaining solution for 1 to 2 days. To accelerate destaining process the acetic acid solution was changed regularly.

For coomassie staining of Nupage Bis-Tris gels colloidal coomassie staining solution from Life Technologies was used according to manufacturer's instructions.

2.2.3.9. Immunoblotting

Protein transfer from polyacrylamide gels to PVDF membranes was performed by using the Mini Trans-Blot wet transfer apparatus from BioRad. In brief, the PVDF membrane was incubated for a few minutes in pure methanol while the sponges, whatman papers and the polyacrylamide gel were soaked in cold blotting buffer. Next, the blotting stack was assembled by placing (from bottom to top) wet sponge, wet whatman paper, polyacrylamide gel, PVDF membrane, wet whatman paper and wet sponge together into the blotting chamber. The chamber was filled with a cooling device and blotting buffer. Transfer was performed at 350 mA for 90 min. After blotting, the successful transfer of proteins to the membrane was controlled by staining the membrane with Ponceau S solution. For detection of proteins by immunoblotting, the membrane was blocked for 1 to 2 hours in blocking solution and afterwards incubated over night at 4 °C with the desired primary antibody. Next day, membrane was washed 3 times, 10 min each with TBS-T and incubated with the appropriate secondary antibody for 3 to 4 hours. The membrane was washed again 3 times, 10 min each with TBS-T and incubated for 1 min in chemiluminescence solution before it was wrapped in plastic foil and exposed to X-ray film.

2.2.3.10. Transformation of chemically competent bacteria

E. coli cells pre-aliquoted in a 1.5 ml tube were thawed on ice for 10 min. After thawing, 250 ng plasmid DNA or 5 µl ligation reaction was added to the cells and the tube was put back on

ice for 30 min. Cells were heat shocked for 50 sec at 42 °C and put back on ice for 2 min, before 500 µl liquid LB medium without antibiotics but supplemented with 2% glucose was added to the tube. The sample was incubated for 1 hour at 37 °C while shaking at 700 rpm on an Eppendorf thermo mixer. After incubation, the tube was centrifuged for 1 min at 13200 *g*, the supernatant was discarded and the cell pellet was resuspended in 100 µl LB medium. The bacterial suspension was pipetted onto a LB agar plate containing the appropriate antibiotic, plated with a Drigalski spatula and incubated at 37 °C for at least 16 hours.

2.2.3.11. Preparation of glycerol stocks from bacteria

Glycerol stocks were prepared by pipetting 330 µl of a fresh bacterial culture into a 1.5 ml tube and adding 670 µl glycerol stock buffer. The tube was vortexed briefly, flash frozen in liquid nitrogen and stored at -80 °C.

2.2.3.12. Overexpression of recombinant proteins in bacteria

After transformation of chemically competent BL21 (DE3) or Rosetta (DE3) cells with the desired plasmid, 10 ml SB medium, containing appropriate antibiotics, was pipetted onto the LB agar plate and the cell clones were thoroughly resuspended by detaching them with a glass pipette. Cell suspension was transferred to a baffled 2 l flask containing 500 ml SB medium supplemented with appropriate antibiotics and incubated at 37 °C on a platform shaker at 140 rpm. 1 to 2 hours later the optical density of the culture was determined by measuring the extinction at a wave length of 600 nm using a photometer. When the culture reached an optical density of 0.2 the temperature of the platform shaker was lowered to 27 °C. The extinction of the culture at 600 nm was determined every hour and the temperature was further lowered to 15 °C at an optical density of 0.5 to 0.6. After the culture reached an extinction value between 0.8 and 1.0, 5 ml of the culture was transferred to a 15 ml tube for later use as pre-induction sample and the expression of recombinant protein was induced by adding 1 mM IPTG to the culture. After overnight incubation at 15 °C, 5 ml of the culture was transferred to a 15 ml tube for later use as post-induction sample and the rest of the cells were harvested by centrifugation at 4000 *g*. Supernatant was discarded, cells were washed once with PBS, cell pellet was snap frozen in liquid nitrogen and stored at -80 °C. Pre- and post-induction samples were prepared by resuspending an equal amount of bacterial cells in 3 fold concentrated protein sample buffer. Samples were separated by SDS-PAGE, the gel was stained with Coomassie Blue and successful overexpression was verified by presence of an additional protein band of the right kilodalton size in the post-induction sample.

2.2.3.13. Purification of recombinant GST fusion proteins from bacteria

For purification, frozen cell pellet was thawed on ice for 20 min. Cell pellet was thoroughly resuspended in 20 ml GST lysis buffer and cells were lysed by using a Branson sonifier (65%

amplitude / 10 sec burst / 60 sec pause / 3 to 4 repeats). The bacterial whole cell lysate was transferred to a Corex glass tube and cleared by centrifugation at 13000 *g* for 30 min. Glutathione sepharose beads were added to the cleared supernatant and the mixture was incubated for 3 to 4 hours at 4 °C on the rotator. Afterwards, beads were harvested by centrifugation at 1200 *g* for 3 min and washed for 6 times with 40 ml GST wash buffer. Beads with bound GST proteins were either directly used or bound proteins were eluted from the beads with GST elution buffer and, if needed, dialyzed against PBS or BRB80 buffer overnight for further assays. A fraction of the dialyzed proteins was separated by SDS-PAGE and successful purification was verified by Coomassie Blue staining. To determine the concentration of the purified proteins, a BSA dilution series of known protein concentration was analyzed in parallel on the same SDS-PAGE gel.

2.2.3.14. Actin co-sedimentation assay

F-actin co-sedimentation assay was performed using the Actin Binding Protein Biochem Kit from Cytoskeleton. Actin was polymerized at room temperature for 1 hour and diluted to 5 µM according to the manufacturer's protocol. For co-sedimentation assays, 40 µl F-actin was mixed with 1 µM GST–GAS2L3 full length, deletion mutants or GST protein and incubated for 30 min at room temperature. Mixtures were pelleted by centrifugation at 120000 *g* for 60 min at 24 °C. Supernatant and pellet fractions were recovered and separated by SDS-PAGE. Gels were stained with Coomassie Blue.

2.2.3.15. Microtubule co-sedimentation assay

Monomeric tubulin was a kind gift of Prof. Dr. Oliver Gruss, University of Heidelberg. Tubulin was polymerized at 37 °C for 30 min by addition of 0.5 volumes of glycerol and 1 mM GTP. The polymerized tubulin was diluted to 10 µM with BRB80 buffer supplemented with 20 µM taxol. For co-sedimentation assays, 20 µl of polymerized tubulin was mixed with 1 µM GST–GAS2L3 full length, deletion mutants or GST protein and incubated for 15 min at room temperature. Mixtures were pelleted by centrifugation at 30000 *g* for 30 min at 30°C over a 30% glycerol cushion. Supernatant and pellet fractions were recovered and separated by SDS-PAGE. Gels were stained with Coomassie Blue.

2.2.3.16. Microtubule-F-actin crosslinking assay

The microtubule-F-actin crosslinking assay was performed as described by Miller and colleagues (Miller et al., 2004). Briefly, 1 µM GST–GAS2L3 full length, N-terminus (aa1-310) or C-terminus (aa303-694) was added to 5 µM polymerized tubulin in BRB80 buffer supplemented with 20 µM taxol and incubated for 15 min at room temperature. After addition of 5 µM F-actin, the mixture was incubated for additional 15 min at room temperature and

centrifuged at 5000 *g* for 10 min at 24 °C. Supernatant and pellet fractions were recovered, separated by SDS-PAGE and stained with Coomassie Blue.

2.2.3.17. Microtubule bundling assay

5 µM unlabelled tubulin was mixed with 0.4 µM Cy5-labelled tubulin in BRB80 buffer. The tubulin mixture was polymerized by addition of 20 µM taxol and 1mM GTP for 30 min at 37 °C. After addition of 500 nM GST–GAS2L3 full length, C-terminus (aa303-694) or GST, the mixtures were incubated for additional 30 min at 37 °C. 1.5 µl aliquots were pipetted onto slides, covered with 1.5 µl BRB80 fixing solution and analyzed by fluorescence microscopy.

2.2.3.18. GST pulldown assay

HeLa whole cell lysates containing 250 to 500 µg total protein were incubated with approximately 5 µg immobilized GST fusion proteins over night at 4 °C on a rotator. The next day, beads were harvested by centrifugation at 1200 *g* for 1 min and washed 6 times with 1 ml TNN lysis buffer. After washing beads were resuspended in SDS protein sample buffer, boiled for 5 min at 95 °C, separated on a SDS-PAGE gel and blotted. Bound proteins were analyzed via immunoblotting.

2.2.3.19. His-Tag pulldown assay

His-tagged and GST fusion proteins were overexpressed (section 2.2.3.12), cells were lysed in His-tag lysis buffer by sonification and cleared lysates were prepared (section 2.2.3.13). For pulldown assays, bacterial cell lysate containing approximately 5 µg of His-tagged protein was mixed with bacterial cell lysate containing approximately 0.5 µg of GST fusion protein and incubated at 4 °C over night on a rotator. Next day, Ni-NTA beads were added to the mixture for 1 hour. Afterwards, beads were harvested by centrifugation at 1200 *g* for 1 min and washed 6 times with 1 ml His-tag wash buffer. After washing beads were resuspended in SDS protein sample buffer, boiled for 5 min at 95 °C, separated on a SDS-PAGE gel and blotted. Bound proteins were analyzed via immunoblotting.

2.2.3.20. Kinase assay

For kinase assays HeLa cells were treated for 15 hours with 100 ng/ml nocodazole, harvested with mitotic shake off and lysed with TNN lysis buffer. Endogenous Aurora B or Cyclin B1 kinases were immunoprecipitated over night at 4 °C (section 2.2.3.3). The precipitated kinases were washed three times with 1 ml TNN lysis buffer and two times with 1 ml kinase assay buffer. Afterwards 2 µg GST-GAS2L3, GST, GST-Histone H3(aa1-46) or Histone H1 (Roche) dissolved in kinase buffer supplemented with 20 µM non-radioactive ATP were added together with 10 µCi γ-P32-ATP to the immobilized kinases. The reaction mixtures were incubated for 20 min at 30 °C. The kinase reactions were stopped by addition

of SDS protein sample buffer. Samples were boiled for 5 min at 95 °C and separated on a SDS-PAGE gel. The gel was dried and exposed to X-ray film for analysis. For mass spectrometrical analysis of CDK1 phosphosites, the assay was performed without radioactively labelled ATP. The samples were separated by SDS-PAGE, protein bands were stained with colloidal coomassie staining solution and the gel was sent to the Mass Spectrometry Core Facility of the Center for Molecular Biology of the University of Heidelberg for further analysis.

2.2.3.21. Antigen affinity purification of polyclonal GAS2L3 antibody

Polyclonal GAS2L3 antibody was antigen purified according to the protocol of Dr. Erik Flemington. In brief, BL21 (DE3) cells overexpressing GST and GST-mGas2l3(aa305-683) were lysed by sonification and supernatants were cleared by centrifugation. Glutathione sepharose beads were added to the supernatants containing GST or GST-mGas2l3(aa305-683) and incubated for 1 hour at 4°C on a rotator. Beads were harvested by centrifugation at 1200 g for 3 min at 4 °C and washed 3 times with TBS supplemented with 1% NP-40. 4 ml of crude rabbit serum containing polyclonal GAS2L3 antibody was thawed and diluted with 4 ml PBS. Beads with bound GST were added to the diluted serum and incubated for 5 hours at 4 °C on a rotator, to pre-clear the serum from all antibodies which recognize and specifically bind to GST. The beads with bound GST-mGas2l3(aa305-683) were washed twice with 0.1 M borate buffer (pH 8), once with 0.1 M borate buffer (pH 9), and once with 0.2 M borate buffer (pH 9). After washing, beads were incubated with 40 mM dimethylpimelimidate dissolved in 0.2 M borate buffer (pH 9) for 1 hour at 4 °C on a rotator, to crosslink the GST-mGas2l3(aa305-683) protein to the glutathione sepharose beads. After crosslinking, beads were washed twice with 0.1 M borate buffer (pH 8) and the crosslinking reaction was finally stopped by incubating the beads with 50 mM Tris/HCl (pH 8) for 45 min at 4 °C on a rotator. Afterwards beads were washed 3 times with PBS, once with 0.2 M glycine/HCl (pH 2.5), once with 1M K_2HPO_4, again with 0.2 M glycine/HCl (pH 2.5) and 1M K_2HPO_4 and twice with PBS. The pre-cleared rabbit serum was centrifuged at 1500 g for 3 min at 4 °C to pellet the GST beads. The supernatant fraction was transferred to the cross linked GST-mGas2l3(aa305-683) beads and the pellet fraction was discarded. After over night incubation at 4 °C on a rotator, beads were washed 3 times with PBS supplemented with 0.2% Tween-20 and twice with pure PBS. The bound antibody was eluted 3 consecutive times by adding 750 µl glycine/HCl (pH 2.5) to the beads. The eluates were neutralized immediately by adding 250 µl 1M K_2HPO_4. From all eluates SDS protein samples were prepared, separated by SDS-PAGE and analyzed via Coomassie blue staining. The two eluates with highest antibody concentration were dialyzed for 2 days against PBS, mixed with sterile glycerol (1:1), aliquoted and stored at -20 °C. The specificity of the antigen purified antibody was tested in immunoblotting and immunoprecipitation experiments.

3. Results

3.1. GAS2L3 is regulated on protein level during cell cycle

Previous experiments in the laboratory have shown that GAS2L3 is regulated during the cell cycle in a DREAM-complex dependent manner (Wolter et al., 2012). So far the regulation was only shown on mRNA level. To verify that GAS2L3 is also regulated on protein level during the cell cycle, immunoprecipitation experiments from HeLa cells, synchronized in different cell cycle phases (section 2.2.1.11), were performed. Samples were separated by SDS-PAGE and analyzed via immunoblotting. GAS2L3 protein expression peaked during G2 and M phase of the cell cycle while in G1 phase and in asynchronous cells GAS2L3 was not detectable (fig 3.1a). To verify proper synchronization of cells phosphorylation of Histone H3 on Ser 10, a G2 and M phase specific marker, was analyzed in parallel by immunoblotting (fig 3.1a). To confirm identity of the protein and specificity of the used antibodies, a HeLa cell line stably expressing a tetracycline inducible shRNA against GAS2L3 mRNA was either treated with tetracycline or was left untreated. Immunoprecipitation experiments with GAS2L3 antibody were carried out and samples were separated by SDS-PAGE. GAS2L3 was readily detected by immunoblotting in the untreated sample while the amount of GAS2L3 was strongly reduced in the tetracycline treated one (fig 3.1b).
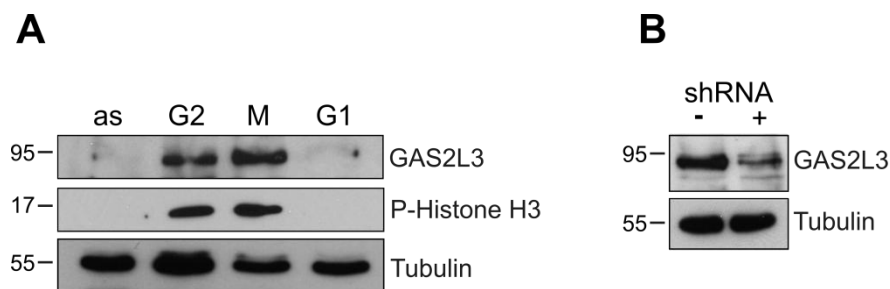
Figure 3.1: Expression of GAS2L3 is cell cycle regulated. A) Endogenous GAS2L3 was immunoprecipitated from synchronized cells. Synchronization of cells was verified by immunoblotting for phosphorylated Histone H3, a marker for G2/M phase of the cell cycle. B) Identity of the endogenous protein was confirmed by expression of a shRNA directed against GAS2L3 mRNA. as: asynchronous cells. Figure was first published in Wolter et al., 2012.

3.2. GAS2L3 is important for proper cytokinesis

It has been shown in previous experiments in the laboratory that depletion of GAS2L3 leads to defects in cytokinesis. To further confirm this observation, HeLa cells were transfected with three different siRNAs against GAS2L3. Percentage of cells with defects in cytokinesis represented either by multinucleation or by abnormally shaped (multi-lobed) nuclei was quantified (fig 3.2). HeLa cells were plated on coverslips, transfected with control or GAS2L3 siRNAs by using Lipofectamine 2000 (section 2.2.1.4) and fixed (section 2.2.1.14) (fig 3.2a).

In parallel, knockdown efficiency of all three GAS2L3 siRNAs was determined by quantitative PCR 48 hours after transfection (fig 3.2b). Percentage of multinucleated cells or cells with multi-lobed nuclei increased to almost 20% after treatment with GAS2L3 specific siRNA while only 3% of the control depleted cells showed defects in cytokinesis (fig 3.2c).
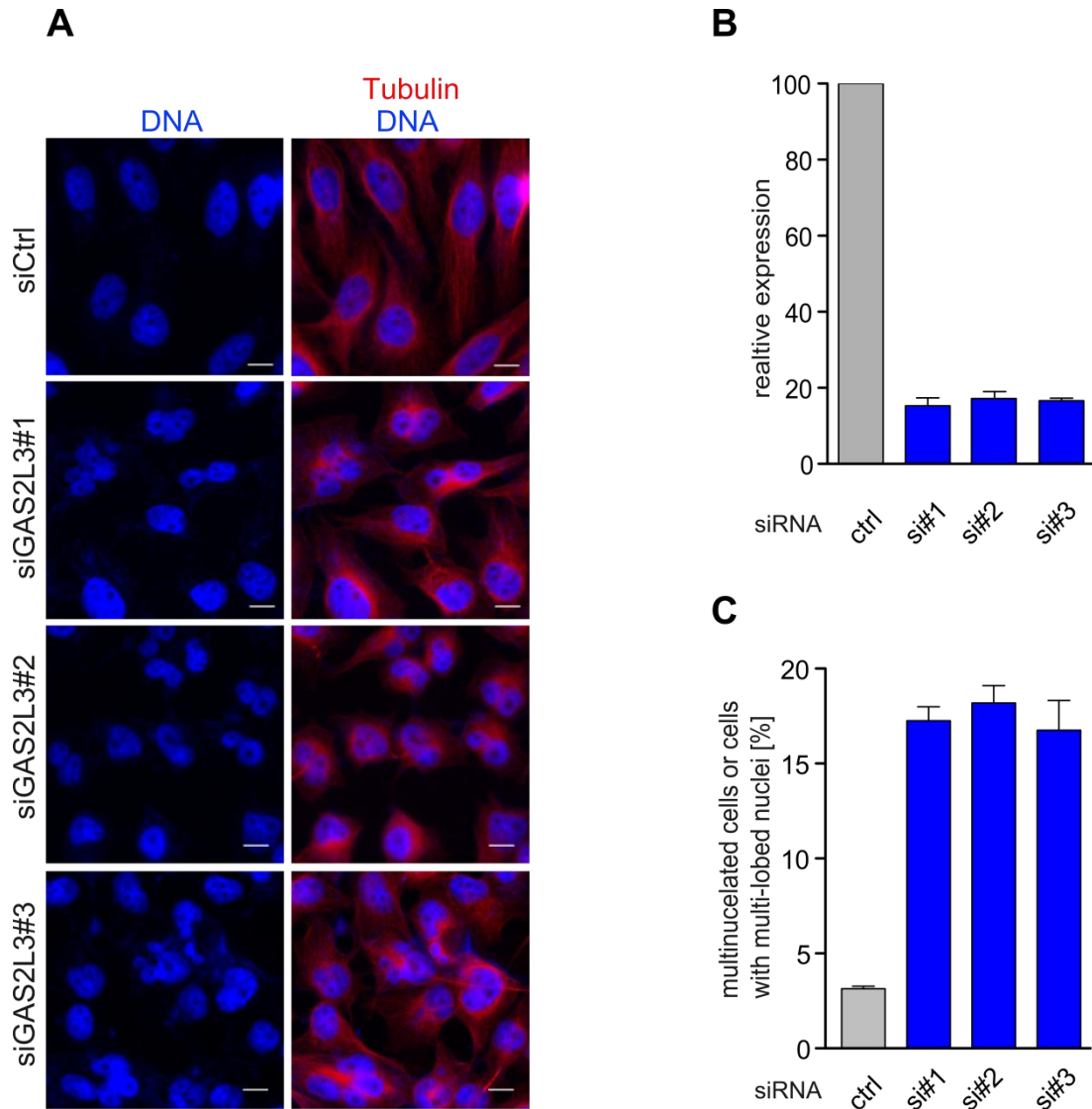
Figure 3.2: Depletion of GAS2L3 leads to defects in cytokinesis. A) GAS2L3 depleted HeLa cells show higher percentage of abnormally shaped nuclei compared to control depleted cells. Nuclei were stained with Hoechst 33258 (blue) and tubulin was counterstained (red). Scale bars: 10 µm. B) Efficient depletion of GAS2L3 by three different siRNAs was verified by qPCR. C) Percentage of multinucleated cells or cells with abnormally shaped nuclei was quantified after GAS2L3 depletion. Results are from three independent experiments. More than 300 cells per experiment were counted. Standard deviations between the three experiments are indicated. Figure was first published in Wolter et al., 2012.

3.3. GAS2L3 is a cytoskeleton associated protein

Due to the domain architecture of GAS2L3 (section 1.3.4) and the localization studies in mammalian cells (Schmitt, 2010; Wolter et al., 2012), it was likely that GAS2L3 directly
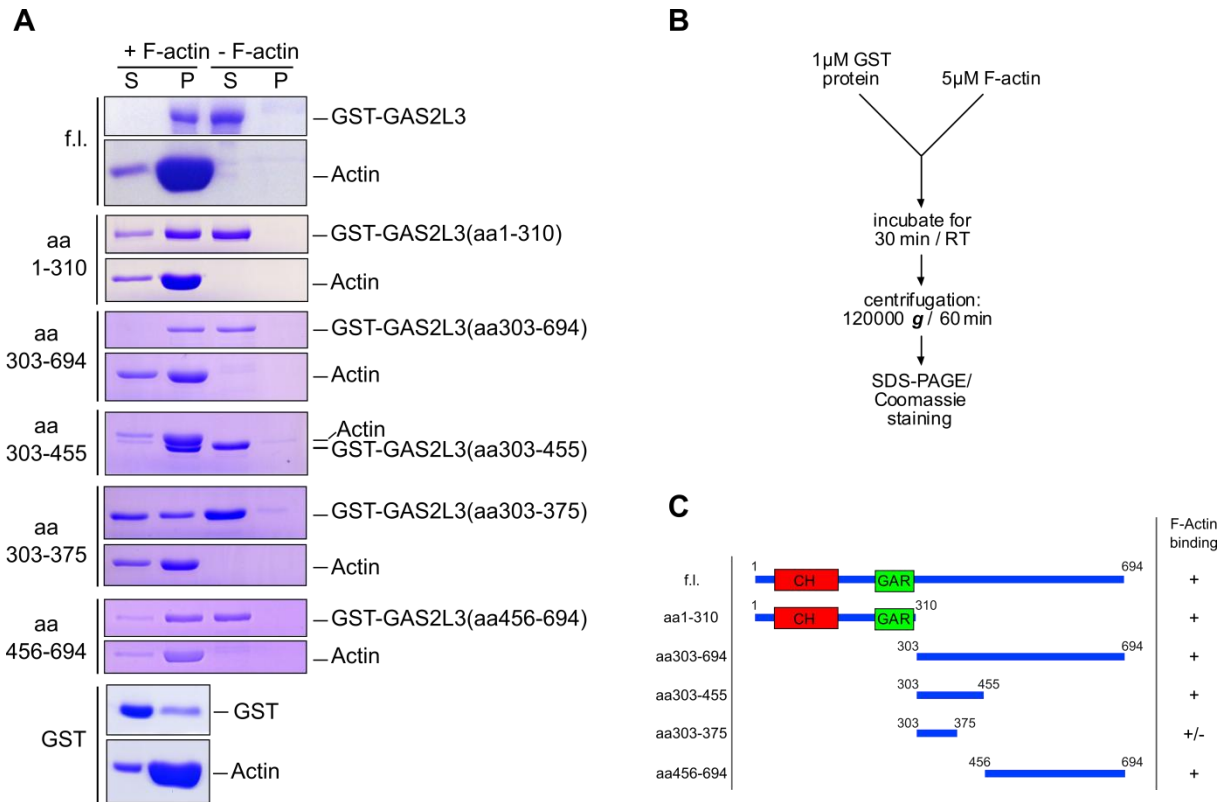
interacts with the cytoskeleton. To address this question a set of GAS2L3 deletion mutants for *in vitro* studies was created. The cDNA sequences of full length GAS2L3 and deletion mutants were amplified by PCR and cloned in frame into pGEX4T-2 vector. This plasmid is used for bacterial overexpression of glutathione-S-transferase (GST) fusion proteins. After purification with glutathione sepharose beads, the GST fusion proteins were eluted from the beads and dialyzed (section 2.2.3.13). Fractions of the purified proteins were analyzed by SDS-PAGE and subsequent Coomassie blue staining. For comparison a BSA dilution series of known protein concentration was analyzed in parallel on the same gel (section 2.2.3.13). After determination of concentration and verification of protein integrity, the purified proteins were used in subsequent *in vitro* experiments.

At first F-actin co-sedimentation assays were performed (section 2.2.3.14) (fig 3.3). Monomeric actin was resuspended in general actin buffer and polymerized to actin filaments (F-actin) by addition of actin polymerization buffer for 1 hour at 24 °C (section 2.2.3.14). 1 µM of the purified GST fusion proteins were incubated together with 5 µM F-actin and subjected to centrifugation at 120000 *g* for 1 hour. The supernatant and pellet fractions were separated by SDS-PAGE and subsequently stained with Coomassie blue (fig 3.3a). Interacting proteins are found in the pellet fraction together with F-actin after centrifugation while non-interacting proteins remain in the supernantant fraction. As control the assay was performed in parallel with GST protein only and with every protein without F-actin. In both cases the tested GST fusion proteins should remain in the supernatant fraction after centrifugation.

The assay was performed with full length GST-GAS2L3 and five different deletion mutants (fig 3.3a). Full length protein and the N-terminal part containing the CH domain showed clear F-actin interaction, indicated by presence of the GST protein in the pellet fraction. Except for GST-GAS2L3(aa303-375), which only showed reduced affinity for F-actin, all of the other tested proteins clearly interacted with F-actin, although they lack a known F-actin binding domain. Importantly, none of the tested proteins was found in the pellet fractions without F-actin (fig 3.3a). The C-terminal part of GAS2L3 harbors at least two different F-actin binding regions, because the non-overlapping mutants GST-GAS2L3(aa303-455) and GST-GAS2L3(aa456-694) showed both a comparable affinity for F-actin (fig 3.3a).

A

+ F-actin - F-actin
S P S P

f.l.
—GST-GAS2L3
—Actin

aa 1-310
—GST-GAS2L3(aa1-310)
—Actin

aa 303-694
—GST-GAS2L3(aa303-694)
—Actin

aa 303-455
—Actin
—GST-GAS2L3(aa303-455)

aa 303-375
—GST-GAS2L3(aa303-375)
—Actin

aa 456-694
—GST-GAS2L3(aa456-694)
—Actin

GST
—GST
—Actin

B

1 µM GST protein   5 µM F-actin

incubate for
30 min / RT

centrifugation:
120000 *g* / 60 min

SDS-PAGE/
Coomassie
staining

C

		F-Actin binding
f.l.	1 [CH] [GAR] 694	+
aa1-310	1 [CH] [GAR] 310	+
aa303-694	303 694	+
aa303-455	303 455	+
aa303-375	303 375	+/-
aa456-694	456 694	+

Figure 3.3: GAS2L3 interacts with F-actin *in vitro*. A) Purified GST or GST-GAS2L3 full length and deletion mutants were incubated with F-actin and centrifuged. Supernatant (S) and pellet (P) fractions were recovered and analyzed via Coomassie blue staining. B) Flow chart describing the F-actin co-sedimentation assay. C) Summary of the interaction data. f.l.: full length, aa: amino acids; RT: room temperature. Panel A and parts of panel C were first published in Wolter et al., 2012.

Next, microtubule co-sedimentation assays were performed (section 2.2.3.15) (fig 3.4). Monomeric tubulin was polymerized to microtubules (MTs) as described in section 2.2.3.15. 1 µM of the purified GST fusion proteins were incubated together with 10 µM taxol stabilized microtubules (MTs) and subjected to centrifugation at 30000 *g* for 30 min. The supernatant and pellet fractions were recovered, separated by SDS-PAGE and subsequently stained with Coomassie blue (fig 3.4a).

Interacting proteins are found in the pellet fraction together with MTs after centrifugation while non-interacting proteins remain in the supernatant fraction. As control, the assay was performed in parallel with GST protein only and with every protein without MTs. In both cases the tested GST fusion proteins should remain in the supernatant fraction after centrifugation.

The assay was performed with full length GST-GAS2L3 and five different deletion mutants (fig 3.4). Full length protein showed a clear interaction with MTs indicated by presence of the GST protein in the pellet fraction. The GST-GAS2L3(aa1-310) protein containing the CH and the GAR domain, which is described as a MT binding domain (Goriounov et al., 2003; Sun et al., 2001), did not interact with MTs. Only GST-GAS2L3(aa303-694) and the smaller non-

overlapping deletion mutants of the C-terminal part, GST-GAS2L3(aa303-455) and GST-GAS2L3(aa456-694) showed a clear interaction with MTs, indicating again two independent C-terminally located binding motifs. Importantly, none of the tested proteins was found in the pellet fractions without MTs.
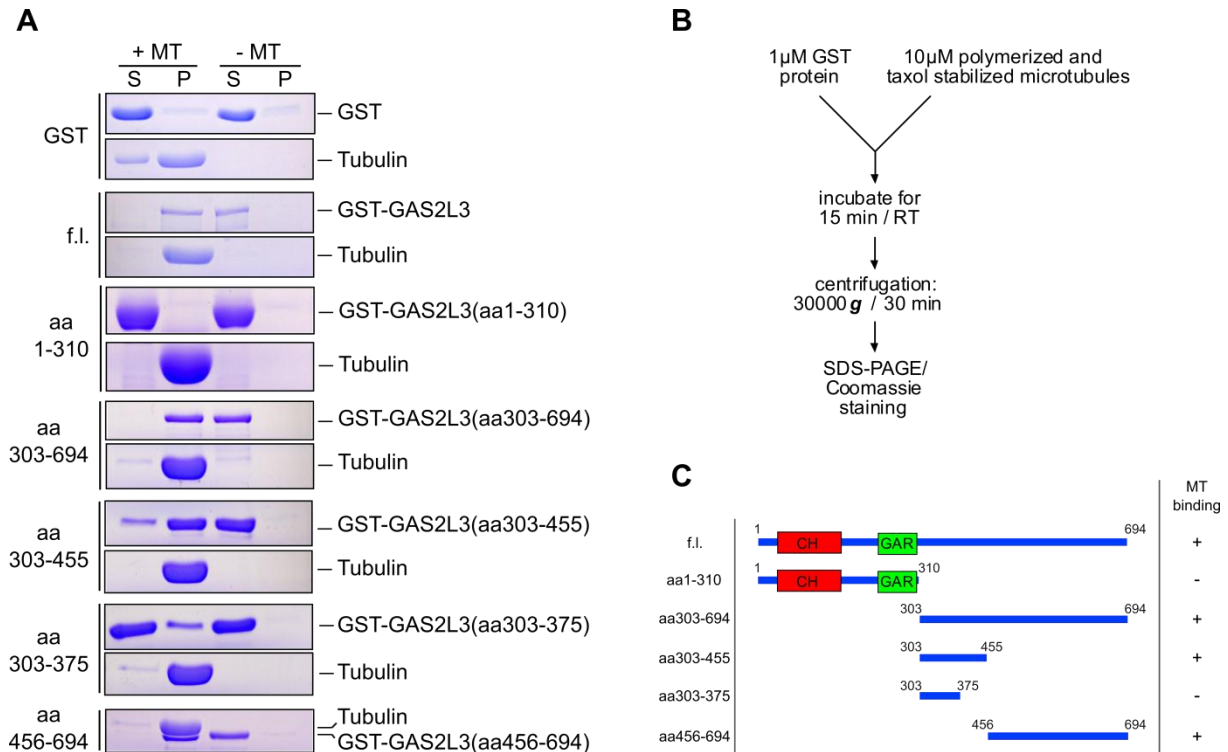
Figure 3.4: GAS2L3 interacts with microtubules *in vitro*. A) Purified GST or GST-GAS2L3 full length and deletion mutants were incubated with microtubules (MT) and centrifuged. Supernatant (S) and pellet (P) fractions were recovered and analyzed via Coomassie blue staining. B) Flow chart describing the MT co-sedimentation assay. C) Summary of the interaction data. f.l.: full length, aa: amino acids; RT: room temperature. Panel A and parts of panel C were first published in Wolter et al., 2012.

Taken together, the co-sedimentation assays revealed, that GAS2L3 can directly interact with F-actin and MTs *in vitro*. It became clear that the F-actin interaction is mediated by the N-terminus of GAS2L3 and at least two binding motifs in the C-terminus, while the MT binding is solely mediated by at least two independent binding motifs in the C-terminal part, but not by the GAR domain. The cartoon depicted in figure 3.5 summarizes the *in vitro* binding data.
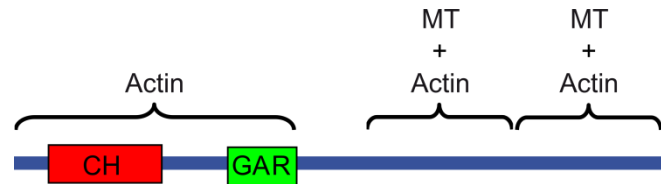
Figure 3.5: Summary of the data obtained from co-sedimentation assays. F-actin binding is mediated by the N-terminus (probably via the CH domain) and at least two independent binding motifs in the C-terminus. Microtubule binding is mediated by at least two independent binding motifs in the C-terminal part of the protein, but not by the GAR domain. Figure was first published in Wolter et al., 2012.

The two co-sedimentation assays were combined to test if GAS2L3 is able to bind to MTs and F-actin simultaneously *in vitro* (section 2.2.3.16) (fig 3.6). 1 µM purified GST fusion proteins were first incubated with 5 µM taxol stabilized MTs at room temperature for 15 min. 5 µM F-actin was added and after additional incubation for 15 min the samples were subjected to low speed centrifugation at 5000 *g* for 10 min. The supernatant and pellet fractions were recovered, separated by SDS-PAGE and subsequently stained with Coomassie blue (fig 3.6a). After low speed centrifugation only MTs formed a pellet, while F-actin stayed in the supernatant fraction (fig 3.6a lanes 1&2 top). Addition of GST-GAS2L3 to F-actin resulted in a pellet formation, indicating an additional F-actin bundling activity of GAS2L3 (fig 3.6a lanes 3&4 top). Incubation of full length protein with MTs indicated a clear interaction (fig 3.6 lanes 5&6 top) confirming the results obtained from the co-sedimentation assays (fig 3.4). The majority of F-actin went to the pellet fraction after incubation with MTs and full length protein, indicating a cytoskeleton crosslinking function of GAS2L3 (fig 3.6 lanes 7&8 top). The C-terminal part was also able to cross link F-actin and MTs *in vitro* (fig 3.6 lanes 7&8 middle), while the N-terminus was not, due to the lack of a MT binding domain (fig 3.6 lanes 7&8 bottom and fig. 3.4). Like the full length protein, the N-terminus showed also an F-actin bundling activity indicated by presence of F-actin in the pellet fraction after low speed centrifugation (fig 3.6 lanes 3&4 bottom), while the C-terminal part was not able to do so (fig 3.6 lanes 3&4 middle).
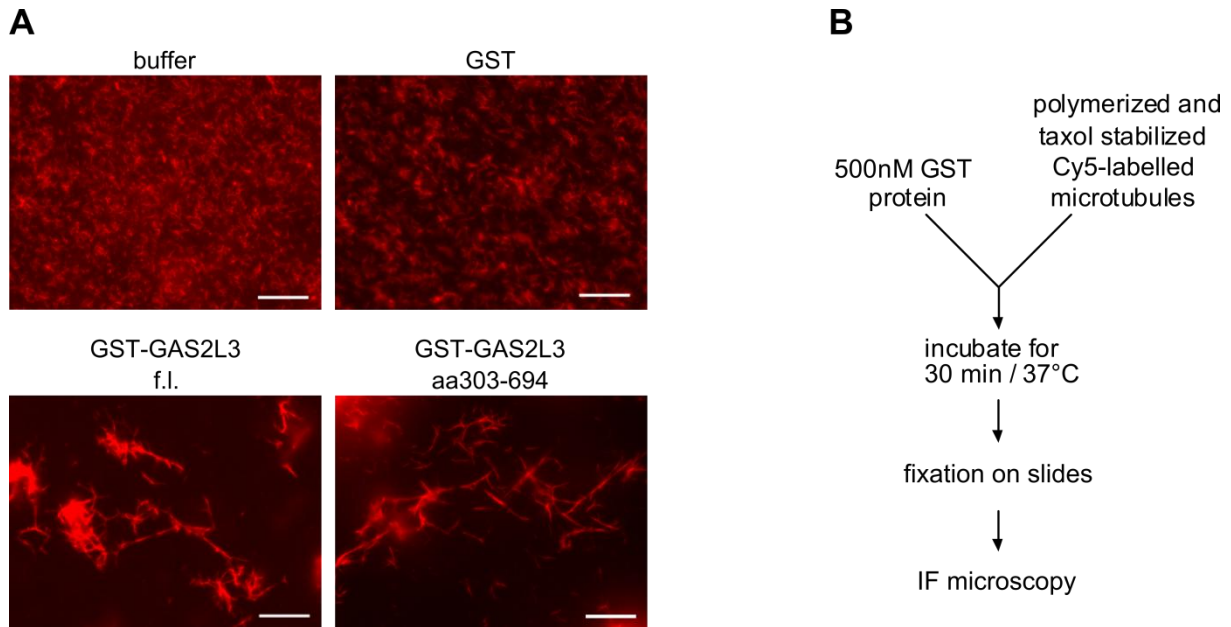
The assay confirmed that GAS2L3 is able to bind simultaneously to F-actin and MTs *in vitro*. It also showed that the N-terminal part of GAS2L3 is not only able to bind, but also to bundle actin filaments and that the C-terminal part is sufficient for crosslinking MTs and F-actin *in vitro*.
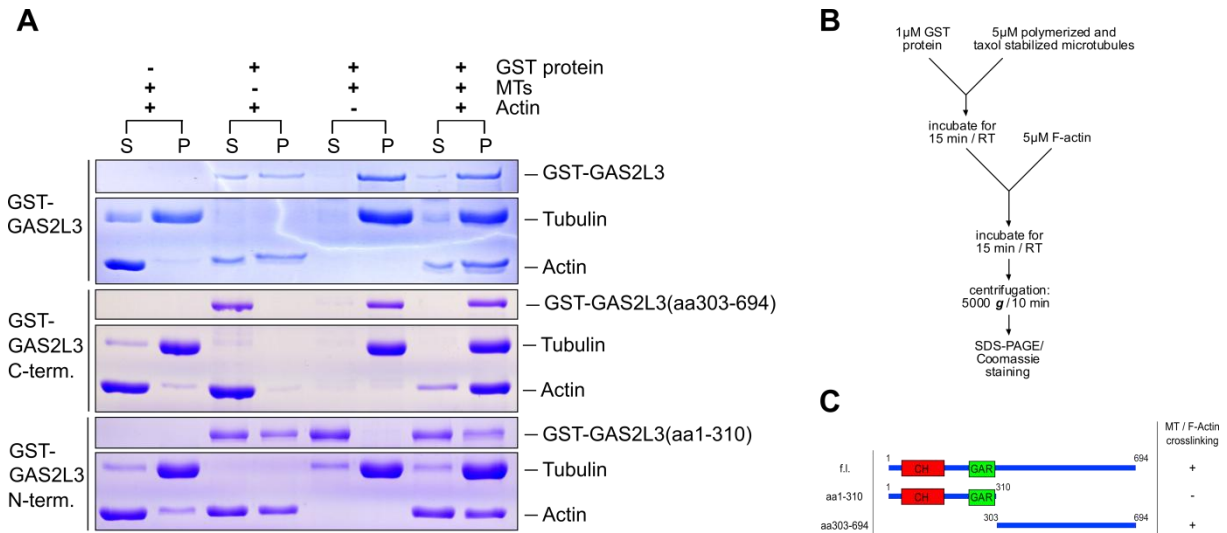
Figure 3.6: GAS2L3 crosslinks microtubules and F-actin *in vitro*. A) Purified GST-GAS2L3 full length and deletion mutants were incubated with microtubules (MTs) and F-actin. Samples were centrifuged, supernatant (S) and pellet (P) fractions were recovered and analyzed via Coomassie blue staining. B) Flow chart describing the MT-F-actin crosslinking assay. C) Summary of the interaction data. f.l.: full length, aa: amino acids; RT: room temperature. Panel A was first published in Wolter et al., 2012.

Additionally it was analyzed, if GAS2L3 has also a MT bundling activity *in vitro*. To address this question, a MT bundling assay was performed (section 2.2.3.17). 500 nM of purified GST fusion proteins were incubated for 30 min with 5 µM taxol stabilized Cy5-labelled MTs at 37 °C. Samples were fixed on slides and analyzed by immunofluorescence microscopy. Incubation of polymerized MTs with MT bundling proteins leads to an accumulation of large filamentous MT structures. As negative control GST protein was used because it only showed low affinity for MTs in co-sedimentation assays (fig 3.4). Addition of GST-GAS2L3 full length and C-terminus resulted in a strong accumulation of filamentous structures compared to the buffer control (fig 3.7). This finding indicated a MT bundling activity of GAS2L3 mediated by the C-terminal part (fig 3.7). In contrast, addition of GST protein alone did not lead to formation of filamentous structures (fig 3.7).

A

B

polymerized and
taxol stabilized
Cy5-labelled
microtubules

500nM GST
protein

incubate for
30 min / 37°C

fixation on slides

IF microscopy

Figure 3.7: GAS2L3 bundles microtubules *in vitro*. A) GST-GAS2L3 full length, C-terminus (aa303-694) or GST were incubated with Cy5-labelled microtubules. Samples were fixed on slides and analyzed by immunofluorescence (IF) microscopy. B) Flow chart describing MT bundling assay. f.l.: full length, aa: amino acids, scale bars: 10 µm. Parts of panel A were first published in Wolter et al., 2012.

Taken together, GAS2L3 is a cytoskeleton associated protein, which is able to bind to F-actin and MTs *in vitro* and which has additionally MT and F-actin bundling activities. The following figure summarizes all the obtained cytoskeleton binding data (fig 3.8).
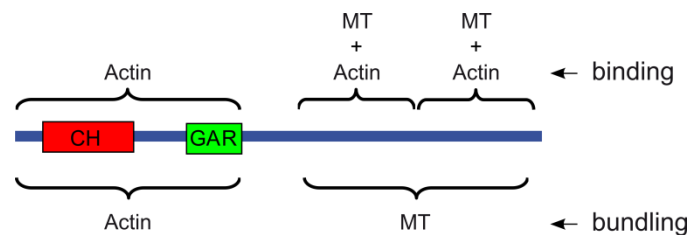
Figure 3.8: Summary of the *in vitro* binding data. The N-terminal part of GAS2L3 has F-actin binding and bundling ability. The C-terminus is able to bind to F-actin and MTs and has additionally a MT bundling activity. Parts of the figure were first published in Wolter et al., 2012.

3.4. GAS2L3 interacts with the chromosomal passenger complex

The GST-GAS2L3 fusion proteins created for *in vitro* MT and F-actin co-sedimentation assays were also used for *in vitro* binding assays to identify new interacting proteins of GAS2L3. In initial experiments the proteins Aurora B, Centrosomal protein of 55 kDa (Cep55), End-binding protein 1 (EB1), MgcRacGAP, Mklp1 and RhoA, which all co-localize with GAS2L3 in human cells, were tested for interaction by using GST pulldown assays (data not shown). HeLa whole cell lysates were incubated with immobilized GST-GAS2L3 or GST

as negative control and bound proteins were analyzed by immunoblotting. None of the tested proteins, except Aurora B kinase, showed an interaction with GAS2L3 (data not shown). As Aurora B kinase is a very important protein and a master regulator of mitosis and cytokinesis (sections 1.4.4 & 1.4.6), it was chosen for further analysis.

GST pulldown assays with different GAS2L3 deletion mutants and full length protein were conducted (section 2.2.3.18) to verify the interaction with Aurora B and map the involved binding region of the GAS2L3 protein (fig 3.9a). HeLa whole cell lysates were incubated with immobilized GST fusion proteins and Aurora B binding was analyzed by immunoblotting. CDK2 was used as control to exclude that recombinant GST fusion proteins bind non-specifically to proteins present in the cell lysate (fig 3.9a). Interaction between Aurora B and full length GAS2L3 protein was detectable like in the initial experiment. All the other deletion mutants harboring the N-terminally located GAR domain also showed a clear interaction with GAS2L3, while the two mutants without this domain did not (fig 3.9a). This experiment led to the conclusion, that the GAR domain of GAS2L3 is mediating the interaction with Aurora B kinase. To further clarify this point, an additional mutant with internally deleted GAR domain (GAS2L3Δ170-309) was created and used for further pulldown experiments (fig 3.9b). Immunoblotting revealed, that GAS2L3(Δ170-309) was not able to bind to Aurora B kinase any more (fig 3.9b). In cells, Aurora B kinase is incorporated into a protein complex which is called chromosomal passenger complex (CPC) (section 1.4). In addition to Aurora B kinase, the CPC consists of three other proteins named Borealin, Incenp and Survivin (section 1.4). To address whether GAS2L3 binds to the whole CPC and not only to Aurora B kinase, binding of two other members of the CPC, Borealin and Survivin, was also analyzed by immunoblotting (fig 3.9b). Borealin and Survivin showed an interaction with all GAS2L3 proteins harboring the GAR domain, but not with the GAS2L3(Δ170-309) mutant (fig 3.9b).
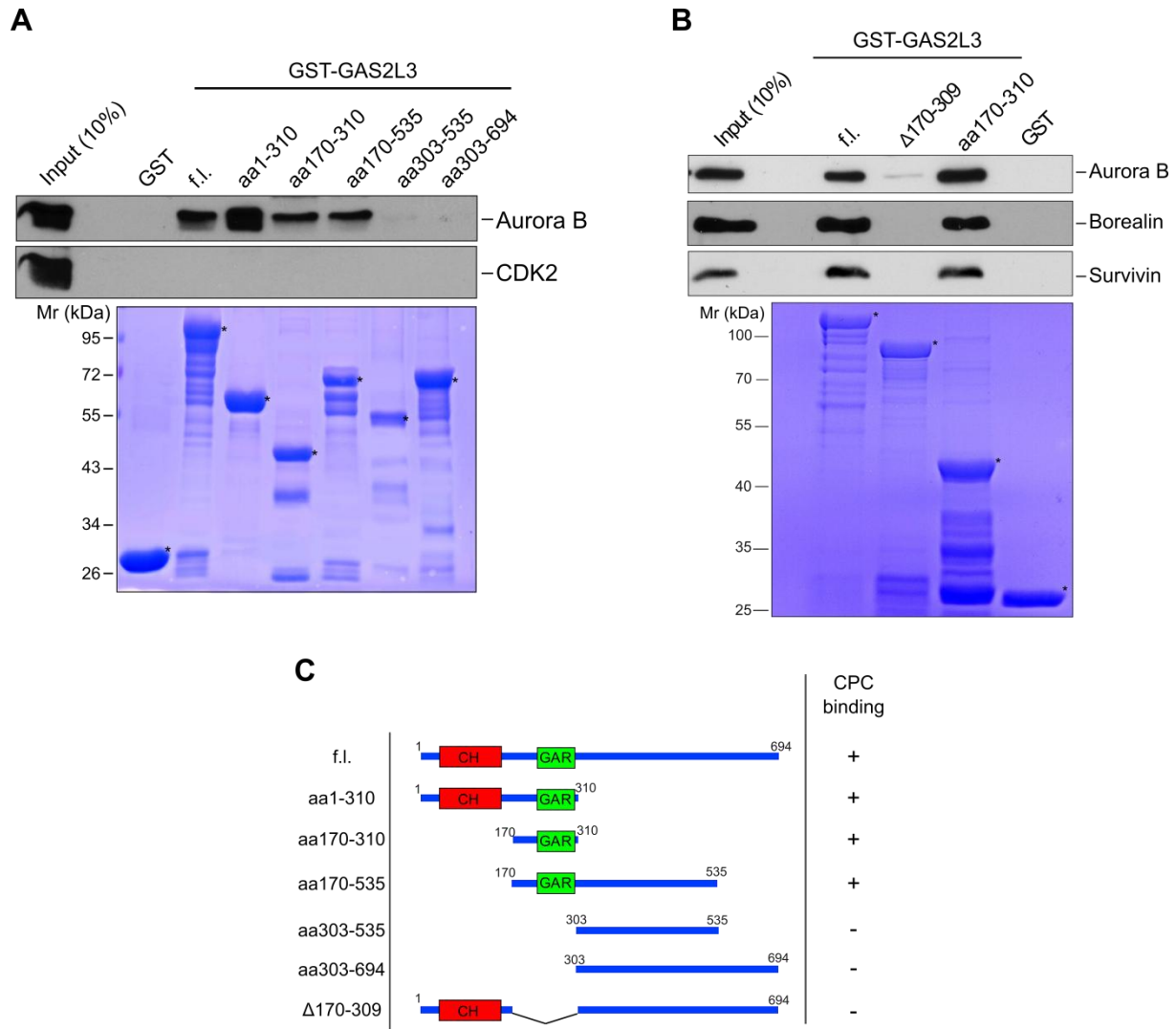
Figure 3.9: The GAR domain of GAS2L3 is required and sufficient to mediate binding to the chromosomal passenger complex *in vitro*. (A) HeLa whole cell lysates were incubated with immobilized GST fusion proteins and binding of Aurora B and CDK2 was analyzed by immunoblotting. Coomassie blue stained gel of the purified GST fusion proteins is shown at the bottom. The positions of the fusion proteins are marked with asterisks. (B) HeLa whole cell lysates were incubated with immobilized GST fusion proteins and binding of Aurora B, Borealin and Survivin was analyzed by immunoblotting. Coomassie blue stained gel of the purified GST fusion proteins is shown at the bottom. The positions of the fusion proteins are marked with asterisks. (C) Summary of the binding data. f.l.: full length, aa: amino acids, CPC: chromosomal passenger complex. Figure was first published in Fackler et al., 2014.

As described earlier, the CPC consists of four members (section 1.4). The question was raised, which of the four proteins is the direct interaction partner of GAS2L3. GST pulldown assays performed with whole cell lysates were not suited to address this question so the decision was taken to bacterially overexpress the CPC members and perform *in vitro* binding assays together with GST-GAS2L3 fusion proteins. The cDNA sequences of the CPC members were amplified by PCR and cloned in frame into the bacterial expression plasmid pRSETA. The resulting constructs were overexpressed in bacteria to obtain His-tagged CPC

proteins. Overexpression of His-tagged Incenp was not possible, so it could not be used for further assays. The other three CPC members were successfully overexpressed and used for *in vitro* binding assays together with GST-GAS2L3 (section 2.2.3.19). Whole cell lysates from *E. coli* cells overexpressing His-tagged CPC proteins and GST-GAS2L3 were prepared and mixed. His-tagged proteins were precipitated with Ni-NTA agarose and bound GST-GAS2L3 protein was detected by immunoblotting (fig 3.10a). His-tagged Borealin and Survivin showed both a clear interaction with GST-GAS2L3, while His-tagged Aurora B did not (fig 3.10a). This result indicates that the direct protein interaction between GAS2L3 and the CPC is mediated by Borealin and Survivin but not by Aurora B kinase.
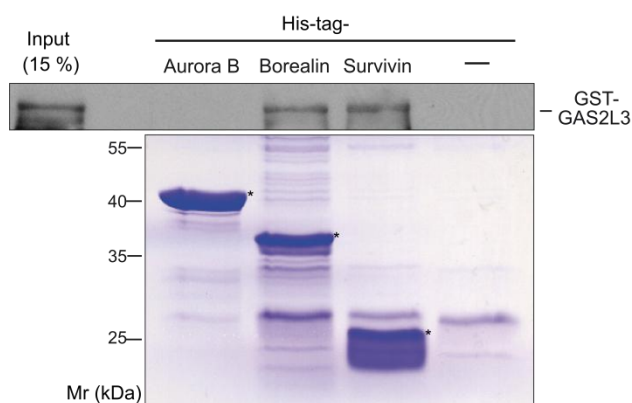
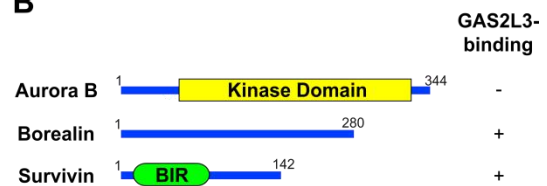**Figure 3.10: GAS2L3 interacts with Borealin and Survivin, but not with Aurora B *in vitro*.** (A) Bacterial cell lysates containing His-tagged recombinant proteins were incubated with bacterial cell lysates containing GST-GAS2L3 fusion protein. His-tagged proteins were precipitated by Ni-NTA agarose and binding of GST-GAS2L3 was analyzed by immunoblotting. Coomassie blue stained gel of the purified His-tagged fusion proteins is shown at the bottom. The positions of the fusion proteins are marked with asterisks. (B) Summary of the binding data. Panel A was first published in Fackler et al., 2014.

To further map the binding regions of Borealin and Survivin which mediate interaction with GAS2L3, deletion mutants of both proteins were created with PCR and cloning them in frame into the pRSETA plasmid. The resulting constructs were overexpressed and used for *in vitro* binding assays together with GST-GAS2L3, GST-GAS2L3(Δ170-309) and GST-GAS2L3(aa170-310) (fig 3.11).

Whole cell lysates from *E. coli* cells overexpressing His-tagged Borealin and Survivin deletion mutants and GST fusion proteins were prepared and mixed. His-tagged proteins were precipitated with Ni-NTA agarose and bound GST fusion proteins were detected by immunoblotting (fig 3.11a). The interaction between full length His-tagged Borealin and Survivin and GST-GAS2L3 full length and GAS2L3(aa170-310) mutant was detectable, while the GAS2L3 mutant lacking the GAR domain (Δ170-309) showed no interaction (fig 3.11a). Additionally the C-terminal mutant of Borealin and the N-terminal mutant of Survivin

containing the BIR domain also showed an interaction with full length GAS2L3 and GAS2L3(aa170-310), but not with GAS2L3(Δ170-309) (fig 3.11a).
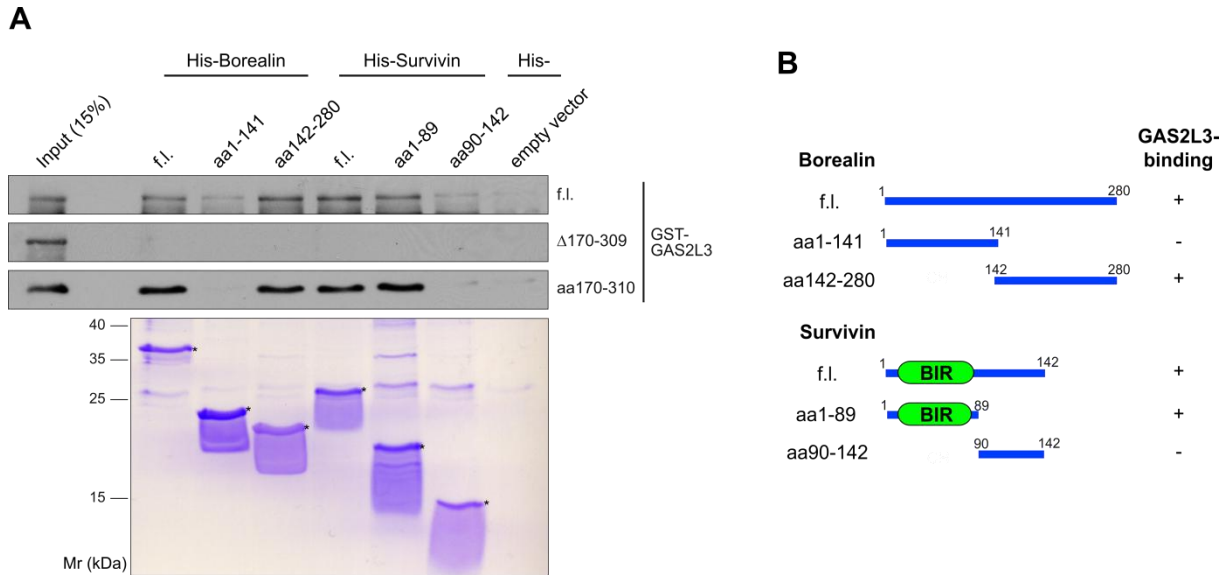
A

B

Figure 3.11: The GAR domain of GAS2L3 interacts with the C-terminus of Borealin and the N-terminus of Survivin. (A) Bacterial cell lysates containing His-tagged recombinant proteins were incubated with bacterial cell lysates containing GST fusion proteins. His-tagged proteins were pulled down by Ni-NTA agarose and binding of GST fusion proteins was analyzed by immunoblotting. Coomassie blue stained gel of the purified His-tagged fusion proteins is shown at the bottom. The positions of the fusion proteins are marked with asterisks. (B) Summary of the binding data. f.l.: full length, aa: amino acids. Figure was first published in Fackler et al., 2014.

The results obtained from all *in vitro* binding assays indicate that the interaction between GAS2L3 and the CPC is mediated by the GAR domain of GAS2L3 and the C-terminal part of Borealin as well as the N-terminal part of Survivin. The cartoon shown in figure 3.12 gives an overview of the interaction between GAS2L3 and the CPC.
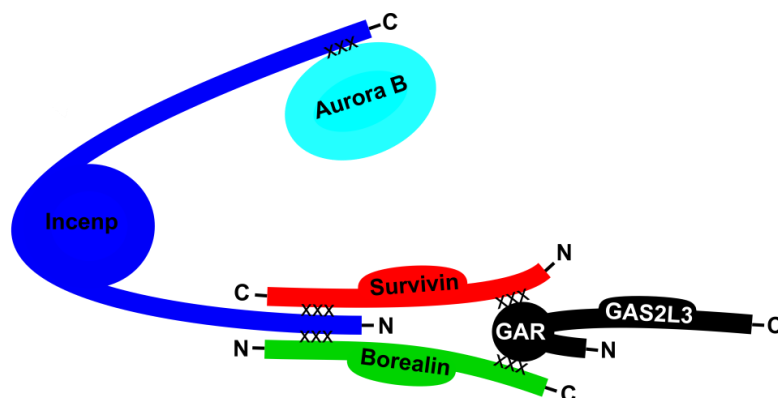
Figure 3.12: GAS2L3 interacts with the chromosomal passenger complex. The GAR domain of GAS2L3 directly interacts with the C-terminus of Borealin and the N-terminus of Survivin. Incenp, Borealin and Survivin form a triple helix bundle. Direct protein-protein interactions between GAS2L3 and CPC subunits are indicated by xxx.

To verify that the interaction is also occurring in living cells, co-immunoprecipitation experiments were carried out. HeLa whole cell lysates were incubated with GAS2L3 and Survivin or with non-specific control IgG antibodies. The antibodies were precipitated by addition of protein G beads and bound proteins were analyzed by immunoblotting. GAS2L3 was efficiently precipitated and the CPC proteins Aurora B and Survivin were readily detectable (fig 3.13a). Vice versa, GAS2L3 and Aurora B were also detectable, when Survivin was precipitated (fig 3.13a). Neither GAS2L3 nor Aurora B or Survivin were detected in samples were non-specific antibodies were used for immunoprecipitation (fig 3.13a). The obtained results indicate that the described *in vitro* interaction between GAS2L3 and the CPC is also occurring in living cells. To further confirm the binding data, a HeLa cell line stably expressing a tetracycline inducible shRNA directed against GAS2L3 mRNA was used. The cells were either treated with tetracycline to induce expression of shGAS2L3 or were left untreated. Whole cell lysates were prepared and incubated with GAS2L3 antibody. Immunoprecipitation experiments were carried out and bound proteins were analyzed by immunoblotting. In the untreated control sample GAS2L3 was efficiently precipitated and the CPC proteins Aurora B and Survivin were detectable (fig 3.13b). In the tetracycline treated sample however, only a small amount of GAS2L3 was precipitated, while the two CPC members Aurora B and Survivin were almost undetectable (fig 3.13b). This result confirmed the specificity of the observed interaction.
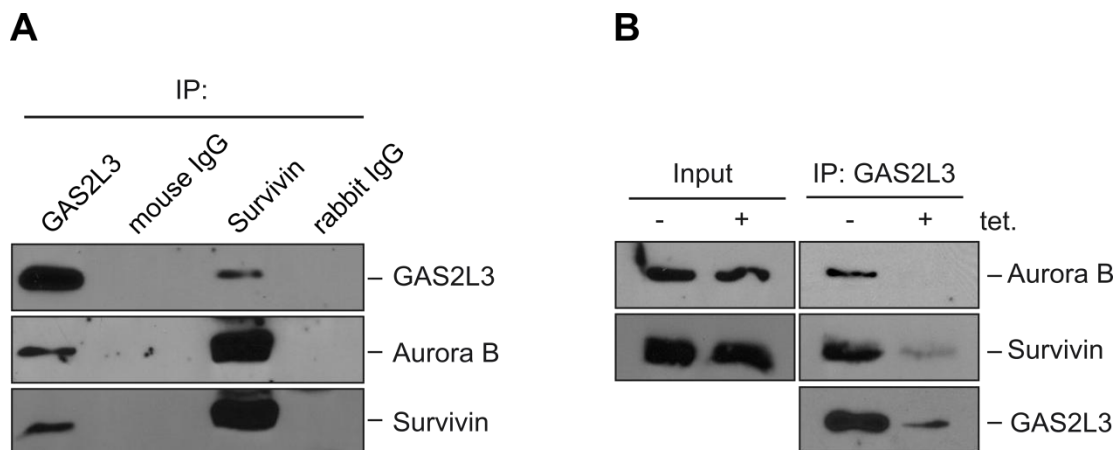
Figure 3.13: GAS2L3 interacts with the chromosomal passenger complex in cells. (A) HeLa whole cell lysates were incubated with GAS2L3 and Survivin or nonspecific mouse and rabbit IgG antibodies. Immunoprecipitation experiments were performed and protein amounts of Aurora B, Survivin and GAS2L3 were analyzed by immunoblotting. (B) Whole cell lysates from HeLa cells stably expressing a tetracycline-inducible GAS2L3 specific shRNA were incubated with GAS2L3 antibody. Immunoprecipitation experiments were performed and protein amounts of Aurora B, Survivin and GAS2L3 were analyzed by immunoblotting. The amounts of bound Aurora B and Survivin were strongly reduced after induction of the shRNA confirming the specificity of the interaction. Figure was first published in Fackler et al., 2014.

3.5. GAS2L3 is phosphorylated by CDK1 but not by Aurora B

Next, it was analyzed if GAS2L3 is not only an interacting protein of the CPC but also a substrate of Aurora B. To address this question, *in vitro* kinase assays with radioactively labelled ATP were performed. Because it was reported recently that CDK1 kinase phosphorylates GAS2L3 *in vivo* (Pe'er et al., 2013), CDK1 was used as a positive control in the *in vitro* kinase assays. Aurora B and CDK1/cyclin B1 were immunoprecipitated from HeLa whole cell lysates (fig 3.14b) and mixed with GST-GAS2L3, GST-Histone H3(aa1-46), Histone H1 or GST protein. GST-Histone H3(aa1-46) served as positive control for Aurora B, Histone H1 as positive control for CDK1 and GST was used as negative control for both kinases. Kinase assays were carried out (section 2.2.3.20) and phosphorylation of the substrate proteins were analyzed by autoradiography. GST-GAS2L3 as well as Histone H1 were strongly phosphorylated by CDK1 kinase (fig 3.14a). In contrast to this finding, no phosphorylation of GAS2L3 by Aurora B kinase was observable, although Histone H3 showed a clear incorporation of radioactively labelled ATP, confirming activity of immunoprecipitated Aurora B kinase (fig 3.14a). Neither Aurora B nor CDK1 kinase phosphorylated GST (fig 3.14a).
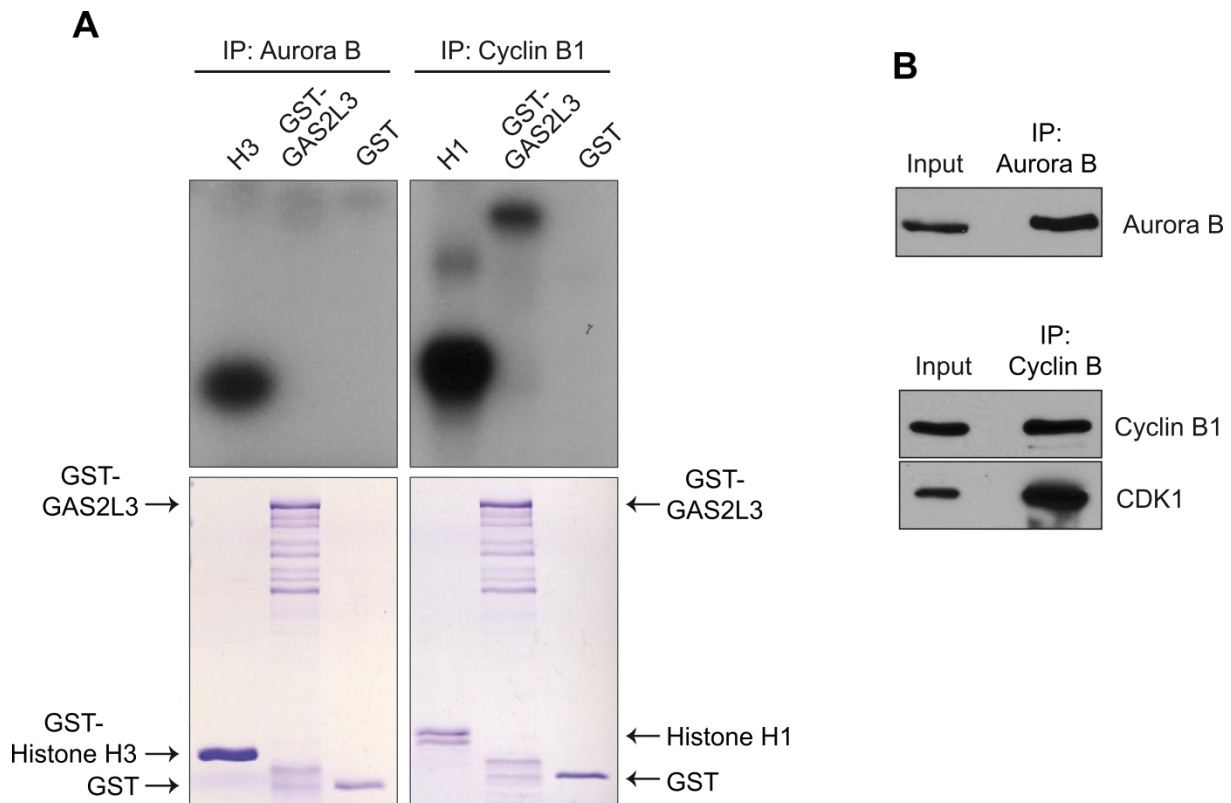
Figure 3.14: GAS2L3 is not a substrate of Aurora B, but is phosphorylated by CDK1. (A) Aurora B or Cyclin B1 were immunoprecipitated from HeLa whole cell lysates. Kinase assays with GST, GST-GAS2L3, GST-Histone H3(aa1-46) and Histone H1 as substrates were performed. Phosphorylation of substrates was visualized by autoradiography. Coomassie blue stained gel of the purified GST fusion proteins is shown at the bottom. (B) Successful immuoprecipitation of Aurora B (top) and CDK1 (bottom) kinases was verified by immunoblotting. Figure was first published in Fackler et al., 2014.

In vitro kinase assays showed, that GAS2L3 was strongly phosphorylated by CDK1 but not by Aurora B kinase. To identify the phosphorylated residues of the GAS2L3 protein, kinase assay with immunoprecipitated CDK1/cyclin B1 complex was repeated without radioactively labelled ATP. The phosphorylated GST-GAS2L3 protein was separated by SDS-PAGE and stained with colloidal coomassie solution. In collaboration with Dr. Thomas Ruppert from the Mass Spectrometry Core Facility of the Center for Molecular Biology, University of Heidelberg, six serine and two threonine residues were found to be modified by phosphorylation (fig 3.15a). All of the identified phosphosites were located in the C-terminal part of the protein (fig 3.15B) and three of them matched perfectly the CDK consensus motif [S*/T*]-P-X-[R/K] (Moreno and Nurse, 1990) (fig 3.15a).

A

Ser 307	VPD**S**PAR
Ser 376	LPN**S**PAA
Ser 418	NTS**S**PAL
Ser 431	ISE**S**PRK
Ser 438	CIS**S**PNT
Thr 441	SPN**T**PKA
Ser 570	SSV**S**PVK
Thr 651	SGK**T**PAS

B
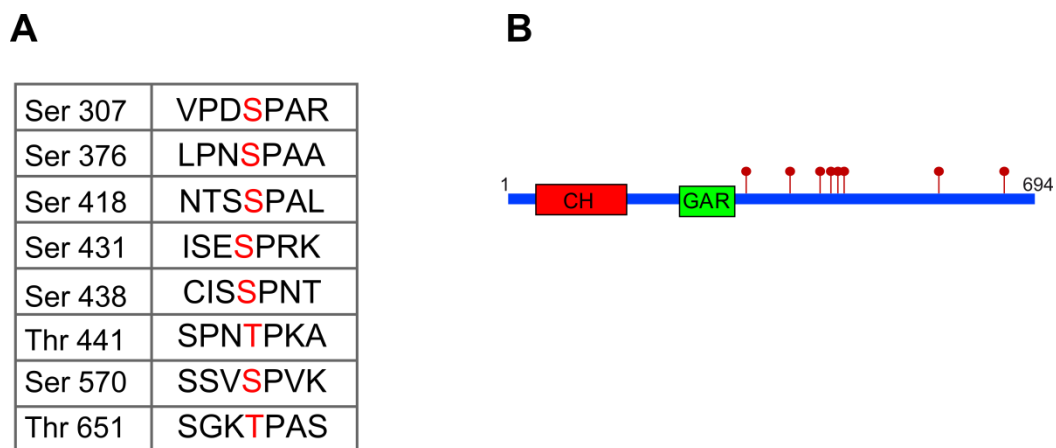
Figure 3.15: CDK1 phosphorylates GAS2L3 at multiple sites. (A) Eight different CDK1 specific GAS2L3 phosphosites were identified by mass spectrometrical analysis. Phosphosites are indicated by number of amino acids and recognition motif. All modified residues are depicted in red. (B) Cartoon describing the location of the phosphorylated amino acids in the GAS2L3 protein. Mass spectrometrical analysis was performed by the Mass Spectrometry Core Facility, ZMBH.

3.6. Depletion of GAS2L3 influences stability and activity of the CPC

To analyze if GAS2L3 influences the activity of the CPC, HeLa cells stably expressing a tetracycline inducible shRNA directed against GAS2L3 mRNA were used. HeLa cells were treated with tetracycline or were left untreated. After addition of nocodazole, whole cell lysates were prepared and separated by SDS-PAGE. Expression levels of CPC proteins and Aurora B substrates were analyzed by immunoblotting. The intensities of the immunoblotting signals were quantified with ImageJ and normalized to the untreated controls. The protein amounts of Borealin and Survivin were lowered in the tetracycline treated sample to approximately 70% of the untreated control (fig 3.16). The two Aurora B substrates P-Histone H3 (Ser 10) and P-CENPA (Ser 7) showed a decrease of the immunoblot signal intensities to approximately 60% of the untreated sample (fig 3.16). However, the protein amounts of

Aurora B and Cyclin B1, which was used as a marker for G2/M phase of the cell cycle, stayed unchanged between control and tetracycline treated samples (fig 3.16). Tubulin was used as loading control and also showed no change in signal intensities (fig 3.16).
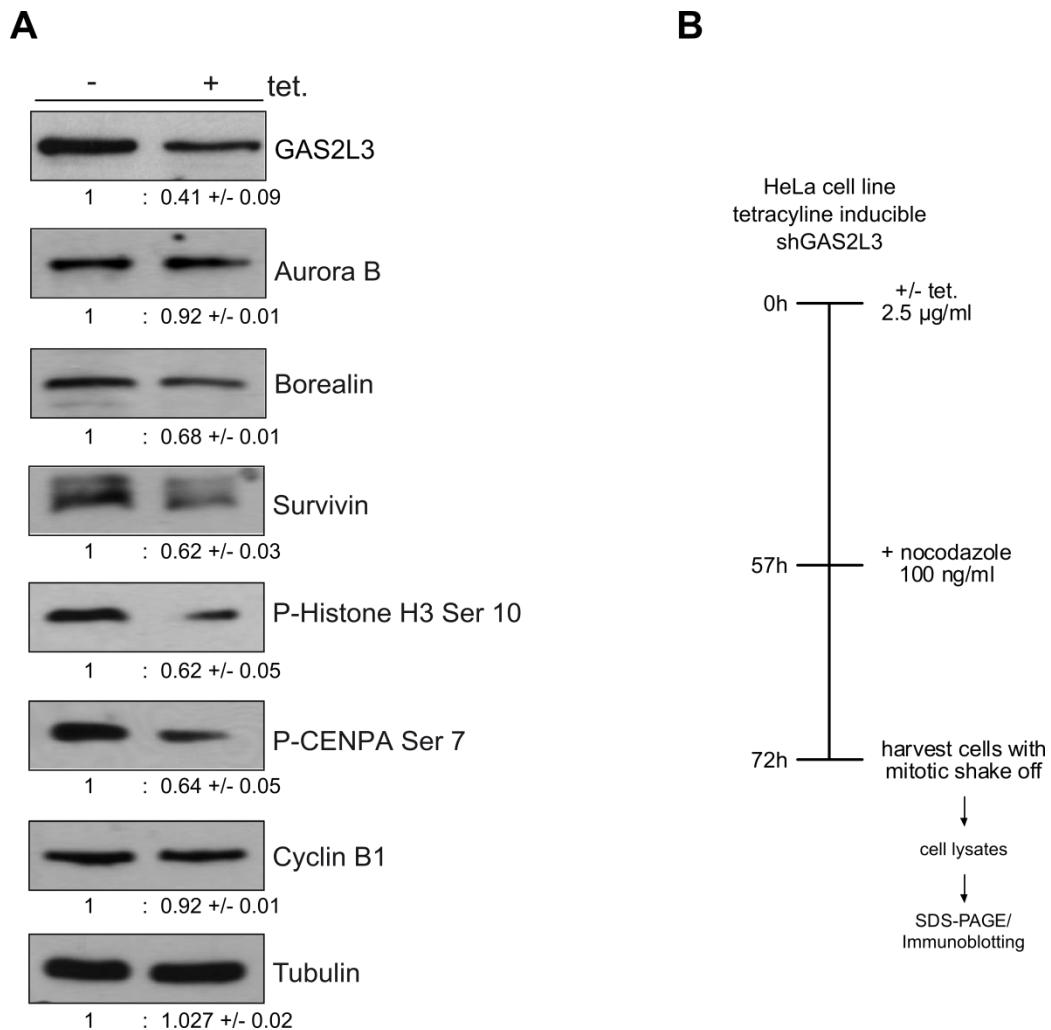
A   **B**

Figure 3.16: GAS2L3 depletion slightly influences stability and activity of the chromosomal passenger complex. (A) HeLa cells stably expressing a tetracycline-inducible GAS2L3 specific shRNA were treated with tetracycline or left untreated. Cell lysates were analyzed by immunoblotting with the indicated antibodies. Protein levels were quantified using Image J and normalized to the untreated control cells. The experiment was performed four times, one representative example is shown. Standard deviations between the four experiments are indicated. (B) Flow chart describing the experiment. Panel A was first published in Fackler et al., 2014.

Taken together these data suggest that GAS2L3 slightly influences the kinase activity of the CPC as well as the stability of its interaction partners Borealin and Survivin but not of Aurora B kinase.

To analyze if the defects in cytokinesis observed after GAS2L3 depletion (fig 3.2) are related to the described influence on CPC activity and stability, pharmacological inhibition of the CPC with the Aurora B specific kinase inhibitor AZD1152 (Mortlock et al., 2007) was used. The amount of AZD1152 was titrated to obtain a reduction in phosphorylation levels of CPC

substrates comparable to shRNA mediated depletion of GAS2L3. HeLa cells stably expressing a tetracycline inducible shRNA against GAS2L3 mRNA were either treated with tetracycline, were left completely untreated or were treated with different concentrations of AZD1152. After addition of nocodazole, whole cell lysates were prepared and separated by SDS-PAGE. Amounts of P-Histone H3, P-CENPA, Cyclin B1 and tubulin were analyzed by immunoblotting. The titration experiments revealed that the concentration of AZD1152 needed to achieve a comparable decrease in immunoblotting signal intensities of CPC substrates like it was observed after GAS2L3 depletion was about 1 nM for P-Histone H3 and about 5 nM for P-CENPA (fig 3.17a). To investigate if AZD1152 leads to cytokinesis defects in this concentration range, cells with tetracycline inducible expression of shGAS2L3 were treated with tetracycline, 5 nm AZD1152 or were left untreated. Cells were fixed and the percentage of multinucleated cells and cells with multi-lobed nuclei was quantified. Approximately 14% of GAS2L3 depleted cells showed defects in cytokinesis while the percentage of multinucleated cells or cells with abnormally shaped nuclei did not siginificantly increase in AZD1152 treated cells compared to control cells (fig 3.17b).
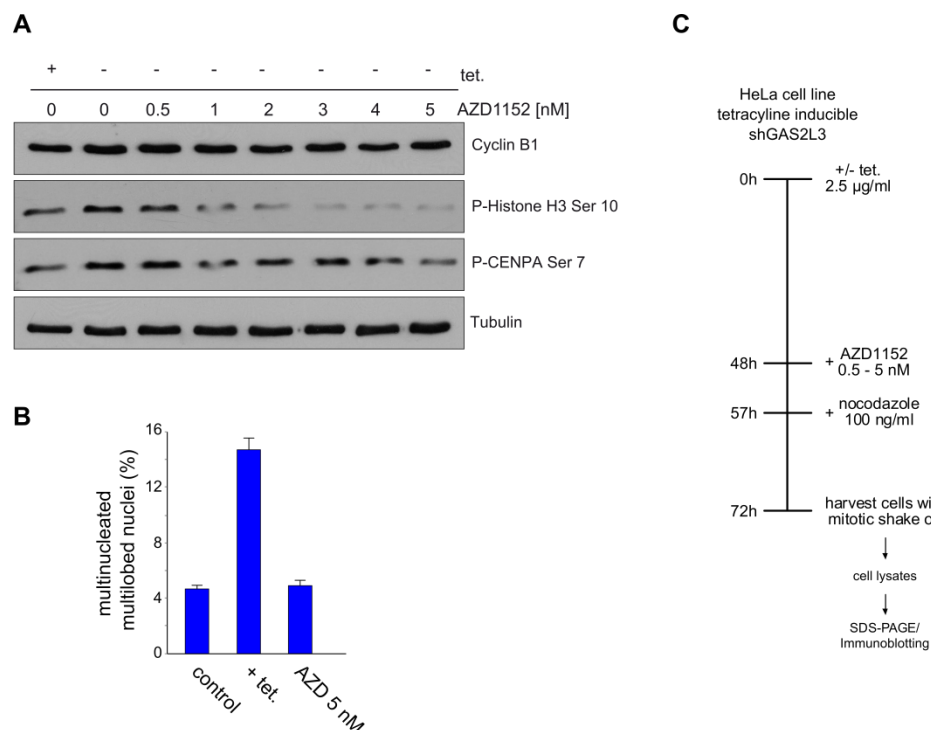
Figure 3.17: Depletion of GAS2L3 phenocopies moderate pharmacological inhibition of the chromosomal passenger complex. (A) HeLa cells stably expressing a tetracycline-inducible GAS2L3 specific shRNA were treated with tetracycline or different concentrations of AZD1152 or were left untreated as control. Cell lysates were analyzed by immunoblotting with the indicated antibodies. (B) Percentage of multinucleated cells and cells with multi-lobed nuclei was quantified in untreated control, tetracycline treated and AZD1152 treated cells. Results are from two independent experiments. More than 300 cells per experiment were counted. Standard deviations between the experiments are indicated (C) Flow chart describing the assay. Panel A and parts of panel B were first published in Fackler et al., 2014.

Thus, although GAS2L3 influences stability of CPC members and kinase activity of the CPC, comparative pharmacological experiments showed that reduction of CPC activity by depletion of GAS2L3 is not strong enough to induce cytokinesis defects.

3.7. Localization of GAS2L3 to the constriction zone depends on the GAR domain

To further analyze if the GAR domain is important for correct localization of GAS2L3 during cytokinesis, eGFP fusion constructs from full length GAS2L3 and GAS2L3(Δ170-309), the mutant unable to interact with the CPC, were generated and transiently overexpressed in HeLa cells. Cells were fixed and analyzed by immunofluorescence microscopy. Both eGFP fusion proteins localized normally to microtubules during interphase (fig 3.18). As previously reported (Wolter et al., 2012) full length GAS2L3 showed a distinct midbody localization during cytokinesis (fig 3.18). The GAS2L3(Δ170-309) mutant protein was still present at the cytokinetic bridge but localized more distal from the midbody compared to the wild type protein (fig 3.18).
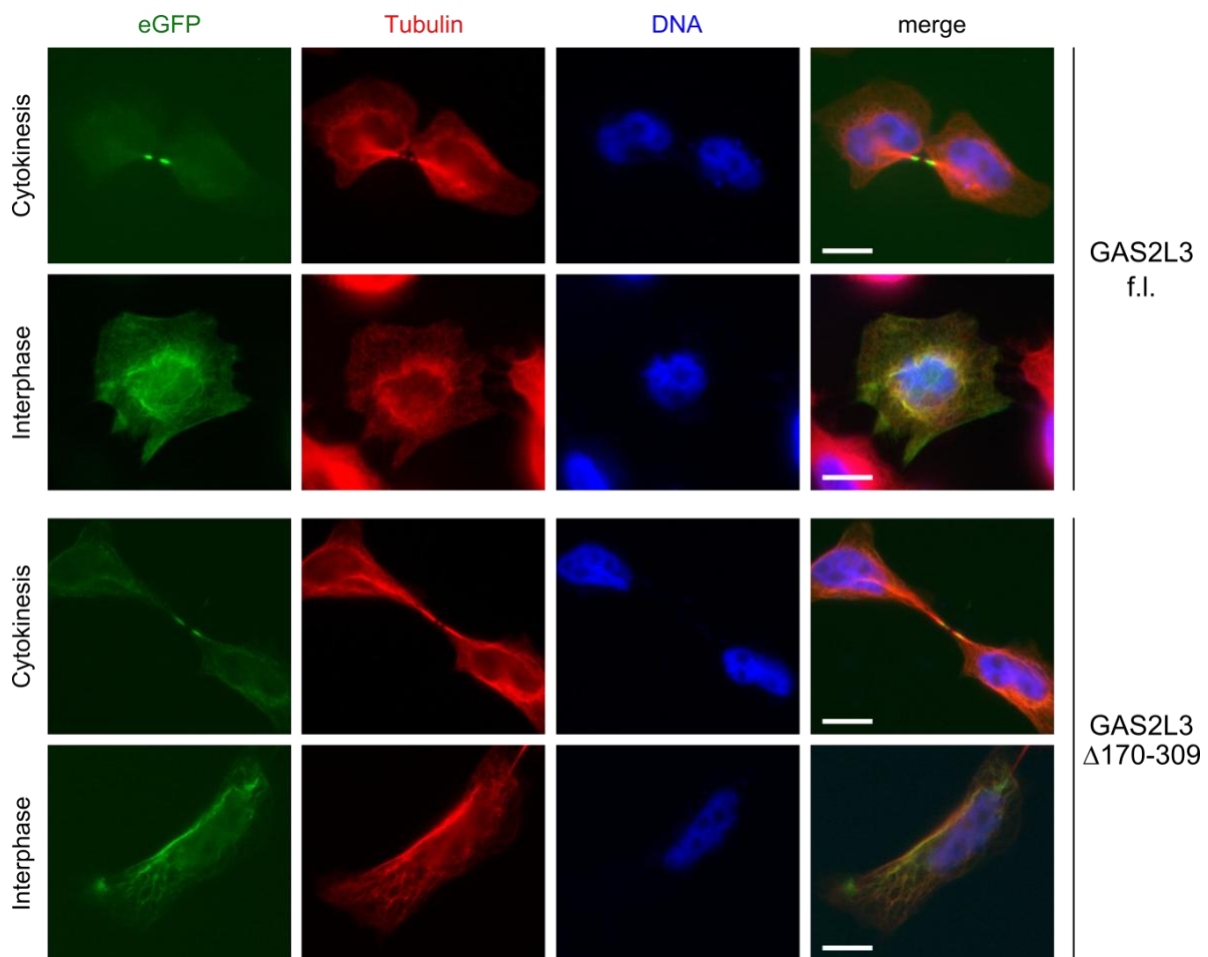
Figure 3.18: The GAR domain is necessary for proper localization of GAS2L3 during cytokinesis. Localization of overexpressed eGFP-GAS2L3 full length and Δ170-309 fusion proteins was analyzed during interphase and cytokinesis. Nuclei were stained with Hoechst 33258 (blue) and tubulin was counterstained (red). Scale bars: 10 μm.

Taken together immunofluorescence microscopy verified that correct localization of GAS2L3 to the midbody during cytokinesis is dependent on the GAR domain (fig 3.18).

3.8. The GAR domain is necessary for proper function of GAS2L3

To investigate if the GAR domain is necessary for proper function of GAS2L3, HeLa cell lines stably expressing tetracycline inducible siRNA resistant eGFP-GAS2L3 full length or Δ170-309 mutant were generated to perform reconstitution assays. Endogenous GAS2L3 protein was depleted by siGAS2L3 while siRNA resistant eGFP-GAS2L3 full length and Δ170-309 proteins were overexpressed in parallel. The aim of this assay was to find out if the reconstituted exogenously expressed proteins are able to compensate for loss of the endogenous protein by rescuing the observed phenotype after GAS2L3 depletion (fig 3.2). To confirm expression of full length eGFP-GAS2L3 and Δ170-309 mutant, cells were induced with tetracycline, whole cell lysates were prepared and eGFP fusion proteins were immunoprecipitated. Samples were analyzed by immunoblotting with GAS2L3 specific antibody (fig 3.19a). The cell lines expressed full length and mutant protein to a comparable level after tetracycline induction. Both eGFP fusion proteins were detectable at the cytokinetic bridge by immunofluorescence microscopy (fig 3.19b and section 3.7). After validation, cell lines were used for reconstitution assays. Cells were treated with tetracycline or were left untreated and subsequently transfected with a siRNA against GAS2L3 (internal # 2) to knockdown the endogenous protein. The cells were fixed and the percentage of multinucleated cells and cells with abnormally shaped nuclei was quantified (fig 3.19c). The quantification results were normalized to uninduced control cells. Expression of eGFP-GAS2L3 full length protein led to a decrease of cells with defective cytokinesis to approximately 70% of the uninduced control (fig 3.19d). The eGFP-GAS2L3(Δ170-309) mutant however did not show any rescue effect, indicating that the GAR domain is important for proper GAS2L3 protein function (fig 3.19d).
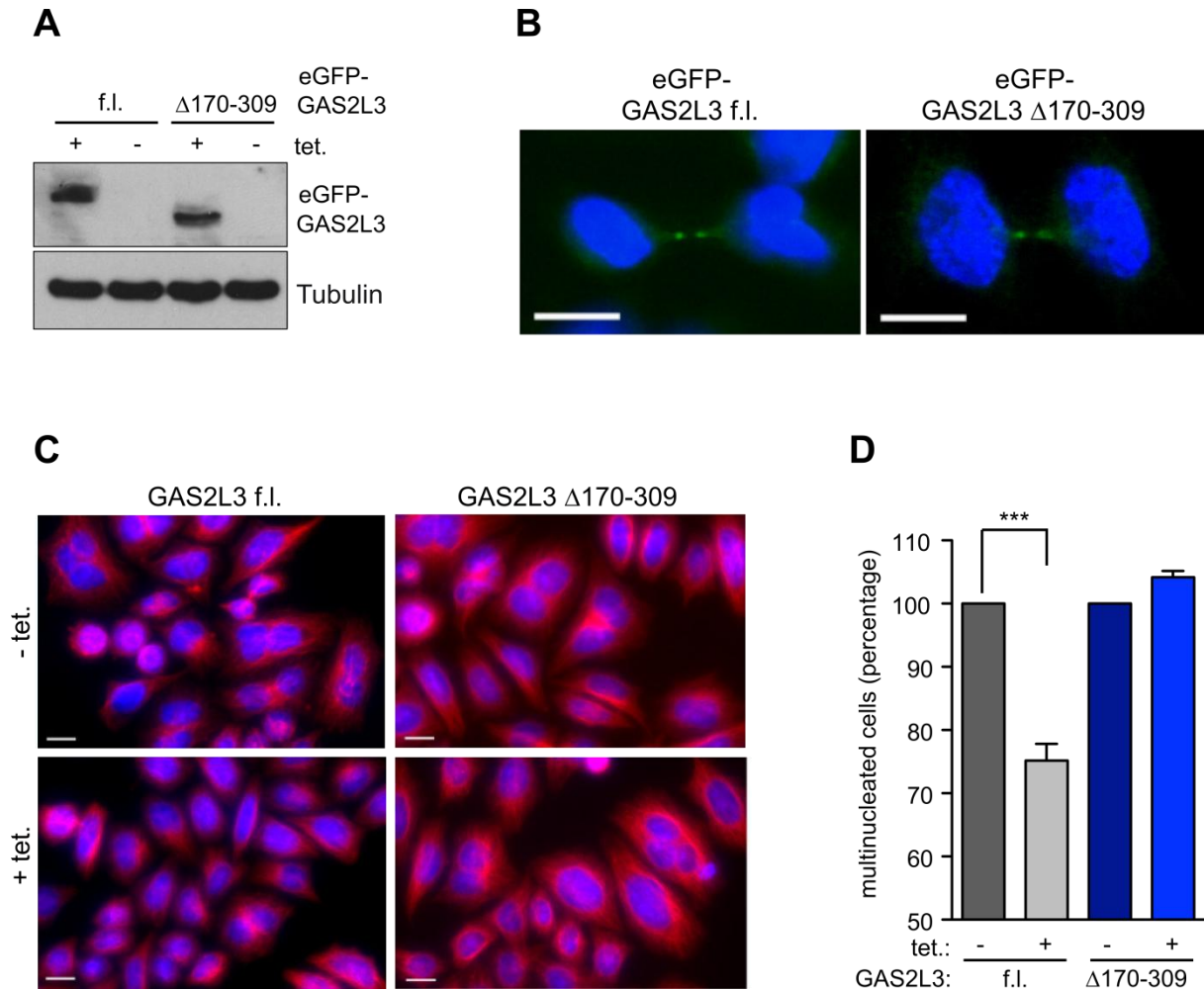
Figure 3.19: The GAR domain of GAS2L3 is necessary for successful completion of cytokinesis. (A) Equal amounts of RNAi-resistant eGFP-GAS2L3 (full length and Δ170-309) proteins are expressed after tetracycline induction. eGFP fusion proteins were immunoprecipitated with GFP antibody detected by immunoblotting with GAS2L3 antibody. (B) eGFP fusion proteins show midbody localization after tetracycline induction. (C) HeLa cells stably expressing tetracycline-inducible and RNAi-resistant eGFP-GAS2L3 (full length and Δ170-309) were pretreated with tetracycline before siRNA transfection as indicated. Nuclei were stained with Hoechst 33258 (blue) and tubulin was counterstained (red). Scale bars: 10 μm. (D) Percentage of multinucleated cells or cells with abnormally shaped nuclei was quantified after GAS2L3 depletion. Quantification results were normalized to untreated control cells. Results are from three independent experiments. More than 400 cells per experiment were counted. Standard deviations between the three experiments are indicated. Figure was first published in Fackler et al., 2014.

3.9. Identification of new interacting proteins of GAS2L3

To identify new interacting proteins of GAS2L3, stable isotope labelling by amino acids in cell culture (SILAC) (section 2.2.3.4) in combination with tandem affinity (TA) purification (section 2.2.3.5) and subsequent mass spectrometrical analysis was used. HeLa cells stably expressing tetracycline inducible HA/Strep/Strep-tagged (HSS-) GAS2L3 were cultivated in "heavy" or "light" SILAC medium for five passages. After successful incorporation of labelled amino acids, expression of HSS-tagged GAS2L3 was induced in cells growing in "heavy" medium while the cells growing in "light" medium were left untreated. To identify interacting

proteins of GAS2L3 specific for early stage of mitosis, cells were trapped in prometaphase by adding nocodazole for 15 hours and harvested by mitotic shake off. For identification of interacting proteins specific for mid-stage and late mitosis, cells were released into fresh medium for 30 and 60 min respectively after nocodazole treatment and harvested (section 2.2.3.4). Cells from all time points were lysed and TA-purification was performed with "heavy" and "light" whole cell lysates (section 2.2.3.5). Final samples were mixed in an equal ratio and separated by Nupage Bis-Tris gel electrophoresis. The gel was stained with colloidal coomassie solution and sent to the Max-Planck-Institute for Biophysical Chemistry, Göttingen where the protein bands were excised, digested with trypsin to achieve small peptids and further analyzed by mass spectrometry. Incorporation of isotopic labelled amino acids ("heavy" amino acids) leads to a mass shift of the corresponding peptide. Comparison of identical peptides with different isotope composition ("heavy" versus "light") by mass spectrometry yields a ratio of intensities, which accurately reflects the abundance ratios for the two peptides respectively proteins. A high "heavy" to "light" ratio represents a high enrichment of the corresponding protein in the HSS-GAS2L3 expressing ("heavy") TA-purification sample compared to the control ("light") sample. This way, interacting proteins can be identified and discriminated from unspecifically bound proteins which have a "heavy" to "light" ratio of about one.

Mass spectrometrical analysis identified 39 proteins with an enrichment value above two. Of all identified proteins, 19 were cytoskeleton-associated proteins, 6 proteins were chaperones or co-chaperones, 8 proteins were involved in gene expression or translation and 6 proteins had other functions (fig 3.20). GAS2L3 was strongly enriched in all three time points (fig 3.20).

no release from nocodazole

gene name	recommended protein name	UniProtKB identifier	fold enrichment
IMPDH2	Inosine-5'-monophosphate dehydrogenase 2	P12268	23,549
LIMA1	LIM domain and actin-binding protein 1	Q9UHB6	19,185
ACTN4	Alpha-actinin-4	O43707	18,586
GAS2L3	GAS2-like protein 3	Q86XJ1	17,479
HSP90AB1	Heat shock protein HSP 90-beta	P08238	14,913
EFHD2	EF-hand domain-containing protein D2	Q96C19	14,83
HSP90AA1	Heat shock protein HSP 90-alpha	P07900	14,211
DBN1	Drebrin	Q16643	13,947
HSPA8	Heat shock cognate 71 kDa protein	P11142	12,214
EEF1A1	Elongation factor 1-alpha 1	P68104	11,481
HSPA1A/1B	Heat shock 70 kDa protein 1A/1B	P08107	10,725
ACTN1	Alpha-actinin-1	P12814	10,562
CAPZB	F-actin-capping protein subunit beta	P47756	10,112
SPTAN1	Spectrin alpha-chain	Q13813	9,3414
TUBB4B	Tubulin beta-4B chain	P68371	8,7675
SPTBN1	Spectrin beta-chain	Q01082	8,2895
PLEC	Plectin	Q15149	8,1855
HNRNPH1	Heterogenous nuclear ribonucleoprotein H	P31943	8,0382
CAPZA1	F-actin-capping protein subunit alpha1	P52907	7,5982
HNRNPM	Heterogenous nuclear ribonucleoprotein M	P52272	6,6445
PSMD2	26S proteasome non-ATPase regulatory subunit 2	Q13200	6,4376
TUBB	Tubulin beta chain	P07437	5,8535
MYH9	Myosin-9	P35579	4,7407
EEF2	Elongation factor 2	P13639	4,0644
HNRNPH3	Heterogenous nuclear ribonucleoprotein H3	P31942	4,0518
IGF2BP3,	Insulin-like growth factor 2 mRNA-binding protein 3	O00425	3,8825
FLNA	Filamin-A	P21333	3,6465
RPL23	60S ribosomal protein L23	P62829	3,5082
VIM	Vimentin	P08670	3,4184
DDX6	Probable ATP-dependent RNA helicase DDX6	P26196	2,4811
ACTBL2	Beta-actin-like protein 2	Q562R1	2,2232
FASN	Fatty acid synthase	P49327	2,1747
HSPA5	78 kDA glucose-regulated protein	P11021	2,0733

30 min release from nocodazole

gene name	recommended protein name	UniProtKB identifier	fold enrichment
GAS2L3	GAS2-like protein 3	Q86XJ1	10,037
BAG2	BAG family molecular chaperone regulator 2	O95816	3,4129
DSG2	Desmoglein-2	Q14126	2,6236
H1F0	Histone H1.0	P07305	2,5495
NES	Nestin	P48681	2,2316
NEXN	Nexilin	Q0ZGT2	2,2035
IMPDH2	Inosine-5'-monophosphate dehydrogenase 2	P12268	2,1387
SMC2	Structural maintenance of chromosomes protein 2	O95347	2,073

60 min release from nocodazole

gene name	recommended protein name	UniProtKB identifier	fold enrichment
GAS2L3	GAS2-like protein 3	Q86XJ1	25,972

Figure 3.20: Mass spectrometrical analysis revealed 38 potentially new GAS2L3 interacting proteins. Gene and recommended protein names are presented together with the UniProt knowledge base identifier. Fold enrichment is given for every protein. GAS2L3 (marked in red) was heavily enriched in all three time points. Only proteins with at least two fold enrichment are shown. Mass spectrometrical analysis was performed by the group of Prof. Dr. Urlaub, MPI Göttingen.

For further validation of the mass spectrometrical results, six proteins from the list which might be connected to the observed *in vivo* phenotype upon loss of GAS2L3 (section 3.10), were chosen to be tested for interaction in co-immunoprecipitation experiments together with HSS-GAS2L3. The cDNAs of Actinin 1, Actinin 4, BAG-2, CapZa1, CapZb and Hsc70 were amplified by PCR and cloned into the pcDNA3_Flag vector. Additionally a Flag-tagged construct of BAG-3, a protein closely related to BAG-2 but not found on the list, was also created. All proteins were successfully overexpressed in HeLa cells stably expressing tetracycline inducible HSS-GAS2L3. Co-immunoprecipitation experiments were performed by incubating whole cell lysates with Strep-Tactin sepharose beads. Bound proteins were separated by SDS-PAGE and analyzed by immunoblotting. All Flag-tagged proteins were detectable in the co-immunoprecipitation samples when HSS-tagged GAS2L3 was present (fig 3.21a). In the absence of exogenously expressed GAS2L3, no Flag-tagged proteins, except Hsc70, were detectable (fig 3.21a). Binding results indicate specific protein interactions between GAS2L3 and all tested proteins, except Hsc70.
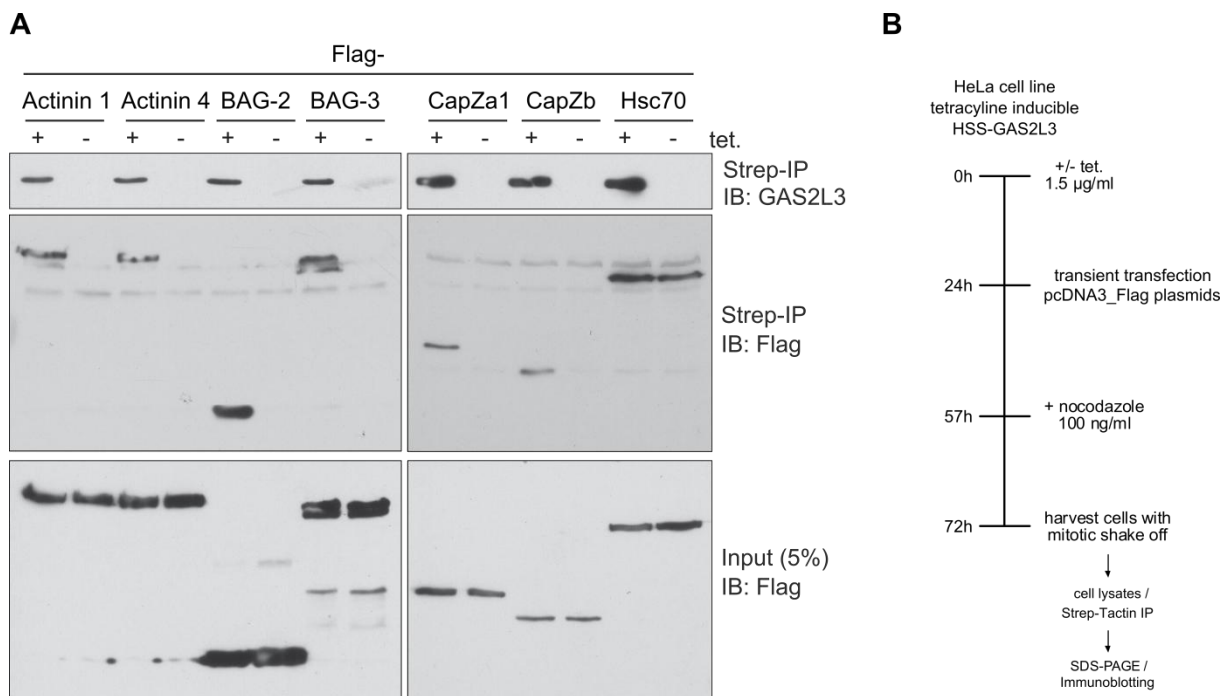
Figure 3.21: GAS2L3 interacts with cytoskeleton associated proteins and co-chaperones identified by mass spectrometrical analysis. Indicated Flag-tagged proteins were transiently overexpressed in HeLa cells stably expressing tetracycline-inducible HSS-tagged GAS2L3. HeLa cells were treated with tetracycline or left untreated and lysed. Whole cell lysates were incubated with Strep-Tactin sepharose beads. Immunoprecipitation experiments were performed and bound Flag-tagged proteins were analyzed by immunoblotting. (B) Flow chart describing the experiment.

In conclusion, SILAC in combination with TA-purification and subsequent mass spectrometrical analysis identified a set of new potential interacting proteins of GAS2L3. By

using co-immunoprecipation experiments the validity of the obtained mass spectrometrical results could be confirmed.

3.10. Establishment of an *in vivo* system to study Gas2l3 function

Expression of GAS2L3 in tissues of a male and a female C57 BL/6 wild type mouse at eight weeks of age was analyzed. Total RNA from 15 different tissues was prepared and transcribed to cDNA. By using quantitative PCR, tissue specific expression levels of GAS2L3 relative to the housekeeping gene hypoxanthine-phosphoribosyltransferase 1 (Hprt-1) were determined. For better comparability, the obtained expression data was normalized to the tissue with the lowest expression. GAS2L3 mRNA was detectable in all analyzed tissues (fig 3.22). Thymus, small intestine and spleen showed highest expression level, while fat tissue and kidney showed lowest GAS2L3 expression (fig 3.22).
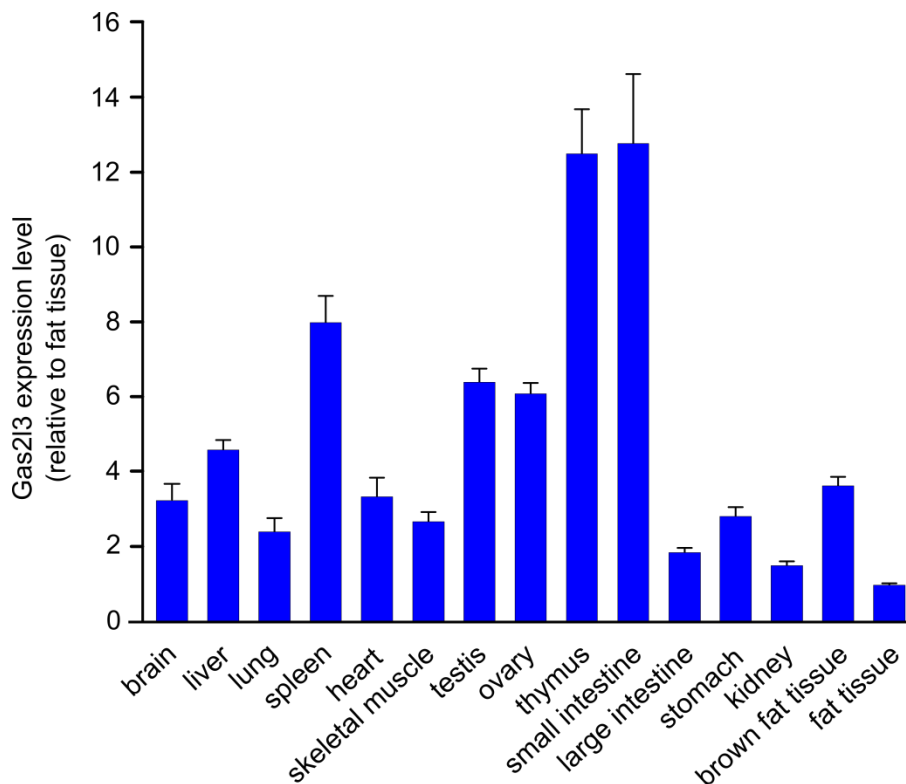
Figure 3.22: GAS2L3 is ubiquitously expressed in mouse tissues. Total RNA from the indicated mouse organs was prepared and reverse transcribed to cDNA. The expression level of GAS2L3 in the different mouse tissues was determined by qPCR and normalized to the tissue with lowest expression (fat tissue). GAS2L3 expression was analyzed in tissues of eight weeks old C57 BL/6 wild type mice.

GAS2L3 was identified as a protein playing an important role in mitosis, cytokinesis and maintenance of genomic stability (Wolter et al., 2012). To get a deeper insight into the *in vivo* function of GAS2L3, a knockout mouse was generated in collaboration with the Max-Planck-Institute of Molecular Cell Biology and Genetics, Dresden. Two different embryonic stem (ES) cell clones already carrying a targeted Gas2l3 allele were obtained from the European

Conditional Mouse Mutagenesis (EUCOMM) program. All EUCOMM cell lines are derived from an ES cell line with C57 BL/6N genetic background. In those ES cells one non-agouti locus was replaced by the dominant agouti wild type locus, which allows identification of ES cell-derived mice by agouti coat color (Pettitt et al., 2009). The Gas2l3$^{ta/+}$ ES cell clones were created by gene targeting of one Gas2l3 allele using a targeting vector with conditional potential (EUCOMM ID: 45033). The exon six of the Gas2l3 gene is flanked by loxP sites (floxed) in the targeted Gas2l3 allele (fig 3.23a). The targeted allele harbours an insertion cassette located between two flippase recognition target (FRT) sites. The insertion cassette consists of a splice acceptor site (EN2), followed by an internal ribosome entry site (IRES) and the beta-galactosidase reporter gene (ßgal). Furthermore it contains a neomycin resistance gene driven by the human beta actin promotor (ßact::neo). Correct orientation of the insertion cassette in the targeted Gas2l3 allele was verified by long range PCR using gene and insertion cassette specific primers (fig 3.23). Two primer pairs were used for each site of the insertion cassette (fig 3.23a&b). Correct orientation of the 3' site could be verified by long range PCR in both ES cell clones (fig 3.23c). The two primer pairs specific for the 5' site did not yield any PCR product (data not shown).
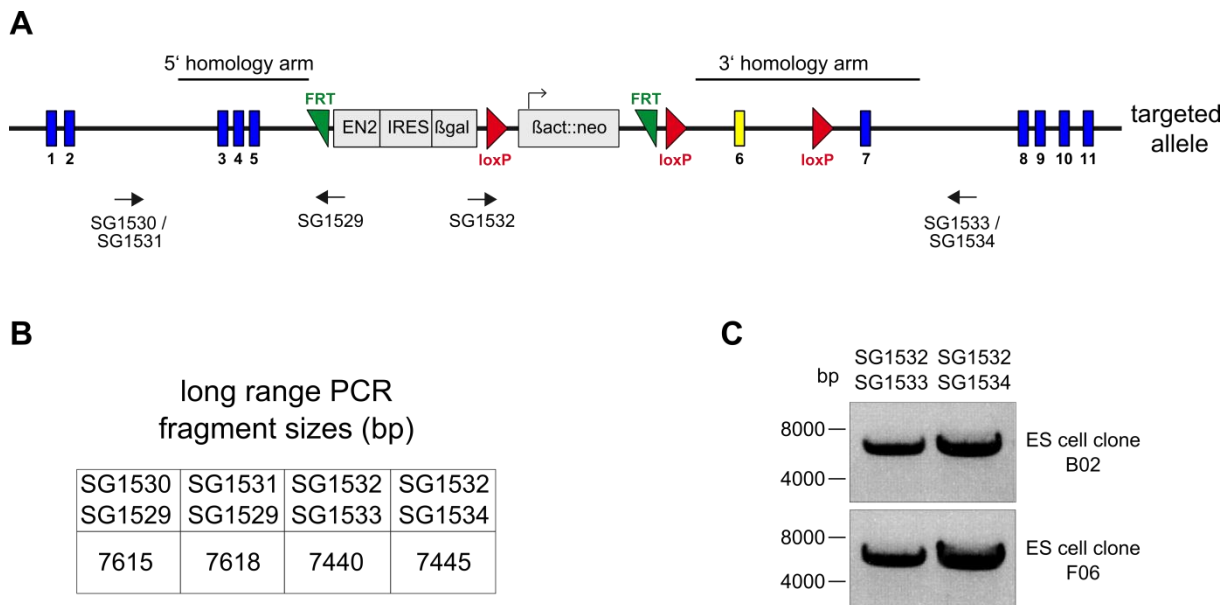
A

B

long range PCR
fragment sizes (bp)

SG1530 SG1529	SG1531 SG1529	SG1532 SG1533	SG1532 SG1534
7615	7618	7440	7445

C

Figure 3.23: Long range PCR confirms correct orientation of the insertion cassette in the targeted Gas2l3 allele of embryonic stem cells. (A) Location of the primers used for long range PCR. (B) Long range PCR fragment sizes obtained by the different primer pairs. (C) Correct orientation of the insertion cassette was confirmed in two different embryonic stem cell clones harboring the targeted Gas2l3 allele. EN2: splice acceptor site, IRES: internal ribosome entry site, ßGal: ß-Galactosidase, ßact::neo: neomycin resistance gene under control of ß-actin promoter, FRT: flippase recognition target, loxP: locus of X-over P1, bp: base pairs

Chimeric mice were generated by transfer of embryonic stem cells to blastocysts and subsequent implantation into uteri of foster mice. Chimeric mice were born and mated to C57

BL/6 mice. Germline transmission of the targeted allele was confirmed by genotyping the offspring pubs with primers specific for the targeted allele by PCR (data not shown). After presence of the targeted allele was verified, positive tested mice were transferred to the mouse facility of the Biocenter Würzburg. Figure 3.24 gives an overview of the breeding strategy for generation of conditional (fig 3.24a) and knockout alleles (fig 3.24b) of Gas2l3.
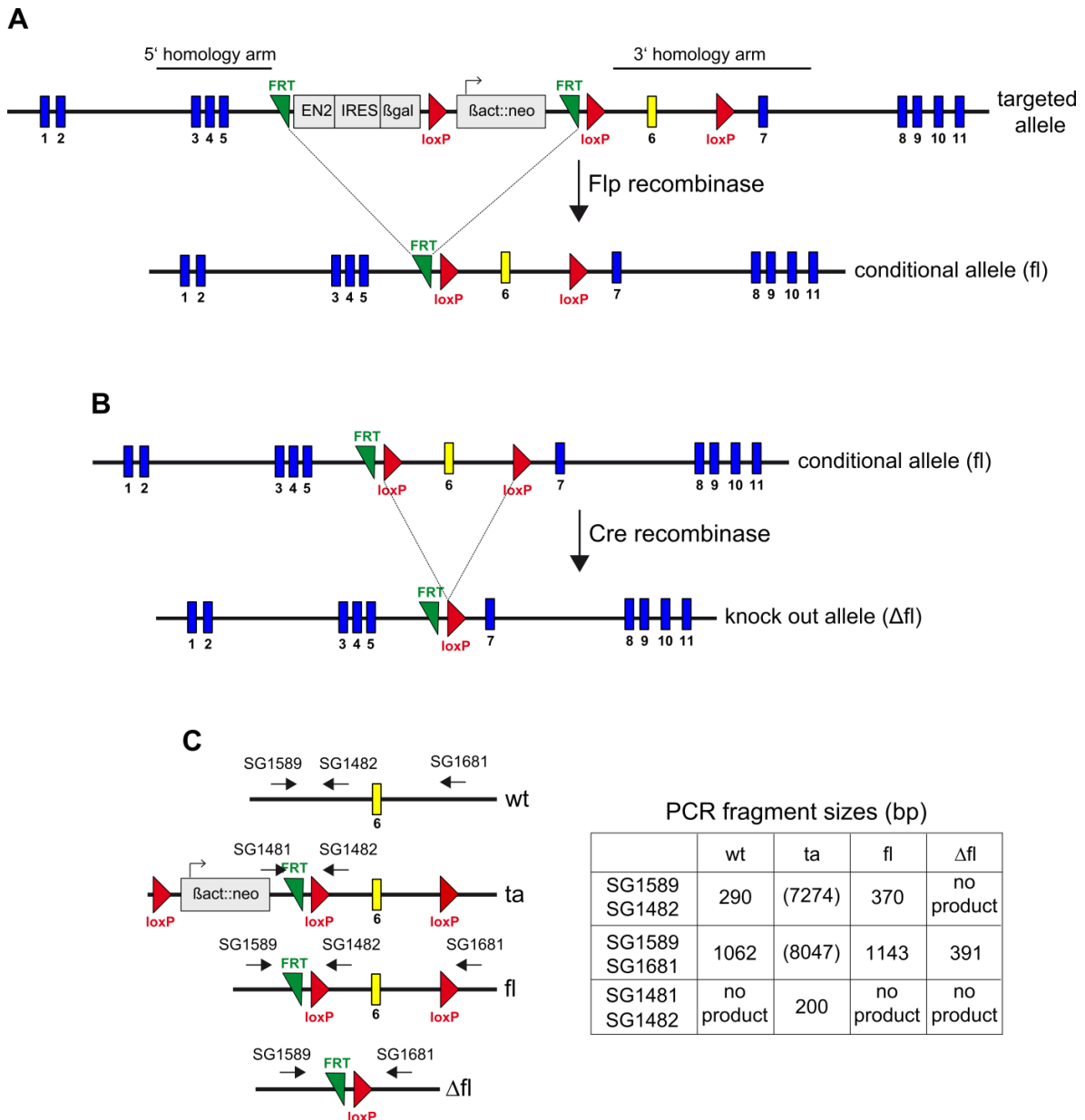
Figure 3.24: Breeding strategy for generation of conditional and knockout alleles of Gas2l3. (A) Mice harboring the targeted allele of Gas2l3 were crossed with Flp recombinase expressing mice to delete the insertion cassette between the FRT sites. The resulting conditional (fl) allele contains one FRT site and two loxP sites flanking exon 6. B) Mice with fl allele were further crossed with Cre recombinase expressing mice to delete the loxP flanked exon 6. The resulting knockout (Δfl) allele contains one FRT site and one loxP site. (C) Location of the primers used for genotyping of the different alleles. The fragment sizes for the different genotyping PCRs are depicted in the table on the right side. Values in brackets represent theoretical fragment sizes. EN2: splice acceptor site, IRES: internal ribosome entry site, ßGal: ß-Galactosidase, ßact::neo: neomycin resistance gene under control of ß-actin promoter, FRT: flippase recognition target, loxP: locus of X-over P1, wt: wild type, ta: targeted, fl: floxed (flanked by loxP sites), Δfl: deleted floxed (knockout), bp: base pairs

Deletion of the floxed exon on genomic DNA level creates a mutated version of the Gas2l3 gene. The mutated gene is transcribed into a frame shifted Gas2l3 mRNA, which in turn encodes for a truncated non-functional Gas2l3 protein. All the pubs obtained from every breeding step were genotyped by using PCR in combination with allele specific primers (fig 3.24c). All expected PCR fragment sizes are shown (fig 3.24c).

Mice harboring the targeted allele were crossed with mice expressing flippase (Flp) recombinase constitutively under control of the human ACTB promoter (Rodríguez et al., 2000) to delete the insertion cassette between the flippase recognition target (FRT) sites. By performing this breeding step, mice with a conditional allele of Gas2l3 (also called floxed or fl allele) were created. A breeding scheme including possible genotypes is shown in figure 3.25a. The offspring was genotyped by using PCR with primers specific for the targeted and floxed allele (fig 3.25b). Presence of Flp recombinase was verified by PCR (fig 3.25b). All mice carrying the floxed allele were positively tested for Flp recombinase while mice still carrying the targeted allele did not harbor Flp recombinase (fig 3.25b). Deletion of the insertion cassette and correct recombination of the allele was verified by sequencing the PCR product resembling the floxed allele (data not shown).
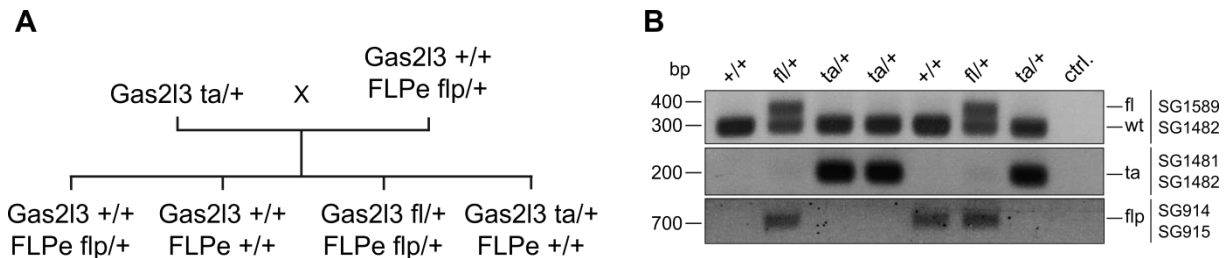
Figure 3.25: Breeding strategy for mice harboring a conditional Gas2l3 allele. (A) Gas2l3$^{ta/+}$ mice were crossed with a mouse strain expressing Flp recombinase to obtain mice with conditional (floxed) Gas2l3 allele. (B) Mice were genotyped by using PCR. All mice carrying the conditional allele were tested positive for Flp recombinase and negative for the targeted allele. Gas2l3 genotypes are indicated on top.

To create a conditional, tamoxifen inducible knockout strain, Gas2l3$^{fl/+}$ mice were crossed with CreER^{T2} mice. This strain expresses CreER^{T2} recombinase in every tissue after tamoxifen induction and can be used for conditional deletion of floxed exons located between the locus over X-over P1 (loxP) sites *in vivo* (Hameyer et al., 2007). The offspring was genotyped with PCR by using primers specifically recognizing the floxed Gas2l3 and the CreER^{T2} allele (data not shown). Gas2l3$^{fl/+}$ CreER$^{T2\ cre/+}$ mice were further intercrossed to create mice homozygous for both alleles. The offspring was genotyped with the above mentioned PCR protocol. All mice were healthy and the genotypes were present in the expected mendelian ratio (data not shown).

To have an inducible Gas2l3 knockout system for cell culture based assays available, mouse embryonic fibroblasts (MEFs) were isolated from embryos derived from crosses of Gas2l3$^{fl/+}$ with Gas2l3$^{fl/+}$ CreER$^{T2\ cre/cre}$ mice (fig 3.26a). The prepared MEF clones were genotyped by PCR using specific primers for the conditional Gas2l3 and the CreER^{T2} alleles (fig 3.26b). All obtained clones were CreER^{T2} positive, while the Gas2l3 genotype was either wild type (Gas2l3$^{+/+}$), heterozygous (Gas2l3$^{fl/+}$) or homozygous (Gas2l3$^{fl/fl}$) for the floxed Gas2l3 allele (fig 3.26b).
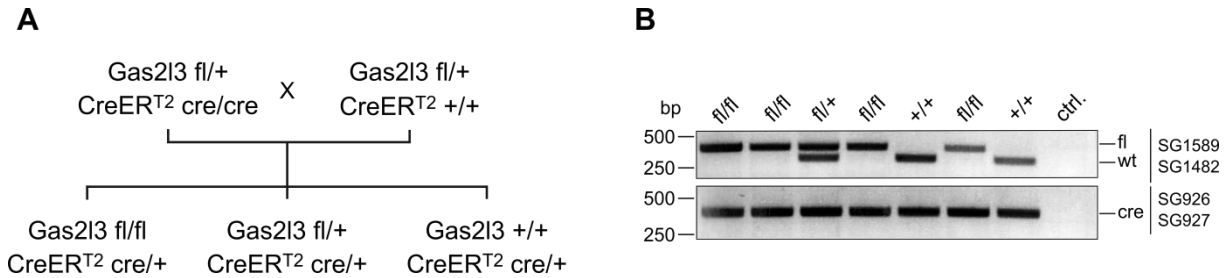
A

B

Figure 3.26: Breeding strategy for isolation of Gas2l3$^{fl/fl}$ CreER$^{T2\ cre/+}$ mouse embryonic fibroblasts. (A) Gas2l3$^{fl/+}$ CreER$^{T2\ cre/cre}$ mice were crossed with Gas2l3$^{fl/+}$ CreER$^{T2\ +/+}$ mice to obtain embryos for isolation of mouse embryonic fibroblasts (MEFs). (B) MEFs were genotyped by using PCR. All MEF clones were tested positive for Cre recombinase. Gas2l3 genotypes are indicated on top.

Inducibility of gene knockout in Gas2l3$^{fl/fl}$ CreER$^{T2\ cre/+}$ MEFs by tamoxifen was verified. Cells were treated with 4-hydroxytamoxifen (OHT) or were left untreated and genomic DNA and total RNA was prepared. Efficiency of Cre mediated recombination on genomic level was verified by PCR (fig 3.27a). Total RNA was transcribed to cDNA and successful deletion of the floxed exon was verified by quantitative PCR using exon specific primers (fig 3.27b). To verify that expression of Gas2l3 protein is lost in Gas2l3$^{fl/fl}$ CreER$^{T2\ cre/+}$ MEFs after tamoxifen induction, immortalized cells were treated with OHT or were left untreated, whole cell lysates were prepared and Gas2l3 was immunoprecipitated. To confirm identity of the protein and specificity of the antibody, HA-tagged murine Gas2l3 was transiently overexpressed in HEK 293 cells and immunoprecipitated with Gas2l3 and HA specific antibodies. The samples obtained from the HEK 293 cells and MEFs were loaded onto the same polyacrylamide gel, separated by SDS-PAGE and analyzed in parallel by immunoblotting. It could be confirmed that Gas2l3 protein expression was lost in Gas2l3$^{fl/fl}$ CreER$^{T2\ cre/+}$ MEFs after OHT treatment (fig 3.27c).
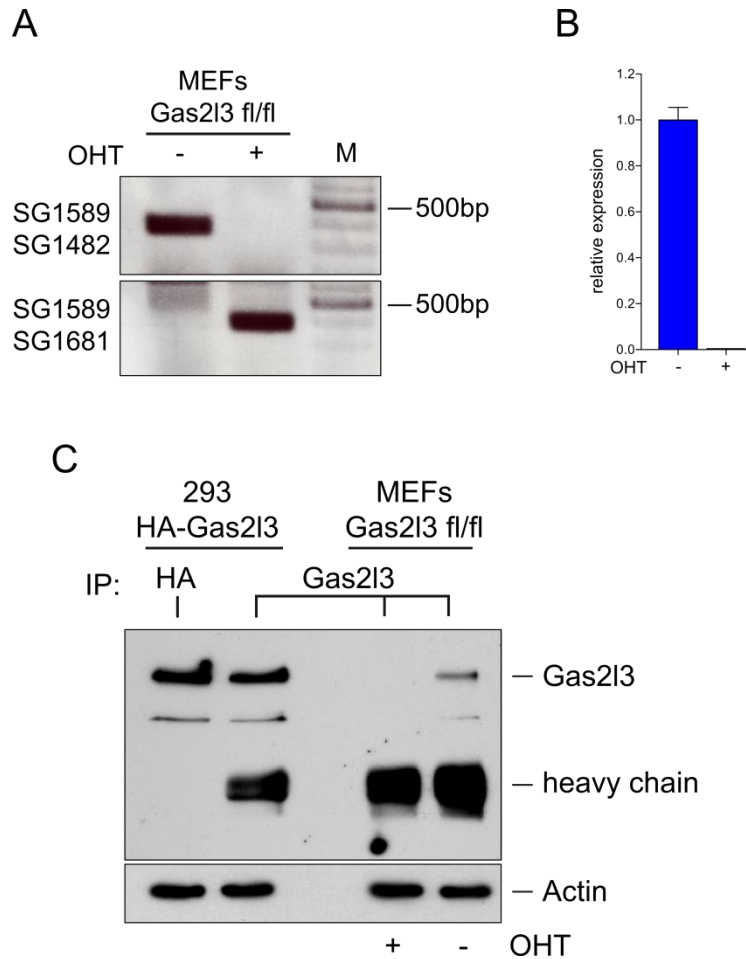
Figure 3.27: Gas2l3 expression is lost in Gas2l3$^{fl/fl}$ CreER$^{T2\ cre/+}$ MEFs after hydroxytamoxifen administration. (A) Knockout of Gas2l3 on genomic DNA level after OHT treatment was verified by performing genotyping PCR with the indicated primers. (B) Loss of full length Gas2l3 mRNA in OHT treated MEFs was verified by using qPCR. Primers specifically recognizing the floxed exon of Gas2l3 mRNA were used. (C) Gas2l3 protein is not detectable any more after OHT treatment. Whole cell lysates of immortalized Gas2l3$^{fl/fl}$ CreER$^{T2\ cre/+}$ MEFs were incubated with GAS2L3 antibody. Immunoprecipitation experiments were performed and amount of bound Gas2l3 was analyzed by immunoblotting. To verify the identity of the endogenous protein, murine HA-tagged Gas2l3 was transiently overexpressed in HEK 293 cells and immunoprecipitated with HA and GAS2L3 antibody. Immunoprecipitation experiments were performed and samples were analyzed together with the endogenous protein samples by immunoblotting.

To create a non-conditional knockout strain, Gas2l3$^{fl/+}$ mice were crossed with Zp3cre mice. This strain expresses Cre recombinase under control of the Zona pellucida 3 (Zp3) promoter and can be used for germline deletion of floxed alleles (de Vries et al., 2000). The offspring was genotyped by PCR using primers specific for the floxed Gas2l3 and the Cre allele (data not shown). Females heterozygous for both alleles (Gas2l3$^{fl/+}$ and Zp3cre$^{cre/+}$) were mated with C57 BL/6 wild type males to achieve germline deletion of Gas2l3. The offspring was genotyped by PCR using primers specifically recognizing Gas2l3 knockout and wild type allele. Heterozygous mice (Gas2l3$^{\Delta fl/+}$) were intercrossed to create non-conditional Gas2l3

knockout mice (fig 3.28a). The offspring was genotyped by using the same PCR protocol already mentioned (fig 3.28b).

A

B
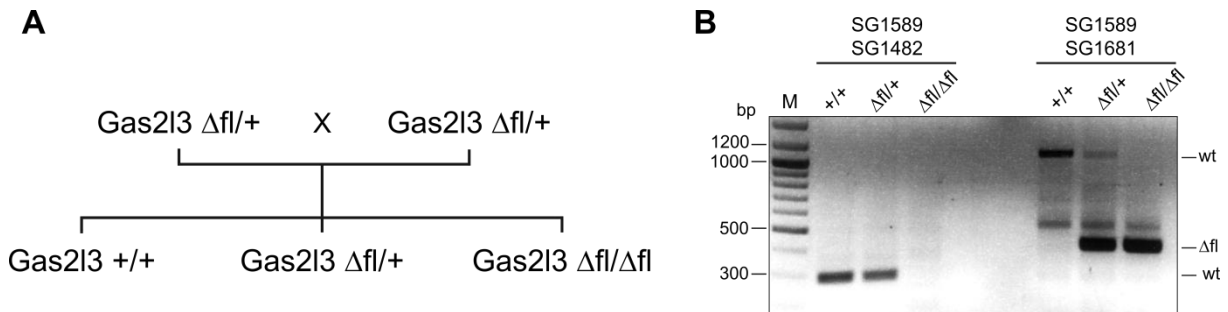
Figure 3.28: Breeding strategy to generate non-conditional Gas2l3 knockout mice. (A) Gas2l3$^{\Delta fl/+}$ mice were intercrossed to obtain non-conditional Gas2l3$^{\Delta fl/\Delta fl}$ knockout mice. (B) Mice were genotyped by using PCR. A genotyping example of a wild type, a heterozygous and a knockout mouse is shown.

At weaning age (approximately 21 days), only ten out of a total of 187 mice were identified to have a Gas2l3 knockout genotype (Δfl/Δfl) (fig 3.29). All other mice showed either wild type (+/+) or heterozygous (Δfl/+) Gas2l3 genotype (fig 3.29).

genotype	observed	expected
+/+	58	46.75
Δfl/+	119	93.50
Δfl/Δfl	10	46.75
total	187	187.00

Figure 3.29: Loss of Gas2l3 leads to an increase in mortality. Breeding pairs were set up by mating two heterozygous Gas2l3$^{\Delta fl/+}$ females with one heterozygous Gas2l3$^{\Delta fl/+}$ male. In total, seven breeding pairs were set up. Pubs were genotyped at three weeks of age. Only ten knockout mice were obtained from a total of 187 mice.

Knockout mice which survived post weaning age were phenotypically normal but died suddenly between 4 and 16 weeks of age. To analyze if male and female Gas2l3$^{\Delta fl/\Delta fl}$ mice are fertile, a breeding pair of knockout mice was set up. Pubs were born and genotyped by PCR using specific primers for the wild type and knockout allele. All pubs harbored two Gas2l3 knockout (Δfl) alleles (fig 3.30).
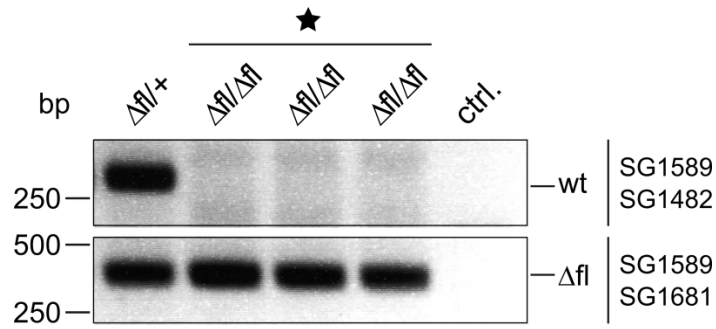
Figure 3.30: Gas2l3 knockout mice are fertile. Male and female Gas2l3 knockout mice were intercrossed, offspring pubs were born and genotyped by PCR after weaning. Genotyping result indicates that all pubs from the litter (marked by the black star) showed knockout genotype. As positive control a heterozygous mouse was genotyped in parallel.

Knockout mice were sacrificed and organs were analyzed macroscopically. Most of the organs looked normal, except the heart which was severely hypertrophic showing heavily enlarged atria and ventricles (data not shown). This heart specific phenotype was observed in 8 different knockout mice ranging between 4 and 16 weeks of age (data not shown). Expression analysis in mouse organs showed (fig 3.22) that Gas2l3 is only moderately expressed in adult heart muscle. To further analyze if Gas2l3 is strongly expressed during heart development, expression level of Gas2l3 relative to Hprt-1 was analyzed by quantitative PCR in rat heart cDNA samples from embryonic, postnatal and adult stages. For better comparability, the obtained expression data was normalized to the developmental stage with lowest expression. Gas2l3 expression level was declining during heart development, showing highest expression at embryonic stages and lowest expression at adult stage (fig 3.31). Rat1 cells were used as positive control (fig 3.31).
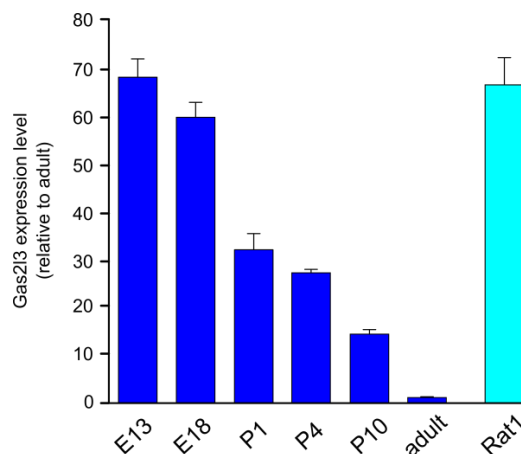
Figure 3.31: Expression of Gas2l3 is declining during rat heart development. Total RNA from heart was prepared at the indicated developmental stages and reverse transcribed to cDNA. The expression level of Gas2l3 at different developmental stages was determined by qPCR and normalized to the stage with lowest expression (adult stage). Rat1 cells were used as a positive control. E: embryonic day, P: postnatal day. cDNA samples were a gift from Prof. Dr. Engel, University of Erlangen

4. Discussion

GAS2L3 was identified as a target gene of the DREAM complex in a microarray screen performed in Lin9 knockout MEFs (Reichert et al., 2010). Experiments revealed that GAS2L3 is important for maintenance of genomic stability (Wolter et al., 2012). The main tasks of this thesis were to further characterize the biochemical properties and physiological functions of GAS2L3 and to establish a knockout mouse model.

4.1. GAS2L3 is regulated during cell cycle

It was shown that GAS2L3 is regulated during cell cycle on transcriptional level in a DREAM complex dependent manner and that its expression peaks during G2/M phase of the cell cycle (Wolter et al., 2012). Because it is known that a high mRNA transcription level does not necessarily correlate with a high expression level of the coded protein (Vogel and Marcotte, 2012), protein levels of endogenous GAS2L3 were analyzed in synchronized cells (fig 3.1a). It could be verified that expression of GAS2L3 peaks during G2 and M phase of the cell cycle, while it was undetectable in G1 phase and asynchronously growing cells confirming the RNA expression data (Wolter et al., 2012). In concordance with this finding a recent study reported, that GAS2L3 is targeted for ubiquitylation by the APC/C^{Cdh1} but not by the APC/C^{Cdc20} complex at the end of mitosis and degraded by the proteasome in a D-box dependent manner (Pe'er et al., 2013).

4.2. GAS2L3 is important for proper cytokinesis

It was reported that depletion of GAS2L3 leads to formation of multinucleated cells (Schmitt, 2010). To analyze the observed phenotype and the cellular consequences upon depletion of GAS2L3 in more detail, the protein was depleted with siRNAs (fig 3.2). Experiments revealed that depletion of GAS2L3 significantly increased the percentage of multinucleated cells or cells with abnormally shaped multi-lobed nuclei compared to untreated control cells (fig 3.2c). This finding confirmed former results and demonstrated that GAS2L3 protein function is important for maintenance of nucleus integrity in HeLa cells.

4.3. GAS2L3 is a cytoskeleton associated protein

GAS2L3 harbors two conserved domains which are implicated in cytoskeleton interaction (section 1.3). Former localization studies confirmed that GAS2L3 is associated with the microtubule cytoskeleton in cells (Wolter et al., 2012). To further characterize which protein domains are directly involved in cytoskeleton interactions, *in vitro* co-sedimentation assays were performed with a set of GAS2L3 deletion mutants (fig 3.3 & 3.4).

Full length GAS2L3 interacted with F-actin *in vitro* (fig 3.3). Further co-sedimentation assays revealed that the N-terminal as well as the C-terminal part of GAS2L3 is able to interact with F-actin. The N-terminus of GAS2L3 was assumed to be interacting with F-actin because it harbors the conserved CH domain, a known F-actin binding domain (section 1.3). The interaction of the C-terminal part of GAS2L3 with F-actin was not expected because it does not contain any known F-actin binding domain. Interestingly it was shown that the C-terminus harbors at least two different, non-overlapping F-actin binding regions (fig 3.3).

Microtubule (MT) co-sedimentation assays further revealed that binding of GAS2L3 to MTs is mediated by the C-terminal part of the protein (fig 3.4). This result was surprising, because it was assumed that the MT binding is mediated by the conserved GAR domain, which is reported to be a MT binding domain at least in GAS2L1, GAS2L2 and MACF (Goriounov et al., 2003; Sun et al., 2001). Interestingly the data shows that the C-terminus contains at least two different, non-overlapping MT binding regions (fig 3.4) which cannot be clearly separated from the C-terminally located F-actin binding regions. Another study confirmed the *in vitro* interaction of GAS2L3 with MTs and F-actin (Stroud et al., 2011). Although this report confirmed the observation that GAS2L3 interacts with F-actin by the CH domain and with MTs by its C-terminus and not by its GAR domain, it failed to show an interaction of the C-terminus with F-actin (Stroud et al., 2011).

The C-terminus of GAS2L3 does not contain any conserved MT or F-actin binding domain. From other cytoskeleton associated proteins it is known that the interactions with MTs and F-actin are mediated by electrostatic forces due to differently charged surfaces. The positively charged N-terminal part of the Ndc80 protein complex for example binds to negatively charged C-terminal tails of tubulin molecules (section 1.4.5.1). The C-terminus of GAS2L3 has also a positive net charge (+49) which could contribute to the interaction with negatively charged MTs and F-actin.

Combination of F-actin and MT co-sedimentation assay further revealed that full length GAS2L3 and the C-terminal part are able to crosslink MTs and F-actin *in vitro* what can be explained by the observation that the C-terminus harbors at least two non-overlapping MT and F-actin binding domains. This assay also demonstrated that the N-terminal part of GAS2L3 has an F-actin bundling activity probably mediated by the CH domain. Additionally an *in vitro* MT bundling assay was performed (fig 3.7), which clearly showed that the C-terminal part and full length GAS2L3 protein is able to bundle MTs *in vitro*.

Taken together all the *in vitro* binding data it was clearly demonstrted that GAS2L3 is a cytoskeleton associated protein which is able to bundle and bind to MTs and F-actin *in vitro*. It is tempting to speculate what the exact function of the interaction with the cytoskeleton

network is. One possible explanation might be that GAS2L3 acts as a cytolinker which is involved in the regulation of the MT and actin cytoskeleton. This idea was also proposed by another study which also showed that binding strength of GAS2L3 to MTs and F-actin is regulated by the GAR domain (Stroud et al., 2011). Compared to other known cytoskeleton crosslinking proteins like the giant spectraplakins (section 1.3), GAS2L3 is a quite small protein, what makes a general cytolinker function (connecting F-actin and MTs in the cell over long distances) not very likely. It is more plausible that GAS2L3 acts as a G2/M phase specific crosslinking protein which is involved in crosstalk of actin and microtubule cytoskeleton. GAS2L3 might participate in processes like positioning of the cleavage furrow where crosslinking of the actin and microtubule cytoskeleton is needed in close proximity. Interestingly it was shown by time-lapse microscopy that the observed phenotype after GAS2L3 depletion (fig 3.2) is not mediated by failure of cleavage furrow ingression but rather by abnormal oscillations of the mitotic spindle and chromatin starting at the end of mitosis (Wolter et al., 2012). Similar oscillation phenotypes were also reported after depletion of proteins like Anillin and mDia2 which are known to play important roles in positioning of the cleavage furrow (Piekny and Glotzer, 2008; Straight et al., 2005; Watanabe et al., 2008; Zhao and Fang, 2005).

4.4. GAS2L3 interacts with the chromosomal passenger complex

Pulldown experiments were performed to identify new interacting proteins of GAS2L3. In initial experiments Aurora B, the catalytic subunit of the CPC (section 1.4.3), was identified as a potential interaction partner of GAS2L3. Further *in vitro* pulldown experiments confirmed the interaction and showed that the GAR domain is necessary and sufficient to mediate binding to the CPC (fig 3.9).

Experiments with recombinant CPC and GAS2L3 proteins revealed that Borealin and Survivin but not Aurora B are directly interacting with GAS2L3 (fig 3.10). Domain specific characterization demonstrated that the observed interactions are mediated between the GAR domain of GAS2L3 and the C-terminal part of Borealin as well as the N-terminal part of Survivin (fig 3.11). Interestingly the domains of Borealin and Survivin involved in the interaction with GAS2L3 are not incorporated into the triple helix bundle which is formed by the N-terminal parts of Borealin and Incenp and the C-terminal part of Survivin (fig 3.12) (section 1.4). It is known that the BIR domain located in the N-terminus of Survivin is important for proper positioning of the CPC to centromeres by binding phosphorylated Thr 3 of Histone H3 (section 1.4.4). Although localization of GAS2L3 to centromeres could not be detected in cells, GAS2L3 might still be somehow involved in regulating this interaction. Apart from the *in vitro* binding assays the interaction between the CPC and GAS2L3 was also verified in living cells by co-immunoprecipitation experiments (fig 3.13).

4.5. GAS2l3 is phosphorylated by CDK1 but not by Aurora B

Kinase assays revealed that GAS2L3 was not phosphorylated by Aurora B but strongly phosphorylated by CDK1 *in vitro* (fig 3.14). This finding is in concordance with another study which reported recently that GAS2L3 is phosphorylated by CDK1 in HEK 293 cells in late mitosis (Pe'er et al., 2013). In this study the two phosphosites Ser 307 and Ser 607 were identified while in our *in vitro* phosphorylation experiments eight different CDK1 phosphosites could be identified by mass spectrometrical analysis (fig 3.15a). Importantly Ser 307 was also found to be phosphorylated in our experiments while phosphorylation of Ser 607 was not detected (fig 3.15a). All identified phosphosites were located in the C-terminal part of GAS2L3 (fig 3.15b) which mediates binding to MTs and F-actin (fig 3.5). From other cytoskeleton associated proteins it is known that the binding affinity to MTs and F-actin is regulated by phosphorylation (section 1.4.5.1). It is tempting to speculate that phosphorylation of the C-terminal part of GAS2L3 by CDK1 might also influence binding affinity for F-actin and/or MTs and by this regulate function or localization of the protein.

4.6. Depletion of GAS2L3 influences stability and activity of the CPC

It was shown that depletion of GAS2L3 leads to a slight reduction of Borealin and Survivin protein levels compared to the untreated control while the amount of Aurora B was not altered (fig 3.16). The two CPC substrates CENPA and Histone H3 showed also a slight decrease in phosphorylation at serine 7 and serine 10 upon GAS2L3 depletion indicating a reduced overall activity of the CPC (fig 3.16).

It is tempting to speculate that GAS2L3 acts as a stabilizer or scaffold of the CPC and that loss of GAS2L3 destabilizes the direct interaction partners Borealin and Survivin and by this the whole CPC. It was reported that the two CPC members Borealin and Survivin are influencing the protein stability of each other, although the exact mechanism of this interdependent regulation is not fully clear. In 2004 it was shown that depletion of Borealin leads to degradation of Survivin while stability of Aurora B and Incenp was not altered (Gassmann et al., 2004). Another study reported in 2012 however that loss of Borealin not only leads to degradation of Survivin but also of the other CPC proteins (Liu et al., 2012). Interestingly the C-terminal part of Borealin, the region which is directly interacting with GAS2L3, was shown to be involved in regulation of Borealin stability (Date et al., 2012). This might explain the reduction in protein levels upon GAS2L3 depletion and further strengthens the hypothesis that GAS2L3 acts as a stabilizer or scaffold of the CPC and by this indirectly influences CPC activity.

Another possible explanation for the reduction in overall CPC activity would be that loss of GAS2L3 negatively influences the localization of the CPC. In such a scenario mislocalization

of the CPC would result in reduced CPC activity and decreased phosphorylation of CPC substrates. Immunofluorescence microscopy experiments however showed that depletion of GAS2L3 does not lead to mislocalization of Aurora B respectively the CPC in mitosis and cytokinesis (data not shown and Wolter et al., 2012) what raises doubts that GAS2L3 is involved in proper localization of the CPC.

It is known that inhibition of Aurora B activity leads to cytokinesis failure and multinucleation (Ruchaud et al., 2007). To further investigate, if the phenotype upon GAS2L3 depletion (fig 3.2) is connected to the observed decrease in CPC activity (fig 3.16), pharmacological inhibition of Aurora B with the chemical inhibitor AZD1152 was used (Mortlock et al., 2007). It was found out that low concentrations of AZD1152 were sufficient to phenocopy GAS2L3 depletion (fig 3.17a). Importantly, the used concentration of AZD1152 did not significantly increase the fraction of cells with abnormally shaped nuclei compared to untreated control cells (fig 3.17b). This observation is in concordance with a recent study reporting that the used concentration of AZD1152 is a subcritical dose which does not lead to cytokinesis defects (Moulding et al., 2012). The decrease in CPC activity mediated by GAS2L3 depletion is obviously not strong enough to be responsible for the observed cytokinesis phenotype upon GAS2L3 depletion.

4.7. Localization of GAS2L3 to the constriction zone depends on the GAR domain

To further address if the GAR domain is important for proper localization of GAS2L3, full length eGFP-GAS2L3 and Δ170-309 mutant were transiently overexpressed in HeLa cells and cellular localization was analyzed. Both proteins co-localized with the MT cytoskeleton during interphase (fig 3.18). This finding was in concordance with the fact, that both proteins harbor the C-terminally located MT binding region identified by *in vitro* co-sedimentation assays (fig 3.4). As reported previously (Wolter et al., 2012) full length GAS2L3 localized to the midbody during cytokinesis (fig 3.18). Although the GAS2L3(Δ170-309) mutant protein was still present at the cytokinetic bridge, it localized more distal from the midbody compared to the wild type protein (fig 3.18). It was reported that GAS2L3 co-localizes with Aurora B at the midbody (Pe'er et al., 2013; Wolter et al., 2012), so it was tempting to speculate that the observed mislocalization of the GAS2L3(Δ170-309) mutant protein might be connected to the loss of interaction with the CPC. Immunofluorescence microscopy experiments and subsequent line scan analysis revealed that GAS2L3(Δ170-309) did not co-localize with Aurora B at the midbody, while a clear co-localization between Aurora B and full length GAS2L3 protein was detectable (Fackler et al., 2014). Furthermore it was shown that full length GAS2L3 is flanked by Aurora B at the midbody and GAS2L3 fluorescent signal peaks, where Aurora B and Tubulin signals are less intense (Fackler et al., 2014; Pe'er et al., 2013).

Higher resolution imaging revealed that full length GAS2L3 localized about 1-2 μm away from the midbody center exactly to the constriction zone, while the GAS2L3(Δ170-309) mutant protein was excluded from this region (Fackler et al., 2014). The constriction zone corresponds to the narrowest part of the microtubule bridge connecting the proto-daughter cells and it represents the area where abscission takes place at the end of cytokinesis. It can be easily identified by a less intense immunofluorescence signal of Tubulin and other proteins like Aurora B or Mklp2, which is probably caused by densely packed proteins and microtubules hardly accessible for antibodies during immunofluorescence labelling (Elia et al., 2011; Guizetti et al., 2011; Hu et al., 2012; Raiborg and Stenmark, 2011). Due to the fact that the midbody is a highly dynamic cellular structure, the different localization patterns of full length GAS2L3 and the Δ170-309 deletion mutant during cytokinesis were further confirmed and validated by using Spastin and the kinesin Mklp2 (section 1.4.4) as constriction site and midbody markers for additional immunofluorescence studies (Fackler et al., 2014). Interestingly it was shown, that the Δ170-309 deletion mutant did not co-localize with Spastin at the constriction zone and Mklp2 at the midbody, while full length GAS2L3 showed a clear co-localization with both proteins (Fackler et al., 2014).

In summary immunofluorescence microscopy experiments revealed that the CPC localizes GAS2L3 to the constriction zone in a GAR domain dependent manner. The observed localization differences of full length GAS2L3 and GAS2L3(Δ170-309) at the midbody further strengthen the biochemical interaction data and point to a function of GAS2L3 in late cytokinesis and abscission. This finding is in concordance with a recent study, which identified GAS2L3 as a novel constriction site associated protein (Pe'er et al., 2013).

4.8. The GAR domain is necessary for proper function of GAS2L3

To further investigate, if the GAR domain is important for proper function of GAS2L3, reconstitution assays with GAS2L3 full length and Δ170-309 mutant were performed (fig 3.19). The aim of these assays was to analyze if reconstituted exogenously expressed full length and Δ170-309 mutant protein is able to compensate for loss of endogenous GAS2L3. As expected, expression of eGFP-GAS2L3 full length protein led to a significant decrease of cells with defective cytokinesis (fig 3.19d). Expression of the eGFP-GAS2L3(Δ170-309) mutant however did not decrease the percentage of cells with abnormally shaped nuclei compared to the uninduced control (fig 3.19d). The obtained results indicate that the GAR domain is necessary for proper GAS2L3 protein function but it is not clear if the inability of the GAR deletion mutant to rescue the cytokinesis phenotype of GAS2L3 depleted cells is directly connected to the interaction with the CPC. As mentioned before, comparative pharmacological inhibition experiments demonstrated that GAS2L3 depletion only leads to a subcritical inhibition of CPC activity which does not cause cytokinesis defects (fig 3.17). Due

to this it is tempting to speculate, that the interaction between the CPC and GAS2L3 is important for other cellular processes like regulation of abscission. It was shown that GAS2L3 is an abscission site associated protein which perfectly co-localizes with Spastin and CHMP4B (Fackler et al., 2014; Pe'er et al., 2013), two proteins either associated with (Spastin) or incorporated into (CHMP4B) the ESCRT-III complex, which is known to be the major regulator of abscission (Schiel et al., 2013). Importantly it is known that the CPC subunit Borealin, which directly interacts with GAS2L3, is also implicated in regulation of abscission by interacting with CHMP4C another subunit of the ESCRT-III complex (sections 1.4.1 & 1.4.5.2). It is easy to speculate that GAS2L3 might be involved in mediating the interaction between the CPC and subunits of the ESCRT-III complex. It is plausible that loss of interaction between GAS2L3 and the CPC disturbs correct signaling between the CPC and the ESCRT-III complex what in turn might deregulate abscission and finally lead to defective cytokinesis and the observed phenotype.

4.9. Identification of new interacting proteins of GAS2L3

For identification of new interacting proteins of GAS2L3 stable isotope labelling by amino acids in cell culture (SILAC) in combination with tandem affinity purification and subsequent mass spectrometrical analysis was performed.

38 proteins with an enrichment of at least two (fig 3.20) were identified as potentially new GAS2L3 interacting proteins. 18 proteins were cytoskeleton associated, 6 proteins were either chaperones or co-chaperones, 8 proteins were involved in gene expression or translation and 6 proteins had other functions (fig 3.20). It was reported recently that many cytoskeleton associated proteins tend to bind unspecifically to sepharose beads during affinity purification experiments (Trinkle-Mulcahy et al., 2008). To verify that the enriched proteins were specific interactors of GAS2L3 and not background contaminants, six different proteins from the list were chosen for further validation by co-immunoprecipitation experiments. Those proteins were the F-actin cross-linking proteins Actinin 1 and Actinin 4, two subunits of the F-actin capping protein CapZ alpha 1 (CapZa1) and CapZ beta (CapZb), the chaperone heat shock cognate 71 kDa protein (Hsc70) and the co-chaperone BAG family molecular chaperone regulator 2 (BAG-2). The co-chaperone BAG-3, which is closely related to BAG-2 and known to form heteromeric complexes with some of the proteins from the list like CapZb, Hsc70 and Filamin (Hishiya et al., 2010; Ulbricht et al., 2013), was also chosen although it was not found on the original list. The Actinins 1 and 4, BAG-2, BAG-3 and both subunits of the F-actin capping protein CapZ interacted with GAS2L3 in co-immunoprecipitation experiments while Hsc70 showed unspecific binding in absence of GAS2L3 (fig 3.21a). The co-immunoprecipitation experiments confirmed the mass spectrometrical results but further biochemical characterization will be necessary to get a

deeper insight into the physiological role of the observed interactions. Future studies will show if all of the proteins are direct interaction partners of GAS2L3 or if some of them are indirectly binding to GAS2L3 via other proteins or the actin or microtubule cytoskeleton. Taken together it was shown that SILAC in combination with tandem affinity purification and subsequent mass spectrometrical analysis is a powerful tool to identify new interacting proteins.

4.10. Establishment of an *in vivo* system to study Gas2l3 function

Expression of Gas2l3 in tissues was analyzed to get a broad overview of Gas2l3 abundance in the mouse (fig 3.22). Gas2l3 expression profile correlated well with the proliferative ability of the different tissues. While fast proliferating tissues like spleen, thymus and small intestine with a high percentage of cells in G2/M phase of the cell cycle showed highest expression of Gas2l3 (fig 3.22), the tissues with lower proliferative ability, where cells are mainly in G0 phase of the cell cycle (e.g. fat tissue or kidney) showed lower expression levels (fig 3.22). This finding is in concordance with the described cell cycle specific regulation of Gas2l3 (fig 3.1 and Wolter et al., 2012) and its role during mitosis and cytokinesis (fig 3.2 and Wolter et al., 2012). A recent study reported that Gas2l3 is also ubiquitously expressed in human tissues and cell lines (Stroud et al., 2011) confirming the expression data obtained from mouse (fig 3.22). Interestingly the authors reported that GAS2L3 is not expressed in HT1080 cells (Stroud et al., 2011). HT1080 cells, a fibrosarcoma cell line derived from a 35 year old male patient (Rasheed et al., 1974), might therefore be used as a valuable system for further research.

Although much effort was expended to shed light on the function of GAS2L3 in mitosis, cytokinesis and maintenance of genomic stability (Wolter et al., 2012), the role of Gas2l3 was solely investigated in cancer cell lines but not in living organisms. To gain further insight into the physiological role of GAS2L3, a knockout mouse model for *in vivo* studies was created. In collaboration with the Transgenic Core Facility of the Max-Planck-Institute of Molecular Cell Biology and Genetics mice carrying a targeted Gas2l3 allele were generated. Those mice were further crossed with flippase (FLP) and Cre recombinase expressing mice (fig 3.24) to create conditional and non-conditional Gas2l3 knockout mice.

The conditional Gas2l3 knockout strain was used to create mouse embryonic fibroblasts (MEFs). MEF clones homozygous for the floxed Gas2l3 allele were obtained and efficiency of the inducible Gas2l3 knockout system after administration of 4-hydroxytamoxifene was determined on genomic DNA, mRNA and protein level (fig 3.27). Surprisingly the conditional knockout MEFs did not show any obvious cytokinesis defects after Gas2l3 deletion like it was reported for cancer cell lines like HeLa cells (fig 3.2). Even after long term deletion of Gas2l3 no significant increase in multinucleation or abnormally shaped nuclei could be observed

compared to untreated control MEFs (data not shown). Possible explanations would be, that Gas2l3 is not so important for cytokinesis of embryonic fibroblasts than it is for other cell types or that complete loss of Gas2l3 is compensated by other proteins or cellular mechanisms which are not active in highly transformed cancer cells.

The conditional CreER^{T2} system is not suited to achieve full recombination of floxed alleles *in vivo* because it was shown that some tissues show no or only low levels of recombination after tamoxifene administration (Reichert et al., 2010). For complete Gas2l3 knockout *in vivo* a non-conditional Gas2l3 knockout strain was established by intercrossing mice harboring a delta floxed (Δfl) allele (fig 3.28). The mendelian ratio of the offspring pubs showed a strong deviation to the disadvantage of knockout mice at weaning age (fig 3.29). Only ten out of a total of 187 mice were identified to be Gas2l3 knockout animals (fig 3.29), which resembles only 5.35% (25% expected). From the remaining 177 mice 31.02% (25% expected) had a wild type (Gas2l3$^{+/+}$) and 63.64% (50% expected) a heterozygous (Gas2l3$^{Δfl/+}$) genotype (fig 3.29). The small number of knockout mice at weaning age indicates either early postnatal or late embryonic lethality. Early embryonic lethality, like it was observed upon Lin9 deletion (Reichert et al., 2010), could be excluded due to the fact that at least a small number of knockout mice were born and reached adulthood (fig 3.29). Importantly the Gas2l3 knockout mice which survived post weaning age did not show any obvious abnormalities and looked phenotypically normal but died suddenly between 4 and 16 weeks of age (data not shown). Intercrossing of male and female knockout mice revealed that both genders are fertile although the received litter was small and harbored only 3 pubs (fig 3.30).

Adult knockout mice were sacrificed and organs were analyzed macroscopically. Most of the knockout organs looked normal compared to wild type controls, only the hearts of knockout animals looked remarkable different compared to wild type hearts (data not shown). All analyzed knockout hearts were severely hypertrophic with heavily enlarged atria and ventricles (data not shown). This data indicates that knockout mice suffer from a heart tissue specific phenotype, which leads to a severe cardiac hypertrophy which might be the explanation for the high mortality rate before weaning age.

Interestingly many of the Gas2l3 interacting proteins identified by mass spectrometrical analysis (fig 3.20) are known to be important for maintenance of skeletal and heart muscle integrity (Coats and Elliott, 2013; Garcia-Pavia et al., 2013; Selcen and Engel, 2011). Loss of the co-chaperone BAG-3 or the F-actin binding protein Actinin for example leads to severe cardiomyopathies and premature death (Citro et al., 2013; Feldman et al., 2014; Lee et al., 2012; Mohapatra et al., 2003; Norton et al., 2011; Selcen et al., 2009). The phenotype observed upon loss of these proteins is very similar to the one observed after deletion of Gas2l3. BAG-3, Actinin and the capping protein subunits CapZa1 and CapZb localize to the

so called Z-disc (Arimura et al., 2011; Beggs et al., 1992; Labeit, 2011; Schafer et al., 1993), a subcellular structure of skeletal and cardiac muscle cells which is important for attachment of actin filaments and muscle contractility (Frank and Frey, 2011; Knöll et al., 2011; Luther, 2009). It is tempting to speculate that Gas2l3 might be involved in maintenance of heart muscle integrity by interacting with Z-disc proteins and that loss of Gas2l3 leads to cardiac muscle defects which in turn cause premature death. In such a scenario Gas2l3 would probably act as a scaffold protein stabilizing Z-disc structures. One drawback of this idea is that a stabilizing function of Gas2l3 would probably mean that Gas2l3 protein has to be present in high abundancy in cardiomyocytes. Keeping in mind that Gas2l3 is only moderately expressed in adult heart muscle (fig 3.22) and that almost all cardiomyocytes in the adult heart are terminally differentiated and have exited cell cycle, (Pasumarthi and Field, 2002) a situation where Gas2l3 is barely expressed (Wolter et al., 2012), this hypothesis seems to be challenged.

Another possibility to explain the heart phenotype might be that loss of Gas2l3 causes defects early during heart development. This idea was addressed by analyzing Gas2l3 expression levels during different stages of heart development (fig 3.31). Gas2l3 expression level was highest at embryonic stages but it declined during postnatal stages and finally went down to a very low level at adult stage (fig 3.31). Interestingly the Gas2l3 expression profile perfectly correlates with cell cycle activity. During embryogenesis all cells are actively dividing while in early postnatal stages cell cycle activity of cardiomyocytes declines and finally stops shortly after birth (Pasumarthi and Field, 2002; Zebrowski and Engel, 2013). In adult stage, only low proliferation activity is detectable in the heart (Senyo et al., 2013; Zebrowski and Engel, 2013). The obtained results strengthen the idea that the observed heart phenotype upon loss of Gas2l3 might be caused by a developmental defect occurring during late embryonic or early postnatal stages.

4.11. Conclusion

In this thesis GAS2L3 was characterized according to its biochemical properties. It was shown that GAS2L3 is a cytoskeleton associated protein which is able to interact with different cytoskeleton networks. Protein interaction studies revealed that GAS2L3 interacts with the CPC via its GAR domain and that this interaction is important for correct midbody localization of GAS2L3 during cytokinesis. Although much effort was expended to clarify the role of GAS2L3 its physiological function is still not unequivocally clear. The data obtained so far (this thesis and Wolter et al., 2012) indicates that GAS2L3 might be involved in regulation of cytokinesis and abscission. This idea is in concordance with a recently published report (Pe'er et al., 2013). To clarify more precisely the role of GAS2L3 in abscission, further studies are needed. Because GAS2L3 shows perfect co-localization with subunits of the

ESCRT-III complex (Fackler et al., 2014; Pe'er et al., 2013) it would be interesting to investigate if GAS2L3 is interacting with this multi-protein complex. An interaction might point to a direct involvement of GAS2L3 in regulation of abscission.

The *in vivo* data indicates so far, that Gas2l3 is important for proper functioning of the heart. At the moment it is not possible to say what the exact role of Gas2l3 in this scenario is. One possibility would be that it is important for proper heart development and that loss of Gas2l3 during early developmental stages leads to heart defects. This idea is supported by the fact that Gas2l3 is strongly expressed during heart development but barely detectable on mRNA level in the adult heart (fig 3.31). Another hypothesis is that Gas2l3 is important for maintenance of muscle integrity in the adult heart. This idea is supported by the newly identified protein interactors (fig 3.20 & 3.21) which show a similar knockout phenotype like GAS2L3 (section 4.10). A third possibility would be that Gas2l3 has a dual function by acting as cytokinesis regulator during heart development as well as stabilizer of the cardiac cytoskeleton at adult stage.

It is obvious that further experiments are necessary to clarify the exact role of Gas2l3 *in vivo*. It would be for example important to know if Gas2l3 protein is detectable in adult cardiomyocytes and if it localizes to the Z-disc. It is also important to further analyze at which developmental stage (embryonic, postnatal or adult) the observed heart phenotype is occurring.

5. Summary

GAS2L3 was identified recently as a target gene of the DREAM complex (Reichert et al., 2010; Wolter et al., 2012). It was shown that GAS2L3 is expressed in a cell cycle specific manner and that depletion of the protein leads to defects in cytokinesis and genomic instability (Wolter et al., 2012).

Major aim of this thesis was, to further characterize the biochemical properties and physiological function of GAS2L3.

By *in vitro* co-sedimentation and bundling assays, GAS2L3 was identified as a cytoskeleton associated protein which bundles, binds and crosslinks F-actin and MTs. GST pulldown assays and co-immunoprecipitation experiments revealed that GAS2L3 interacts *in vitro* and *in vivo* with the chromosomal passenger complex (CPC), a very important regulator of mitosis and cytokinesis, and that the interaction is mediated by the GAR domain of GAS2L3 and the C-terminal part of Borealin and the N-terminal part of Survivin. Kinase assays showed that GAS2L3 is not a substrate of the CPC but is strongly phosphorylated by CDK1 *in vitro*. Depletion of GAS2L3 by shRNA influenced protein stability and activity of the CPC. However pharmacological studies showed that the decreased CPC activity is not responsible for the observed cytokinesis defects upon GAS2L3 depletion. Immunofluorescence experiments revealed that GAS2L3 is localized to the constriction zone by the CPC in a GAR dependent manner and that the GAR domain is important for proper protein function.

New interacting proteins of GAS2L3 were identified by stable isotope labelling by amino acids in cell culture (SILAC) in combination with tandem affinity purification and subsequent mass spectrometrical analysis. Co-immunoprecipitation experiments further confirmed the obtained mass spectrometrical data.

To address the physiological function of GAS2L3 *in vivo*, a conditional and a non-conditional knockout mouse strain was established. The non-conditional mouse strain showed a highly increased mortality rate before weaning age probably due to heart failure. The physiological function of GAS2L3 *in vivo* as well as the exact reason for the observed heart phenotype is not known at the moment.

6. Zusammenfassung

GAS2L3 wurde vor kurzem als Zielgen des DREAM Komplex identifiziert (Reichert et al., 2010; Wolter et al., 2012). Es konnte gezeigt werden, dass die Expression von GAS2L3 Zellzyklus abhängig reguliert wird und dass Depletion des Proteins zu Fehlern in der Zytokinese und genomischer Instabilität führt (Wolter et al., 2012).

Hauptziel dieser Doktorarbeit war es, GAS2L3 hinsichtlich seiner biochemischen Eigenschaften und physiologischer Funktion näher zu charakterisieren.

Unter Verwendung verschiedener *in vitro* Experimente konnte gezeigt werden, dass GAS2L3 sowohl F-Aktin als auch Mikrotubuli binden, bündeln und quervernetzen kann. *In vitro* und *in vivo* Protein-Protein Interaktionsexperimente zeigten, dass GAS2L3 mit dem „chromosomal passenger complex" (CPC), einem wichtigen Mitose- und Zytokineseregulator, interagiert und dass diese Interaktion durch die GAR Domäne von GAS2L3 und den C-Terminus von Borealin beziehungsweise den N-terminus von Survivin vermittelt wird. Phosphorylierungsexperimente zeigten deutlich, dass GAS2L3 kein Substrat des CPC ist, jedoch von CDK1 phosphoryliert wird. Zellbiologische Experimente belegten, dass Depletion von GAS2L3 mittels shRNA die Proteinstabilität und Aktivität des CPC beeinflusst. Experimente mit einem chemischen Aurora B Inhibitor dokumentierten, dass die verringerte CPC Aktivität nicht die Ursache der beobachteten Zytokinesefehler nach GAS2L3 Depletion ist. Immunfluoreszenzexperimente machten deutlich, dass GAS2L3 mit Hilfe des CPC an der Abschnürungszone lokalisiert wird und dass die Lokalisation abhängig von der GAR Domäne erfolgt.

Mit Hilfe von SILAC in Kombination mit Tandem-Affinitätsaufreinigung und anschließender massenspektrometrischer Auswertung wurden neue Proteininteraktoren von GAS2L3 identifiziert. Protein-Protein Interaktionsexperimente bestätigten die massenspektrometrisch ermittelten Daten.

Um die physiologische Funktion von GAS2L3 *in vivo* näher analysieren zu können, wurden verschiedene Knockout Mauslinien etabliert. Die nicht-konditionelle Mauslinie zeigte erhöhte Sterblichkeit vor dem Absetzalter wahrscheinlich verursacht durch Herzversagen. Die genaue physiologische Funktion von GAS2L3 und der Grund für den beobachteten Herzphänotyp sind momentan noch unbekannt.

7. References

Adams, R.R., Wheatley, S.P., Gouldsworthy, A.M., Kandels-Lewis, S.E., Carmena, M., Smythe, C., Gerloff, D.L., and Earnshaw, W.C. (2000). INCENP binds the Aurora-related kinase AIRK2 and is required to target it to chromosomes, the central spindle and cleavage furrow. Curr. Biol. CB *10*, 1075–1078.

Adams, R.R., Maiato, H., Earnshaw, W.C., and Carmena, M. (2001). Essential roles of Drosophila inner centromere protein (INCENP) and Aurora-B in histone H3 phosphorylation, metaphase chromosome alignment, kinetochore disjunction, and chromosome segregation. J Cell Biol *153*, 865–880.

Ainsztein, A.M., Kandels-Lewis, S.E., Mackay, A.M., and Earnshaw, W.C. (1998). INCENP centromere and spindle targeting: identification of essential conserved motifs and involvement of heterochromatin protein HP1. J Cell Biol *143*, 1763–1774.

Alberts, B., Johnson, A., and Lewis, J. (2008). Molecular Biology of the Cell (New York: Garland Pub).

Alushin, G.M., Ramey, V.H., Pasqualato, S., Ball, D.A., Grigorieff, N., Musacchio, A., and Nogales, E. (2010). The Ndc80 kinetochore complex forms oligomeric arrays along microtubules. Nature *467*, 805–810.

Ambrosini, G., Adida, C., and Altieri, D.C. (1997). A novel anti-apoptosis gene, survivin, expressed in cancer and lymphoma. Nat. Med *3*, 917–921.

Andrews, P.D., Ovechkina, Y., Morrice, N., Wagenbach, M., Duncan, K., Wordeman, L., and Swedlow, J.R. (2004). Aurora B regulates MCAK at the mitotic centromere. Dev. Cell *6*, 253–268.

Arimura, T., Ishikawa, T., Nunoda, S., Kawai, S., and Kimura, A. (2011). Dilated cardiomyopathy-associated BAG3 mutations impair Z-disc assembly and enhance sensitivity to apoptosis in cardiomyocytes. Hum. Mutat. *32*, 1481–1491.

Asai, T., Liu, Y., Di Giandomenico, S., Bae, N., Ndiaye-Lobry, D., Deblasio, A., Menendez, S., Antipin, Y., Reva, B., Wevrick, R., et al. (2012). Necdin, a p53 target gene, regulates the quiescence and response to genotoxic stress of hematopoietic stem/progenitor cells. Blood *120*, 1601–1612.

Ban, R., Nishida, T., and Urano, T. (2011). Mitotic kinase Aurora-B is regulated by SUMO-2/3 conjugation/deconjugation during mitosis. Genes Cells *16*, 652–669.

Barrett, R.M., Colnaghi, R., and Wheatley, S.P. (2011). Threonine 48 in the BIR domain of survivin is critical to its mitotic and anti-apoptotic activities and can be phosphorylated by CK2 in vitro. Cell Cycle *10*, 538–548.

Bayliss, R., Sardon, T., Vernos, I., and Conti, E. (2003). Structural basis of Aurora-A activation by TPX2 at the mitotic spindle. Mol. Cell *12*, 851–862.

Beardmore, V.A., Ahonen, L.J., Gorbsky, G.J., and Kallio, M.J. (2004). Survivin dynamics increases at centromeres during G2/M phase transition and is regulated by microtubule-attachment and Aurora B kinase activity. J Cell Sci *117*, 4033–4042.

References

Beggs, A.H., Byers, T.J., Knoll, J.H., Boyce, F.M., Bruns, G.A., and Kunkel, L.M. (1992). Cloning and characterization of two human skeletal muscle alpha-actinin genes located on chromosomes 1 and 11. J. Biol. Chem. *267*, 9281–9288.

Beijersbergen, R.L., Kerkhoven, R.M., Zhu, L., Carlée, L., Voorhoeve, P.M., and Bernards, R. (1994). E2F-4, a new member of the E2F gene family, has oncogenic activity and associates with p107 in vivo. Genes Dev. *8*, 2680–2690.

Benetti, R., Del Sal, G., Monte, M., Paroni, G., Brancolini, C., and Schneider, C. (2001). The death substrate Gas2 binds m-calpain and increases susceptibility to p53-dependent apoptosis. EMBO J. *20*, 2702–2714.

Benetti, R., Copetti, T., Dell'Orso, S., Melloni, E., Brancolini, C., Monte, M., and Schneider, C. (2005). The calpain system is involved in the constitutive regulation of beta-catenin signaling functions. J. Biol. Chem. *280*, 22070–22080.

Bishop, J.D., and Schumacher, J.M. (2002). Phosphorylation of the carboxyl terminus of inner centromere protein (INCENP) by the Aurora B Kinase stimulates Aurora B kinase activity. J Biol Chem *277*, 27577–27580.

Bourhis, E., Hymowitz, S.G., and Cochran, A.G. (2007). The mitotic regulator Survivin binds as a monomer to its functional interactor Borealin. J Biol Chem *282*, 35018–35023.

Bradford, M.M. (1976). A rapid and sensitive method for the quantitation of microgram quantities of protein utilizing the principle of protein-dye binding. Anal. Biochem. 248–254.

Brancolini, C., and Schneider, C. (1994). Phosphorylation of the growth arrest-specific protein Gas2 is coupled to actin rearrangements during Go-->G1 transition in NIH 3T3 cells. J. Cell Biol. *124*, 743–756.

Brancolini, C., Bottega, S., and Schneider, C. (1992). Gas2, a growth arrest-specific protein, is a component of the microfilament network system. J. Cell Biol. *117*, 1251–1261.

Brancolini, C., Benedetti, M., and Schneider, C. (1995). Microfilament reorganization during apoptosis: the role of Gas2, a possible substrate for ICE-like proteases. EMBO J. *14*, 5179–5190.

De Bruin, A., Maiti, B., Jakoi, L., Timmers, C., Buerki, R., and Leone, G. (2003). Identification and characterization of E2F7, a novel mammalian E2F family member capable of blocking cellular proliferation. J. Biol. Chem. *278*, 42041–42049.

Buck, V., Allen, K.E., Sørensen, T., Bybee, A., Hijmans, E.M., Voorhoeve, P.M., Bernards, R., and La Thangue, N.B. (1995). Molecular and functional characterisation of E2F-5, a new member of the E2F family. Oncogene *11*, 31–38.

Capalbo, L., Montembault, E., Takeda, T., Bassi, Z.I., Glover, D.M., and D'Avino, P.P. (2012). The chromosomal passenger complex controls the function of endosomal sorting complex required for transport-III Snf7 proteins during cytokinesis. Open Biol. *2*, 120070.

Carlton, J.G., Caballe, A., Agromayor, M., Kloc, M., and Martin-Serrano, J. (2012). ESCRT-III governs the Aurora B-mediated abscission checkpoint through CHMP4C. Science *336*, 220–225.

Carmena, M., Ruchaud, S., and Earnshaw, W.C. (2009). Making the Auroras glow: regulation of Aurora A and B kinase function by interacting proteins. Curr Opin Cell Biol *21*, 796–805.

References

Carmena, M., Wheelock, M., Funabiki, H., and Earnshaw, W.C. (2012). The Chromosomal Passenger Complex (CPC): From Easy Rider to the Godfather of Mitosis. Nat. Rev. Mol. Cell Biol. *13*, 789–803.

Carnero, A., and Hannon, G.J. (1998). The INK4 family of CDK inhibitors. Curr. Top. Microbiol. Immunol. *227*, 43–55.

Cartwright, P., Müller, H., Wagener, C., Holm, K., and Helin, K. (1998). E2F-6: a novel member of the E2F family is an inhibitor of E2F-dependent transcription. Oncogene *17*, 611–623.

Carvalho, A., Carmena, M., Sambade, C., Earnshaw, W.C., and Wheatley, S.P. (2003). Survivin is required for stable checkpoint activation in taxol-treated HeLa cells. J Cell Sci *116*, 2987–2998.

Castresana, J., and Saraste, M. (1995). Does Vav bind to F-actin through a CH domain? FEBS Lett. *374*, 149–151.

Cesario, J.M., Jang, J.K., Redding, B., Shah, N., Rahman, T., and McKim, K.S. (2006). Kinesin 6 family member Subito participates in mitotic spindle assembly and interacts with mitotic regulators. J. Cell Sci. *119*, 4770–4780.

Chantalat, L., Skoufias, D.A., Kleman, J.P., Jung, B., Dideberg, O., and Margolis, R.L. (2000). Crystal structure of human survivin reveals a bow tie-shaped dimer with two unusual alpha-helical extensions. Mol. Cell *6*, 183–189.

Cheeseman, I.M., Chappie, J.S., Wilson-Kubalek, E.M., and Desai, A. (2006). The conserved KMN network constitutes the core microtubule-binding site of the kinetochore. Cell *127*, 983–997.

Cheng, L., Zhang, J., Ahmad, S., Rozier, L., Yu, H., Deng, H., and Mao, Y. (2011). Aurora B regulates formin mDia3 in achieving metaphase chromosome alignment. Dev. Cell *20*, 342–352.

Christensen, J., Cloos, P., Toftegaard, U., Klinkenberg, D., Bracken, A.P., Trinh, E., Heeran, M., Di Stefano, L., and Helin, K. (2005). Characterization of E2F8, a novel E2F-like cell-cycle regulated repressor of E2F-activated transcription. Nucleic Acids Res. *33*, 5458–5470.

Chu, Y., Yao, P.Y., Wang, W., Wang, D., Wang, Z., Zhang, L., Huang, Y., Ke, Y., Ding, X., and Yao, X. (2011). Aurora B kinase activation requires survivin priming phosphorylation by PLK1. J. Mol. Cell Biol. *3*, 260–267.

Ciferri, C., Pasqualato, S., Screpanti, E., Varetti, G., Santaguida, S., Dos Reis, G., Maiolica, A., Polka, J., De Luca, J.G., De Wulf, P., et al. (2008). Implications for kinetochore-microtubule attachment from the structure of an engineered Ndc80 complex. Cell *133*, 427–439.

Citro, R., d' Avenia, M., De Marco, M., Giudice, R., Mirra, M., Ravera, A., Silverio, A., Farina, R., Silvestri, F., Gravina, P., et al. (2013). Polymorphisms of the antiapoptotic protein bag3 may play a role in the pathogenesis of tako-tsubo cardiomyopathy. Int. J. Cardiol. *168*, 1663–1665.

Coats, C.J., and Elliott, P.M. (2013). Genetic biomarkers in hypertrophic cardiomyopathy. Biomark. Med. *7*, 505–516.

References

Coelho, P.A., Queiroz-Machado, J., Carmo, A.M., Moutinho-Pereira, S., Maiato, H., and Sunkel, C.E. (2008). Dual role of topoisomerase II in centromere resolution and aurora B activity. PLoS Biol. *6*, e207.

Coller, H.A. (2007). What's taking so long? S-phase entry from quiescence versus proliferation. Nat. Rev. Mol. Cell Biol. *8*, 667–670.

Colnaghi, R., and Wheatley, S.P. (2010). Liaisons between survivin and Plk1 during cell division and cell death. J Biol Chem *285*, 22592–22604.

Connell, C.M., Colnaghi, R., and Wheatley, S.P. (2008). Nuclear survivin has reduced stability and is not cytoprotective. J Biol Chem *283*, 3289–3296.

Cooke, C.A., Heck, M.M., and Earnshaw, W.C. (1987). The inner centromere protein (INCENP) antigens: movement from inner centromere to midbody during mitosis. J. Cell Biol. *105*, 2053–2067.

Dai, J., and Higgins, J.M. (2005). Haspin: a mitotic histone kinase required for metaphase chromosome alignment. Cell Cycle *4*, 665–668.

Date, D., Dreier, M.R., Borton, M.T., Bekier, M.E., and Taylor, W.R. (2012). Effects of phosphatase and proteasome inhibitors on Borealin phosphorylation and degradation. J Biochem *151*, 361–369.

DeLuca, J.G., Gall, W.E., Ciferri, C., Cimini, D., Musacchio, A., and Salmon, E.D. (2006). Kinetochore microtubule dynamics and attachment stability are regulated by Hec1. Cell *127*, 969–982.

DeLuca, K.F., Lens, S.M., and DeLuca, J.G. (2011). Temporal changes in Hec1 phosphorylation control kinetochore-microtubule attachment stability during mitosis. J Cell Sci *124*, 622–634.

Dieterich, K., Soto Rifo, R., Faure, A.K., Hennebicq, S., Ben Amar, B., Zahi, M., Perrin, J., Martinez, D., Sèle, B., Jouk, P.-S., et al. (2007). Homozygous mutation of AURKC yields large-headed polyploid spermatozoa and causes male infertility. Nat. Genet. *39*, 661–665.

Dorée, M., and Galas, S. (1994). The cyclin-dependent protein kinases and the control of cell division. FASEB J. Off. Publ. Fed. Am. Soc. Exp. Biol. *8*, 1114–1121.

Du, J., Kelly, A.E., Funabiki, H., and Patel, D.J. (2012). Structural basis for recognition of H3T3ph and Smac/DIABLO N-terminal peptides by human Survivin. Structure *20*, 185–195.

Dukes, J.D., Richardson, J.D., Simmons, R., and Whitley, P. (2008). A dominant-negative ESCRT-III protein perturbs cytokinesis and trafficking to lysosomes. Biochem. J. *411*, 233–239.

Dyson, N. (1998). The regulation of E2F by pRB-family proteins. Genes Dev. *12*, 2245–2262.

Elia, N., Sougrat, R., Spurlin, T.A., Hurley, J.H., and Lippincott-Schwartz, J. (2011). Dynamics of endosomal sorting complex required for transport (ESCRT) machinery during cytokinesis and its role in abscission. Proc. Natl. Acad. Sci. U. S. A. *108*, 4846–4851.

Espeut, J., Cheerambathur, D.K., Krenning, L., Oegema, K., and Desai, A. (2012). Microtubule binding by KNL-1 contributes to spindle checkpoint silencing at the kinetochore. J. Cell Biol. *196*, 469–482.

References

Eyers, P.A., Erikson, E., Chen, L.G., and Maller, J.L. (2003). A novel mechanism for activation of the protein kinase Aurora A. Curr. Biol. CB *13*, 691–697.

Fackler, M., Wolter, P., and Gaubatz, S. (2014). The GAR domain of GAS2L3 mediates binding to the chromosomal passenger complex and is required for localization of GAS2L3 to the constriction zone during abscission. FEBS J. *281*, 2123–2135.

Feldman, A.M., Begay, R.L., Knezevic, T., Myers, V.D., Slavov, D.B., Zhu, W., Gowan, K., Graw, S.L., Jones, K.L., Tilley, D.G., et al. (2014). Decreased Levels of BAG3 in a Family With a Rare Variant and in Idiopathic Dilated Cardiomyopathy. J. Cell. Physiol. *[Epub ahead of print]*, DOI: 10.1002/jcp.24615.

Felsani, A., Mileo, A.M., and Paggi, M.G. (2006). Retinoblastoma family proteins as key targets of the small DNA virus oncoproteins. Oncogene *25*, 5277–5285.

Fernández-Miranda, G., Pérez de Castro, I., Carmena, M., Aguirre-Portolés, C., Ruchaud, S., Fant, X., Montoya, G., Earnshaw, W.C., and Malumbres, M. (2010). SUMOylation modulates the function of Aurora-B kinase. J. Cell Sci. *123*, 2823–2833.

Fischle, W., Tseng, B.S., Dormann, H.L., Ueberheide, B.M., Garcia, B.A., Shabanowitz, J., Hunt, D.F., Funabiki, H., and Allis, C.D. (2005). Regulation of HP1-chromatin binding by histone H3 methylation and phosphorylation. Nature *438*, 1116–1122.

Foley, E.A., Maldonado, M., and Kapoor, T.M. (2011). Formation of stable attachments between kinetochores and microtubules depends on the B56-PP2A phosphatase. Nat. Cell Biol *13*, 1265–1271.

Frank, D., and Frey, N. (2011). Cardiac Z-disc signaling network. J. Biol. Chem. *286*, 9897–9904.

Fuller, B.G., Lampson, M.A., Foley, E.A., Rosasco-Nitcher, S., Le, K.V., Tobelmann, P., Brautigan, D.L., Stukenberg, P.T., and Kapoor, T.M. (2008). Midzone activation of aurora B in anaphase produces an intracellular phosphorylation gradient. Nature *453*, 1132–1136.

Gamper, I., Koh, K.-R., Ruau, D., Ullrich, K., Bartunkova, J., Piroth, D., Hacker, C., Bartunek, P., and Zenke, M. (2009). GAR22: a novel target gene of thyroid hormone receptor causes growth inhibition in human erythroid cells. Exp. Hematol. *37*, 539–548.e4.

Garcia-Pavia, P., Cobo-Marcos, M., Guzzo-Merello, G., Gomez-Bueno, M., Bornstein, B., Lara-Pezzi, E., Segovia, J., and Alonso-Pulpon, L. (2013). Genetics in dilated cardiomyopathy. Biomark. Med. *7*, 517–533.

Gassmann, R., Carvalho, A., Henzing, A.J., Ruchaud, S., Hudson, D.F., Honda, R., Nigg, E.A., Gerloff, D.L., and Earnshaw, W.C. (2004). Borealin: a novel chromosomal passenger required for stability of the bipolar mitotic spindle. J. Cell Biol. *166*, 179–191.

Gaubatz, S., Wood, J.G., and Livingston, D.M. (1998). Unusual proliferation arrest and transcriptional control properties of a newly discovered E2F family member, E2F-6. Proc. Natl. Acad. Sci. U. S. A. *95*, 9190–9195.

Gavet, O., and Pines, J. (2010). Progressive activation of CyclinB1-Cdk1 coordinates entry to mitosis. Dev. Cell *18*, 533–543.

Giacinti, C., and Giordano, A. (2006). RB and cell cycle progression. Oncogene *25*, 5220–5227.

References

Gimona, M., and Mital, R. (1998). The single CH domain of calponin is neither sufficient nor necessary for F-actin binding. J. Cell Sci. *111 (Pt 13)*, 1813–1821.

Ginsberg, D., Vairo, G., Chittenden, T., Xiao, Z.X., Xu, G., Wydner, K.L., DeCaprio, J.A., Lawrence, J.B., and Livingston, D.M. (1994). E2F-4, a new member of the E2F transcription factor family, interacts with p107. Genes Dev. *8*, 2665–2679.

Girard, F., Strausfeld, U., Fernandez, A., and Lamb, N.J. (1991). Cyclin A is required for the onset of DNA replication in mammalian fibroblasts. Cell *67*, 1169–1179.

Glotzer, M. (2003). Cytokinesis: progress on all fronts. Curr. Opin. Cell Biol. *15*, 684–690.

Glover, D.M., Leibowitz, M.H., McLean, D.A., and Parry, H. (1995). Mutations in aurora prevent centrosome separation leading to the formation of monopolar spindles. Cell *81*, 95–105.

Goriounov, D., Leung, C.L., and Liem, R.K.H. (2003). Protein products of human Gas2-related genes on chromosomes 17 and 22 (hGAR17 and hGAR22) associate with both microfilaments and microtubules. J. Cell Sci. *116*, 1045–1058.

Grossman, D., Kim, P.J., Schechner, J.S., and Altieri, D.C. (2001). Inhibition of melanoma tumor growth in vivo by survivin targeting. Proc Natl Acad Sci USA *98*, 635–640.

Gruneberg, U., Neef, R., Honda, R., Nigg, E.A., and Barr, F.A. (2004). Relocation of Aurora B from centromeres to the central spindle at the metaphase to anaphase transition requires MKlp2. J. Cell Biol. *166*, 167–172.

Guizetti, J., Schermelleh, L., Mäntler, J., Maar, S., Poser, I., Leonhardt, H., Müller-Reichert, T., and Gerlich, D.W. (2011). Cortical constriction during abscission involves helices of ESCRT-III-dependent filaments. Science *331*, 1616–1620.

Hameyer, D., Loonstra, A., Eshkind, L., Schmitt, S., Antunes, C., Groen, A., Bindels, E., Jonkers, J., Krimpenfort, P., Meuwissen, R., et al. (2007). Toxicity of ligand-dependent Cre recombinases and generation of a conditional Cre deleter mouse allowing mosaic recombination in peripheral tissues. Physiol. Genomics *31*, 32–41.

Harper, J.W., Elledge, S.J., Keyomarsi, K., Dynlacht, B., Tsai, L.H., Zhang, P., Dobrowolski, S., Bai, C., Connell-Crowley, L., and Swindell, E. (1995). Inhibition of cyclin-dependent kinases by p21. Mol. Biol. Cell *6*, 387–400.

Harrison, M.M., Ceol, C.J., Lu, X., and Horvitz, H.R. (2006). Some C. elegans class B synthetic multivulva proteins encode a conserved LIN-35 Rb-containing complex distinct from a NuRD-like complex. Proc. Natl. Acad. Sci. U. S. A. *103*, 16782–16787.

Hartwell, L.H., and Weinert, T.A. (1989). Checkpoints: controls that ensure the order of cell cycle events. Science *246*, 629–634.

Hartwig, J.H. (1995). Actin-binding proteins. 1: Spectrin super family. Protein Profile *2*, 703–800.

Hayama, S., Daigo, Y., Yamabuki, T., Hirata, D., Kato, T., Miyamoto, M., Ito, T., Tsuchiya, E., Kondo, S., and Nakamura, Y. (2007). Phosphorylation and activation of cell division cycle associated 8 by aurora kinase B plays a significant role in human lung carcinogenesis. Cancer Res. *67*, 4113–4122.

References

Hayashi-Takanaka, Y., Yamagata, K., Nozaki, N., and Kimura, H. (2009). Visualizing histone modifications in living cells: spatiotemporal dynamics of H3 phosphorylation during interphase. J Cell Biol *187*, 781–790.

Hijmans, E.M., Voorhoeve, P.M., Beijersbergen, R.L., van 't Veer, L.J., and Bernards, R. (1995). E2F-5, a new E2F family member that interacts with p130 in vivo. Mol. Cell. Biol. *15*, 3082–3089.

Hirota, T., Kunitoku, N., Sasayama, T., Marumoto, T., Zhang, D., Nitta, M., Hatakeyama, K., and Saya, H. (2003). Aurora-A and an interacting activator, the LIM protein Ajuba, are required for mitotic commitment in human cells. Cell *114*, 585–598.

Hirota, T., Lipp, J.J., Toh, B.H., and Peters, J.M. (2005). Histone H3 serine 10 phosphorylation by Aurora B causes HP1 dissociation from heterochromatin. Nature *438*, 1176–1180.

Hishiya, A., Kitazawa, T., and Takayama, S. (2010). BAG3 and Hsc70 interact with actin capping protein CapZ to maintain myofibrillar integrity under mechanical stress. Circ. Res. *107*, 1220–1231.

Honda, R., Korner, R., and Nigg, E.A. (2003). Exploring the functional interactions between Aurora B, INCENP, and survivin in mitosis. Mol Biol Cell *14*, 3325–3341.

Howman, E.V., Fowler, K.J., Newson, A.J., Redward, S., MacDonald, A.C., Kalitsis, P., and Choo, K.H. (2000). Early disruption of centromeric chromatin organization in centromere protein A (Cenpa) null mice. Proc. Natl. Acad. Sci. U. S. A. *97*, 1148–1153.

Hsu, J.Y., Sun, Z.W., Li, X., Reuben, M., Tatchell, K., Bishop, D.K., Grushcow, J.M., Brame, C.J., Caldwell, J.A., Hunt, D.F., et al. (2000). Mitotic phosphorylation of histone H3 is governed by Ipl1/aurora kinase and Glc7/PP1 phosphatase in budding yeast and nematodes. Cell *102*, 279–291.

Hu, C.-K., Coughlin, M., and Mitchison, T.J. (2012). Midbody assembly and its regulation during cytokinesis. Mol. Biol. Cell *23*, 1024–1034.

Hua, S., Wang, Z., Jiang, K., Huang, Y., Ward, T., Zhao, L., Dou, Z., and Yao, X. (2011). CENP-U cooperates with Hec1 to orchestrate kinetochore-microtubule attachment. J. Biol. Chem. *286*, 1627–1638.

Humbert, P.O., Verona, R., Trimarchi, J.M., Rogers, C., Dandapani, S., and Lees, J.A. (2000). E2f3 is critical for normal cellular proliferation. Genes Dev. *14*, 690–703.

Hümmer, S., and Mayer, T.U. (2009). Cdk1 negatively regulates midzone localization of the mitotic kinesin Mklp2 and the chromosomal passenger complex. Curr. Biol. CB *19*, 607–612.

Hunter, T., and Pines, J. (1994). Cyclins and cancer. II: Cyclin D and CDK inhibitors come of age. Cell *79*, 573–582.

Hutterer, A., Berdnik, D., Wirtz-Peitz, F., Zigman, M., Schleiffer, A., and Knoblich, J.A. (2006). Mitotic activation of the kinase Aurora-A requires its binding partner Bora. Dev. Cell *11*, 147–157.

Jang, J.K., Rahman, T., and McKim, K.S. (2005). The kinesinlike protein Subito contributes to central spindle assembly and organization of the meiotic spindle in Drosophila oocytes. Mol. Biol. Cell *16*, 4684–4694.

References

Jelluma, N., Brenkman, A.B., van den Broek, N.J.F., Cruijsen, C.W.A., van Osch, M.H.J., Lens, S.M.A., Medema, R.H., and Kops, G.J.P.L. (2008). Mps1 phosphorylates Borealin to control Aurora B activity and chromosome alignment. Cell *132*, 233–246.

Jeyaprakash, A.A., Klein, U.R., Lindner, D., Ebert, J., Nigg, E.A., and Conti, E. (2007). Structure of a Survivin-Borealin-INCENP core complex reveals how chromosomal passengers travel together. Cell *131*, 271–285.

Jeyaprakash, A.A., Basquin, C., Jayachandran, U., and Conti, E. (2011). Structural basis for the recognition of phosphorylated histone H3 by the survivin subunit of the chromosomal passenger complex. Structure *19*, 1625–1634.

Kaitna, S., Mendoza, M., Jantsch-Plunger, V., and Glotzer, M. (2000). Incenp and an Aurora-like kinase form a complex essential for chromosome segregation and efficient completion of cytokinesis. Curr Biol *10*, 1172–1181.

Kang, J., Chaudhary, J., Dong, H., Kim, S., Brautigam, C.A., and Yu, H. (2011). Mitotic centromeric targeting of HP1 and its binding to Sgo1 are dispensable for sister-chromatid cohesion in human cells. Mol. Biol. Cell *22*, 1181–1190.

Kastan, M.B., and Bartek, J. (2004). Cell-cycle checkpoints and cancer. Nature *432*, 316–323.

Katayama, H., Brinkley, W.R., and Sen, S. (2003). The Aurora kinases: role in cell transformation and tumorigenesis. Cancer Metastasis Rev. *22*, 451–464.

Kaur, H., Bekier, M.E., and Taylor, W.R. (2010). Regulation of Borealin by phosphorylation at serine 219. J Cell Biochem *111*, 1291–1298.

Kawashima, S.A., Tsukahara, T., Langegger, M., Hauf, S., Kitajima, T.S., and Watanabe, Y. (2007). Shugoshin enables tension-generating attachment of kinetochores by loading Aurora to centromeres. Genes Dev. *21*, 420–435.

Kelly, A.E., Sampath, S.C., Maniar, T.A., Woo, E.M., Chait, B.T., and Funabiki, H. (2007). Chromosomal enrichment and activation of the aurora B pathway are coupled to spatially regulate spindle assembly. Dev. Cell *12*, 31–43.

Kelly, A.E., Ghenoiu, C., Xue, J.Z., Zierhut, C., Kimura, H., and Funabiki, H. (2010). Survivin reads phosphorylated histone H3 threonine 3 to activate the mitotic kinase Aurora B. Science *330*, 235–239.

Ben Khelifa, M., Zouari, R., Harbuz, R., Halouani, L., Arnoult, C., Lunardi, J., and Ray, P.F. (2011). A new AURKC mutation causing macrozoospermia: implications for human spermatogenesis and clinical diagnosis. Mol. Hum. Reprod. *17*, 762–768.

Ben Khelifa, M., Coutton, C., Blum, M.G.B., Abada, F., Harbuz, R., Zouari, R., Guichet, A., May-Panloup, P., Mitchell, V., Rollet, J., et al. (2012). Identification of a new recurrent aurora kinase C mutation in both European and African men with macrozoospermia. Hum. Reprod. Oxf. Engl. *27*, 3337–3346.

Kim, Y., Holland, A.J., Lan, W., and Cleveland, D.W. (2010). Aurora kinases and protein phosphatase 1 mediate chromosome congression through regulation of CENP-E. Cell *142*, 444–455.

King, R.W., Jackson, P.K., and Kirschner, M.W. (1994). Mitosis in transition. Cell *79*, 563–571.

References

Klein, U.R., Nigg, E.A., and Gruneberg, U. (2006). Centromere targeting of the chromosomal passenger complex requires a ternary subcomplex of Borealin, Survivin, and the N-terminal domain of INCENP. Mol Biol Cell *17*, 2547–2558.

Klein, U.R., Haindl, M., Nigg, E.A., and Muller, S. (2009). RanBP2 and SENP3 function in a mitotic SUMO2/3 conjugation-deconjugation cycle on Borealin. Mol Biol Cell *20*, 410–418.

Knight, A.S., Notaridou, M., and Watson, R.J. (2009). A Lin-9 complex is recruited by B-Myb to activate transcription of G2/M genes in undifferentiated embryonal carcinoma cells. Oncogene *28*, 1737–1747.

Knöll, R., Buyandelger, B., and Lab, M. (2011). The sarcomeric Z-disc and Z-discopathies. J. Biomed. Biotechnol. *2011*, 569628.

Korenbaum, E., and Rivero, F. (2002). Calponin homology domains at a glance. J. Cell Sci. *115*, 3543–3545.

Korenjak, M., Taylor-Harding, B., Binné, U.K., Satterlee, J.S., Stevaux, O., Aasland, R., White-Cooper, H., Dyson, N., and Brehm, A. (2004). Native E2F/RBF complexes contain Myb-interacting proteins and repress transcription of developmentally controlled E2F target genes. Cell *119*, 181–193.

Kramer, E.R., Scheuringer, N., Podtelejnikov, A.V., Mann, M., and Peters, J.M. (2000). Mitotic regulation of the APC activator proteins CDC20 and CDH1. Mol. Biol. Cell *11*, 1555–1569.

Kufer, T.A., Silljé, H.H.W., Körner, R., Gruss, O.J., Meraldi, P., and Nigg, E.A. (2002). Human TPX2 is required for targeting Aurora-A kinase to the spindle. J. Cell Biol. *158*, 617–623.

Kuilman, T., Michaloglou, C., Mooi, W.J., and Peeper, D.S. (2010). The essence of senescence. Genes Dev. *24*, 2463–2479.

Labeit, S. (2011). BAG3 in heart disease: novel clues for cardiomyocyte survival from the Z-disk? Hum. Mutat. *32*, iv.

Laemmli, U.K. (1970). Cleavage of structural proteins during the assembly of the head of bacteriophage T4. Nature *227*, 680–685.

Lampson, M.A., and Cheeseman, I.M. (2010). Sensing centromere tension: Aurora B and the regulation of kinetochore function. Trends Cell Biol *21*, 133–140.

Lan, W., Zhang, X., Kline-Smith, S.L., Rosasco, S.E., Barrett-Wilt, G.A., Shabanowitz, J., Hunt, D.F., Walczak, C.E., and Stukenberg, P.T. (2004). Aurora B phosphorylates centromeric MCAK and regulates its localization and microtubule depolymerization activity. Curr. Biol. CB *14*, 273–286.

Lee, H., Lee, D.J., Oh, S.P., Park, H.D., Nam, H.H., Kim, J.M., and Lim, D.-S. (2006). Mouse emi1 has an essential function in mitotic progression during early embryogenesis. Mol. Cell. Biol. *26*, 5373–5381.

Lee, H.C., Cherk, S.W., Chan, S.K., Wong, S., Tong, T.W., Ho, W.S., Chan, A.Y., Lee, K.C., and Mak, C.M. (2012). BAG3-related myofibrillar myopathy in a Chinese family. Clin. Genet. *81*, 394–398.

References

Lee, K.K., Tang, M.K., Yew, D.T., Chow, P.H., Yee, S.P., Schneider, C., and Brancolini, C. (1999). gas2 is a multifunctional gene involved in the regulation of apoptosis and chondrogenesis in the developing mouse limb. Dev. Biol. *207*, 14–25.

Lee, M.H., Reynisdóttir, I., and Massagué, J. (1995). Cloning of p57KIP2, a cyclin-dependent kinase inhibitor with unique domain structure and tissue distribution. Genes Dev. *9*, 639–649.

Lees, E. (1995). Cyclin dependent kinase regulation. Curr. Opin. Cell Biol. *7*, 773–780.

Lens, S.M., Vader, G., and Medema, R.H. (2006). The case for Survivin as mitotic regulator. Curr Opin Cell Biol *18*, 616–622.

Lewis, P.W., Beall, E.L., Fleischer, T.C., Georlette, D., Link, A.J., and Botchan, M.R. (2004). Identification of a Drosophila Myb-E2F2/RBF transcriptional repressor complex. Genes Dev. *18*, 2929–2940.

Li, X., Sakashita, G., Matsuzaki, H., Sugimoto, K., Kimura, K., Hanaoka, F., Taniguchi, H., Furukawa, K., and Urano, T. (2004). Direct association with inner centromere protein (INCENP) activates the novel chromosomal passenger protein, Aurora-C. J. Biol. Chem. *279*, 47201–47211.

Lipinski, M.M., and Jacks, T. (1999). The retinoblastoma gene family in differentiation and development. Oncogene *18*, 7873–7882.

Litovchick, L., Sadasivam, S., Florens, L., Zhu, X., Swanson, S.K., Velmurugan, S., Chen, R., Washburn, M.P., Liu, X.S., and DeCaprio, J.A. (2007). Evolutionarily conserved multisubunit RBL2/p130 and E2F4 protein complex represses human cell cycle-dependent genes in quiescence. Mol. Cell *26*, 539–551.

Litovchick, L., Florens, L.A., Swanson, S.K., Washburn, M.P., and DeCaprio, J.A. (2011). DYRK1A protein kinase promotes quiescence and senescence through DREAM complex assembly. Genes Dev. *25*, 801–813.

Liu, D., Vader, G., Vromans, M.J., Lampson, M.A., and Lens, S.M. (2009). Sensing chromosome bi-orientation by spatial separation of aurora B kinase from kinetochore substrates. Science *323*, 1350–1353.

Liu, J., Cheng, F., and Deng, L.-W. (2012). MLL5 maintains genomic integrity by regulating the stability of the chromosomal passenger complex through a functional interaction with Borealin. J. Cell Sci. *125*, 4676–4685.

Logan, N., Delavaine, L., Graham, A., Reilly, C., Wilson, J., Brummelkamp, T.R., Hijmans, E.M., Bernards, R., and La Thangue, N.B. (2004). E2F-7: a distinctive E2F family member with an unusual organization of DNA-binding domains. Oncogene *23*, 5138–5150.

Logan, N., Graham, A., Zhao, X., Fisher, R., Maiti, B., Leone, G., and La Thangue, N.B. (2005). E2F-8: an E2F family member with a similar organization of DNA-binding domains to E2F-7. Oncogene *24*, 5000–5004.

Lu, L.-Y., Wood, J.L., Minter-Dykhouse, K., Ye, L., Saunders, T.L., Yu, X., and Chen, J. (2008). Polo-like kinase 1 is essential for early embryonic development and tumor suppression. Mol. Cell. Biol. *28*, 6870–6876.

Luther, P.K. (2009). The vertebrate muscle Z-disc: sarcomere anchor for structure and signalling. J. Muscle Res. Cell Motil. *30*, 171–185.

References

Maerki, S., Olma, M.H., Staubli, T., Steigemann, P., Gerlich, D.W., Quadroni, M., Sumara, I., and Peter, M. (2009). The Cul3-KLHL21 E3 ubiquitin ligase targets aurora B to midzone microtubules in anaphase and is required for cytokinesis. J. Cell Biol. *187*, 791–800.

Maiti, B., Li, J., de Bruin, A., Gordon, F., Timmers, C., Opavsky, R., Patil, K., Tuttle, J., Cleghorn, W., and Leone, G. (2005). Cloning and characterization of mouse E2F8, a novel mammalian E2F family member capable of blocking cellular proliferation. J. Biol. Chem. *280*, 18211–18220.

Maresca, T.J., and Salmon, E.D. (2010). Welcome to a new kind of tension: translating kinetochore mechanics into a wait-anaphase signal. J Cell Sci *123*, 825–835.

Meadows, J.C., Shepperd, L.A., Vanoosthuyse, V., Lancaster, T.C., Sochaj, A.M., Buttrick, G.J., Hardwick, K.G., and Millar, J.B.A. (2011). Spindle checkpoint silencing requires association of PP1 to both Spc7 and kinesin-8 motors. Dev. Cell *20*, 739–750.

Miller, A.L., Wang, Y., Mooseker, M.S., and Koleske, A.J. (2004). The Abl-related gene (Arg) requires its F-actin-microtubule cross-linking activity to regulate lamellipodial dynamics during fibroblast adhesion. J. Cell Biol. *165*, 407–419.

Miller, S.A., Johnson, M.L., and Stukenberg, P.T. (2008). Kinetochore attachments require an interaction between unstructured tails on microtubules and Ndc80(Hec1). Curr. Biol. CB *18*, 1785–1791.

Moberg, K., Starz, M.A., and Lees, J.A. (1996). E2F-4 switches from p130 to p107 and pRB in response to cell cycle reentry. Mol. Cell. Biol. *16*, 1436–1449.

Mohapatra, B., Jimenez, S., Lin, J.H., Bowles, K.R., Coveler, K.J., Marx, J.G., Chrisco, M.A., Murphy, R.T., Lurie, P.R., Schwartz, R.J., et al. (2003). Mutations in the muscle LIM protein and alpha-actinin-2 genes in dilated cardiomyopathy and endocardial fibroelastosis. Mol. Genet. Metab. *80*, 207–215.

Monier, K., Mouradian, S., and Sullivan, K.F. (2007). DNA methylation promotes Aurora-B-driven phosphorylation of histone H3 in chromosomal subdomains. J Cell Sci *120*, 101–114.

Montpetit, B., Hazbun, T.R., Fields, S., and Hieter, P. (2006). Sumoylation of the budding yeast kinetochore protein Ndc10 is required for Ndc10 spindle localization and regulation of anaphase spindle elongation. J Cell Biol *174*, 653–663.

Moreno, S., and Nurse, P. (1990). Substrates for p34cdc2: in vivo veritas? Cell *61*, 549–551.

Morgan, D. (2006). The Cell Cycle: Principles of Control (London : Sunderland, MA: Oxford University Press).

Morgan, D.O. (1997). Cyclin-dependent kinases: engines, clocks, and microprocessors. Annu. Rev. Cell Dev. Biol. *13*, 261–291.

Mortlock, A.A., Foote, K.M., Heron, N.M., Jung, F.H., Pasquet, G., Lohmann, J.-J.M., Warin, N., Renaud, F., De Savi, C., Roberts, N.J., et al. (2007). Discovery, synthesis, and in vivo activity of a new class of pyrazoloquinazolines as selective inhibitors of aurora B kinase. J. Med. Chem. *50*, 2213–2224.

Moulding, D.A., Moeendarbary, E., Valon, L., Record, J., Charras, G.T., and Thrasher, A.J. (2012). Excess F-actin mechanically impedes mitosis leading to cytokinesis failure in X-linked neutropenia by exceeding Aurora B kinase error correction capacity. Blood *120*, 3803–3811.

References

Murnion, M.E., Adams, R.R., Callister, D.M., Allis, C.D., Earnshaw, W.C., and Swedlow, J.R. (2001). Chromatin-associated protein phosphatase 1 regulates aurora-B and histone H3 phosphorylation. J. Biol. Chem. *276*, 26656–26665.

Murray, A.W. (2004). Recycling the cell cycle: cyclins revisited. Cell *116*, 221–234.

Nevins, J.R. (1992). E2F: a link between the Rb tumor suppressor protein and viral oncoproteins. Science *258*, 424–429.

Nguyen, H.G., Chinnappan, D., Urano, T., and Ravid, K. (2005). Mechanism of Aurora-B degradation and its dependency on intact KEN and A-boxes: identification of an aneuploidy-promoting property. Mol Cell Biol *25*, 4977–4992.

Niedzialkowska, E., Wang, F., Porebski, P.J., Minor, W., Higgins, J.M.G., and Stukenberg, P.T. (2012). Molecular basis for phosphospecific recognition of histone H3 tails by Survivin paralogues at inner centromeres. Mol. Biol. Cell *23*, 1457–1466.

Norden, C., Mendoza, M., Dobbelaere, J., Kotwaliwale, C.V., Biggins, S., and Barral, Y. (2006). The NoCut pathway links completion of cytokinesis to spindle midzone function to prevent chromosome breakage. Cell *125*, 85–98.

Norton, N., Li, D., Rieder, M.J., Siegfried, J.D., Rampersaud, E., Züchner, S., Mangos, S., Gonzalez-Quintana, J., Wang, L., McGee, S., et al. (2011). Genome-wide studies of copy number variation and exome sequencing identify rare variants in BAG3 as a cause of dilated cardiomyopathy. Am. J. Hum. Genet. *88*, 273–282.

Nozawa, R.-S., Nagao, K., Masuda, H.-T., Iwasaki, O., Hirota, T., Nozaki, N., Kimura, H., and Obuse, C. (2010). Human POGZ modulates dissociation of HP1alpha from mitotic chromosome arms through Aurora B activation. Nat. Cell Biol. *12*, 719–727.

O'Connor, D.S., Grossman, D., Plescia, J., Li, F., Zhang, H., Villa, A., Tognin, S., Marchisio, P.C., and Altieri, D.C. (2000). Regulation of apoptosis at cell division by p34cdc2 phosphorylation of survivin. Proc. Natl. Acad. Sci. U. S. A. *97*, 13103–13107.

O'Connor, D.S., Wall, N.R., Porter, A.C., and Altieri, D.C. (2002). A p34cdc2 survival checkpoint in cancer. Cancer Cell *2*, 43–54.

Ohi, R., Sapra, T., Howard, J., and Mitchison, T.J. (2004). Differentiation of cytoplasmic and meiotic spindle assembly MCAK functions by Aurora B-dependent phosphorylation. Mol. Biol. Cell *15*, 2895–2906.

Ohtsubo, M., Theodoras, A.M., Schumacher, J., Roberts, J.M., and Pagano, M. (1995). Human cyclin E, a nuclear protein essential for the G1-to-S phase transition. Mol. Cell. Biol. *15*, 2612–2624.

Osterloh, L., von Eyss, B., Schmit, F., Rein, L., Hübner, D., Samans, B., Hauser, S., and Gaubatz, S. (2007). The human synMuv-like protein LIN-9 is required for transcription of G2/M genes and for entry into mitosis. EMBO J. *26*, 144–157.

Pasumarthi, K.B.S., and Field, L.J. (2002). Cardiomyocyte cell cycle regulation. Circ. Res. *90*, 1044–1054.

Pavletich, N.P. (1999). Mechanisms of cyclin-dependent kinase regulation: structures of Cdks, their cyclin activators, and Cip and INK4 inhibitors. J. Mol. Biol. *287*, 821–828.

References

Pe'er, T., Lahmi, R., Sharaby, Y., Chorni, E., Noach, M., Vecsler, M., Zlotorynski, E., Steen, H., Steen, J.A., and Tzur, A. (2013). Gas2l3, a novel constriction site-associated protein whose regulation is mediated by the APC/C Cdh1 complex. PloS One *8*, e57532.

Peters, J.-M. (2006). The anaphase promoting complex/cyclosome: a machine designed to destroy. Nat. Rev. Mol. Cell Biol. *7*, 644–656.

Pettitt, S.J., Liang, Q., Rairdan, X.Y., Moran, J.L., Prosser, H.M., Beier, D.R., Lloyd, K., Bradley, A., and Skarnes, W.C. (2009). Agouti C57BL/6N embryonic stem cells for mouse genetic resources. Nat. Methods *6*, 493–495.

Piekny, A.J., and Glotzer, M. (2008). Anillin is a scaffold protein that links RhoA, actin, and myosin during cytokinesis. Curr. Biol. CB *18*, 30–36.

Pilkinton, M., Sandoval, R., and Colamonici, O.R. (2007). Mammalian Mip/LIN-9 interacts with either the p107, p130/E2F4 repressor complex or B-Myb in a cell cycle-phase-dependent context distinct from the Drosophila dREAM complex. Oncogene *26*, 7535–7543.

Pines, M.K., Housden, B.E., Bernard, F., Bray, S.J., and Röper, K. (2010). The cytolinker Pigs is a direct target and a negative regulator of Notch signalling. Dev. Camb. Engl. *137*, 913–922.

Planas-Silva, M.D., and Weinberg, R.A. (1997). The restriction point and control of cell proliferation. Curr. Opin. Cell Biol. *9*, 768–772.

Pollard, T.D., Earnshaw, W.C., and Lippincott-Schwartz, J. (2007). Cell Biology (Philadelphia: Saunders W.B.).

Porter, L.A., and Donoghue, D.J. (2003). Cyclin B1 and CDK1: nuclear localization and upstream regulators. Prog. Cell Cycle Res. *5*, 335–347.

Posch, M., Khoudoli, G.A., Swift, S., King, E.M., Deluca, J.G., and Swedlow, J.R. (2010). Sds22 regulates aurora B activity and microtubule-kinetochore interactions at mitosis. J. Cell Biol. *191*, 61–74.

Powers, A.F., Franck, A.D., Gestaut, D.R., Cooper, J., Gracyzk, B., Wei, R.R., Wordeman, L., Davis, T.N., and Asbury, C.L. (2009). The Ndc80 kinetochore complex forms load-bearing attachments to dynamic microtubule tips via biased diffusion. Cell *136*, 865–875.

Qian, J., Lesage, B., Beullens, M., Van Eynde, A., and Bollen, M. (2011). PP1/Repo-man dephosphorylates mitotic histone H3 at T3 and regulates chromosomal aurora B targeting. Curr. Biol. CB *21*, 766–773.

Raiborg, C., and Stenmark, H. (2011). Cell biology. A helix for the final cut. Science *331*, 1533–1534.

Ramadan, K., Bruderer, R., Spiga, F.M., Popp, O., Baur, T., Gotta, M., and Meyer, H.H. (2007). Cdc48/p97 promotes reformation of the nucleus by extracting the kinase Aurora B from chromatin. Nature *450*, 1258–1262.

Rasheed, S., Nelson-Rees, W.A., Toth, E.M., Arnstein, P., and Gardner, M.B. (1974). Characterization of a newly derived human sarcoma cell line (HT-1080). Cancer *33*, 1027–1033.

Reichert, N., Wurster, S., Ulrich, T., Schmitt, K., Hauser, S., Probst, L., Götz, R., Ceteci, F., Moll, R., Rapp, U., et al. (2010). Lin9, a subunit of the mammalian DREAM complex, is

essential for embryonic development, for survival of adult mice, and for tumor suppression. Mol. Cell. Biol. *30*, 2896–2908.

Rodríguez, C.I., Buchholz, F., Galloway, J., Sequerra, R., Kasper, J., Ayala, R., Stewart, A.F., and Dymecki, S.M. (2000). High-efficiency deleter mice show that FLPe is an alternative to Cre-loxP. Nat. Genet. *25*, 139–140.

Röper, K., Gregory, S.L., and Brown, N.H. (2002). The "spectraplakins": cytoskeletal giants with characteristics of both spectrin and plakin families. J. Cell Sci. *115*, 4215–4225.

Rosasco-Nitcher, S.E., Lan, W., Khorasanizadeh, S., and Stukenberg, P.T. (2008). Centromeric Aurora-B activation requires TD-60, microtubules, and substrate priming phosphorylation. Science *319*, 469–472.

Rosenberg, J.S., Cross, F.R., and Funabiki, H. (2011). KNL1/Spc105 recruits PP1 to silence the spindle assembly checkpoint. Curr. Biol. CB *21*, 942–947.

Ruchaud, S., Carmena, M., and Earnshaw, W.C. (2007). Chromosomal passengers: conducting cell division. Nat. Rev Mol Cell Biol *8*, 798–812.

Sadasivam, S., Duan, S., and DeCaprio, J.A. (2012). The MuvB complex sequentially recruits B-Myb and FoxM1 to promote mitotic gene expression. Genes Dev. *26*, 474–489.

Sampath, S.C., Ohi, R., Leismann, O., Salic, A., Pozniakovski, A., and Funabiki, H. (2004). The chromosomal passenger complex is required for chromatin-induced microtubule stabilization and spindle assembly. Cell *118*, 187–202.

Sánchez, I., and Dynlacht, B.D. (2005). New insights into cyclins, CDKs, and cell cycle control. Semin. Cell Dev. Biol. *16*, 311–321.

Avo Santos, M., van de Werken, C., de Vries, M., Jahr, H., Vromans, M.J.M., Laven, J.S.E., Fauser, B.C., Kops, G.J., Lens, S.M., and Baart, E.B. (2011). A role for Aurora C in the chromosomal passenger complex during human preimplantation embryo development. Hum. Reprod. Oxf. Engl. *26*, 1868–1881.

Sasai, K., Katayama, H., Stenoien, D.L., Fujii, S., Honda, R., Kimura, M., Okano, Y., Tatsuka, M., Suzuki, F., Nigg, E.A., et al. (2004). Aurora-C kinase is a novel chromosomal passenger protein that can complement Aurora-B kinase function in mitotic cells. Cell Motil. Cytoskeleton *59*, 249–263.

Schafer, D.A., Waddle, J.A., and Cooper, J.A. (1993). Localization of CapZ during myofibrillogenesis in cultured chicken muscle. Cell Motil. Cytoskeleton *25*, 317–335.

Schiel, J.A., Childs, C., and Prekeris, R. (2013). Endocytic transport and cytokinesis: from regulation of the cytoskeleton to midbody inheritance. Trends Cell Biol. *23*, 319–327.

Schmit, F., Korenjak, M., Mannefeld, M., Schmitt, K., Franke, C., von Eyss, B., Gagrica, S., Hänel, F., Brehm, A., and Gaubatz, S. (2007). LINC, a human complex that is related to pRB-containing complexes in invertebrates regulates the expression of G2/M genes. Cell Cycle Georget. Tex *6*, 1903–1913.

Schmitt, K. (2010). Identification and Characterization of GAS2L3 as a Novel Mitotic Regulator in Human Cells (Universität Würzburg, Fakultät für Biologie, Dissertation (urn:nbn:de:bvb:20-opus-52704)).

References

Schneider, C., King, R.M., and Philipson, L. (1988). Genes specifically expressed at growth arrest of mammalian cells. Cell *54*, 787–793.

Selcen, D., and Engel, A.G. (2011). Myofibrillar myopathies. Handb. Clin. Neurol. *101*, 143–154.

Selcen, D., Muntoni, F., Burton, B.K., Pegoraro, E., Sewry, C., Bite, A.V., and Engel, A.G. (2009). Mutation in BAG3 causes severe dominant childhood muscular dystrophy. Ann. Neurol. *65*, 83–89.

Senyo, S.E., Steinhauser, M.L., Pizzimenti, C.L., Yang, V.K., Cai, L., Wang, M., Wu, T.-D., Guerquin-Kern, J.-L., Lechene, C.P., and Lee, R.T. (2013). Mammalian heart renewal by pre-existing cardiomyocytes. Nature *493*, 433–436.

Sessa, F., Mapelli, M., Ciferri, C., Tarricone, C., Areces, L.B., Schneider, T.R., Stukenberg, P.T., and Musacchio, A. (2005). Mechanism of Aurora B activation by INCENP and inhibition by hesperadin. Mol. Cell *18*, 379–391.

Sgorbissa, A., Benetti, R., Marzinotto, S., Schneider, C., and Brancolini, C. (1999). Caspase-3 and caspase-7 but not caspase-6 cleave Gas2 in vitro: implications for microfilament reorganization during apoptosis. J. Cell Sci. *112 (Pt 23)*, 4475–4482.

Shackelford, R.E., Kaufmann, W.K., and Paules, R.S. (1999). Cell cycle control, checkpoint mechanisms, and genotoxic stress. Environ. Health Perspect. *107 Suppl 1*, 5–24.

Sherr, C.J. (1996). Cancer cell cycles. Science *274*, 1672–1677.

Sherr, C.J., and Roberts, J.M. (1999). CDK inhibitors: positive and negative regulators of G1-phase progression. Genes Dev. *13*, 1501–1512.

Skop, A.R., Liu, H., Yates, J., 3rd, Meyer, B.J., and Heald, R. (2004). Dissection of the mammalian midbody proteome reveals conserved cytokinesis mechanisms. Science *305*, 61–66.

Stauber, R.H., Rabenhorst, U., Rekik, A., Engels, K., Bier, C., and Knauer, S.K. (2006). Nucleocytoplasmic shuttling and the biological activity of mouse survivin are regulated by an active nuclear export signal. Traffic Cph. Den. *7*, 1461–1472.

Di Stefano, L., Jensen, M.R., and Helin, K. (2003). E2F7, a novel E2F featuring DP-independent repression of a subset of E2F-regulated genes. EMBO J. *22*, 6289–6298.

Steigemann, P., Wurzenberger, C., Schmitz, M.H.A., Held, M., Guizetti, J., Maar, S., and Gerlich, D.W. (2009). Aurora B-mediated abscission checkpoint protects against tetraploidization. Cell *136*, 473–484.

Stevaux, O., and Dyson, N.J. (2002). A revised picture of the E2F transcriptional network and RB function. Curr. Opin. Cell Biol. *14*, 684–691.

Stewart, S., and Fang, G. (2005). Destruction box-dependent degradation of aurora B is mediated by the anaphase-promoting complex/cyclosome and Cdh1. Cancer Res *65*, 8730–8735.

Stradal, T., Kranewitter, W., Winder, S.J., and Gimona, M. (1998). CH domains revisited. FEBS Lett. *431*, 134–137.

Straight, A.F., Field, C.M., and Mitchison, T.J. (2005). Anillin binds nonmuscle myosin II and regulates the contractile ring. Mol. Biol. Cell *16*, 193–201.

Stroud, M.J., Kammerer, R.A., and Ballestrem, C. (2011). Characterization of G2L3 (GAS2-like 3), a new microtubule- and actin-binding protein related to spectraplakins. J. Biol. Chem. *286*, 24987–24995.

Stroud, M.J., Nazgiewicz, A., McKenzie, E.A., Wang, Y., Kammerer, R.A., and Ballestrem, C. (2014). GAS2-like proteins mediate communication between microtubules and actin through interaction with end-binding proteins. J. Cell Sci. *[Epub ahead of print]*, DOI: 10.1242/jcs.140558.

Sumara, I., Quadroni, M., Frei, C., Olma, M.H., Sumara, G., Ricci, R., and Peter, M. (2007). A Cul3-based E3 ligase removes Aurora B from mitotic chromosomes, regulating mitotic progression and completion of cytokinesis in human cells. Dev. Cell *12*, 887–900.

Sun, C., Nettesheim, D., Liu, Z., and Olejniczak, E.T. (2005). Solution structure of human survivin and its binding interface with Smac/Diablo. Biochemistry (Mosc.) *44*, 11–17.

Sun, D., Leung, C.L., and Liem, R.K. (2001). Characterization of the microtubule binding domain of microtubule actin crosslinking factor (MACF): identification of a novel group of microtubule associated proteins. J. Cell Sci. *114*, 161–172.

Suozzi, K.C., Wu, X., and Fuchs, E. (2012). Spectraplakins: master orchestrators of cytoskeletal dynamics. J. Cell Biol. *197*, 465–475.

Szafer-Glusman, E., Fuller, M.T., and Giansanti, M.G. (2011). Role of Survivin in cytokinesis revealed by a separation-of-function allele. Mol Biol Cell *22*, 3779–3790.

Tanaka, T.U., Rachidi, N., Janke, C., Pereira, G., Galova, M., Schiebel, E., Stark, M.J.R., and Nasmyth, K. (2002). Evidence that the Ipl1-Sli15 (Aurora kinase-INCENP) complex promotes chromosome bi-orientation by altering kinetochore-spindle pole connections. Cell *108*, 317–329.

Tanenbaum, M.E., Macurek, L., van der Vaart, B., Galli, M., Akhmanova, A., and Medema, R.H. (2011). A complex of Kif18b and MCAK promotes microtubule depolymerization and is negatively regulated by Aurora kinases. Curr. Biol. CB *21*, 1356–1365.

Taylor, S., and Peters, J.-M. (2008). Polo and Aurora kinases: lessons derived from chemical biology. Curr. Opin. Cell Biol. *20*, 77–84.

Tooley, J.G., Miller, S.A., and Stukenberg, P.T. (2011). The Ndc80 complex uses a tripartite attachment point to couple microtubule depolymerization to chromosome movement. Mol. Biol. Cell *22*, 1217–1226.

Trimarchi, J.M., and Lees, J.A. (2002). Sibling rivalry in the E2F family. Nat. Rev. Mol. Cell Biol. *3*, 11–20.

Trimarchi, J.M., Fairchild, B., Verona, R., Moberg, K., Andon, N., and Lees, J.A. (1998). E2F-6, a member of the E2F family that can behave as a transcriptional repressor. Proc. Natl. Acad. Sci. U. S. A. *95*, 2850–2855.

Trinkle-Mulcahy, L., Boulon, S., Lam, Y.W., Urcia, R., Boisvert, F.-M., Vandermoere, F., Morrice, N.A., Swift, S., Rothbauer, U., Leonhardt, H., et al. (2008). Identifying specific protein interaction partners using quantitative mass spectrometry and bead proteomes. J. Cell Biol. *183*, 223–239.

References

Tseng, B.S., Tan, L., Kapoor, T.M., and Funabiki, H. (2010). Dual detection of chromosomes and microtubules by the chromosomal passenger complex drives spindle assembly. Dev Cell *18*, 903–912.

Tseng, T.C., Chen, S.H., Hsu, Y.P., and Tang, T.K. (1998). Protein kinase profile of sperm and eggs: cloning and characterization of two novel testis-specific protein kinases (AIE1, AIE2) related to yeast and fly chromosome segregation regulators. DNA Cell Biol. *17*, 823–833.

Tsukahara, T., Tanno, Y., and Watanabe, Y. (2010). Phosphorylation of the CPC by Cdk1 promotes chromosome bi-orientation. Nature *467*, 719–723.

Tyers, M., and Jorgensen, P. (2000). Proteolysis and the cell cycle: with this RING I do thee destroy. Curr. Opin. Genet. Dev. *10*, 54–64.

Ulbricht, A., Eppler, F.J., Tapia, V.E., van der Ven, P.F.M., Hampe, N., Hersch, N., Vakeel, P., Stadel, D., Haas, A., Saftig, P., et al. (2013). Cellular mechanotransduction relies on tension-induced and chaperone-assisted autophagy. Curr. Biol. CB *23*, 430–435.

Uren, A.G., Beilharz, T., O'Connell, M.J., Bugg, S.J., van Driel, R., Vaux, D.L., and Lithgow, T. (1999). Role for yeast inhibitor of apoptosis (IAP)-like proteins in cell division. Proc. Natl. Acad. Sci. U. S. A. *96*, 10170–10175.

Uren, A.G., Wong, L., Pakusch, M., Fowler, K.J., Burrows, F.J., Vaux, D.L., and Choo, K.H. (2000). Survivin and the inner centromere protein INCENP show similar cell-cycle localization and gene knockout phenotype. Curr. Biol. CB *10*, 1319–1328.

Vader, G., and Lens, S.M.A. (2008). The Aurora kinase family in cell division and cancer. Biochim. Biophys. Acta *1786*, 60–72.

Vader, G., Kauw, J.J., Medema, R.H., and Lens, S.M. (2006). Survivin mediates targeting of the chromosomal passenger complex to the centromere and midbody. EMBO Rep *7*, 85–92.

Vagnarelli, P., Ribeiro, S., Sennels, L., Sanchez-Pulido, L., de Lima Alves, F., Verheyen, T., Kelly, D.A., Ponting, C.P., Rappsilber, J., and Earnshaw, W.C. (2011). Repo-Man coordinates chromosomal reorganization with nuclear envelope reassembly during mitotic exit. Dev. Cell *21*, 328–342.

Vancompernolle, K., Gimona, M., Herzog, M., Van Damme, J., Vandekerckhove, J., and Small, V. (1990). Isolation and sequence of a tropomyosin-binding fragment of turkey gizzard calponin. FEBS Lett. *274*, 146–150.

Varma, D., and Salmon, E.D. (2012). The KMN protein network--chief conductors of the kinetochore orchestra. J. Cell Sci. *125*, 5927–5936.

Verdecia, M.A., Huang, H., Dutil, E., Kaiser, D.A., Hunter, T., and Noel, J.P. (2000). Structure of the human anti-apoptotic protein survivin reveals a dimeric arrangement. Nat. Struct. Biol. *7*, 602–608.

Vidal, A., and Koff, A. (2000). Cell-cycle inhibitors: three families united by a common cause. Gene *247*, 1–15.

Vogel, C., and Marcotte, E.M. (2012). Insights into the regulation of protein abundance from proteomic and transcriptomic analyses. Nat. Rev. Genet. *13*, 227–232.

References

Vong, Q.P., Cao, K., Li, H.Y., Iglesias, P.A., and Zheng, Y. (2005). Chromosome alignment and segregation regulated by ubiquitination of survivin. Science *310*, 1499–1504.

De Vries, W.N., Binns, L.T., Fancher, K.S., Dean, J., Moore, R., Kemler, R., and Knowles, B.B. (2000). Expression of Cre recombinase in mouse oocytes: a means to study maternal effect genes. Genes. N. Y. N 2000 *26*, 110–112.

Van der Waal, M.S., Hengeveld, R.C., van der Horst, A., and Lens, S.M. (2012). Cell division control by the chromosomal passenger complex. Exp Cell Res *318*, 1407–1420.

Walker, D.H., and Maller, J.L. (1991). Role for cyclin A in the dependence of mitosis on completion of DNA replication. Nature *354*, 314–317.

Wang, E., Ballister, E.R., and Lampson, M.A. (2011). Aurora B dynamics at centromeres create a diffusion-based phosphorylation gradient. J Cell Biol *194*, 539–549.

Wang, F., Dai, J., Daum, J.R., Niedzialkowska, E., Banerjee, B., Stukenberg, P.T., Gorbsky, G.J., and Higgins, J.M.G. (2010). Histone H3 Thr-3 phosphorylation by Haspin positions Aurora B at centromeres in mitosis. Science *330*, 231–235.

Watanabe, S., Ando, Y., Yasuda, S., Hosoya, H., Watanabe, N., Ishizaki, T., and Narumiya, S. (2008). mDia2 induces the actin scaffold for the contractile ring and stabilizes its position during cytokinesis in NIH 3T3 cells. Mol. Biol. Cell *19*, 2328–2338.

Wei, R.R., Al-Bassam, J., and Harrison, S.C. (2007). The Ndc80/HEC1 complex is a contact point for kinetochore-microtubule attachment. Nat. Struct. Mol. Biol. *14*, 54–59.

Welburn, J.P.I., Vleugel, M., Liu, D., Yates, J.R., 3rd, Lampson, M.A., Fukagawa, T., and Cheeseman, I.M. (2010). Aurora B phosphorylates spatially distinct targets to differentially regulate the kinetochore-microtubule interface. Mol. Cell *38*, 383–392.

Werner, A., Flotho, A., and Melchior, F. (2012). The RanBP2/RanGAP1*SUMO1/Ubc9 complex is a multisubunit SUMO E3 ligase. Mol Cell *46*, 287–298.

Wheatley, S.P., Carvalho, A., Vagnarelli, P., and Earnshaw, W.C. (2001). INCENP is required for proper targeting of Survivin to the centromeres and the anaphase spindle during mitosis. Curr. Biol. CB *11*, 886–890.

Wheatley, S.P., Henzing, A.J., Dodson, H., Khaled, W., and Earnshaw, W.C. (2004). Aurora-B phosphorylation in vitro identifies a residue of survivin that is essential for its localization and binding to inner centromere protein (INCENP) in vivo. J Biol Chem *279*, 5655–5660.

Wheatley, S.P., Barrett, R.M., Andrews, P.D., Medema, R.H., Morley, S.J., Swedlow, J.R., and Lens, S.M.A. (2007). Phosphorylation by aurora-B negatively regulates survivin function during mitosis. Cell Cycle Georget. Tex *6*, 1220–1230.

Wittmann, T., Wilm, M., Karsenti, E., and Vernos, I. (2000). Tpx2, a Novel Xenopus Map Involved in Spindle Pole Organization. J. Cell Biol. *149*, 1405–1418.

Wolter, P., Schmitt, K., Fackler, M., Kremling, H., Probst, L., Hauser, S., Gruss, O.J., and Gaubatz, S. (2012). GAS2L3, a target gene of the DREAM complex, is required for proper cytokinesis and genomic stability. J. Cell Sci. *125*, 2393–2406.

Wu, C.L., Zukerberg, L.R., Ngwu, C., Harlow, E., and Lees, J.A. (1995). In vivo association of E2F and DP family proteins. Mol. Cell. Biol. *15*, 2536–2546.

References

Wyler, E., Zimmermann, M., Widmann, B., Gstaiger, M., Pfannstiel, J., Kutay, U., and Zemp, I. (2011). Tandem affinity purification combined with inducible shRNA expression as a tool to study the maturation of macromolecular assemblies. RNA N. Y. N *17*, 189–200.

Xu, Z., Ogawa, H., Vagnarelli, P., Bergmann, J.H., Hudson, D.F., Ruchaud, S., Fukagawa, T., Earnshaw, W.C., and Samejima, K. (2009). INCENP-aurora B interactions modulate kinase activity and chromosome passenger complex localization. J. Cell Biol. *187*, 637–653.

Yamagishi, Y., Honda, T., Tanno, Y., and Watanabe, Y. (2010). Two histone marks establish the inner centromere and chromosome bi-orientation. Science *330*, 239–243.

Yan, H., Thomas, J., Liu, T., Raj, D., London, N., Tandeski, T., Leachman, S.A., Lee, R.M., and Grossman, D. (2006). Induction of melanoma cell apoptosis and inhibition of tumor growth using a cell-permeable Survivin antagonist. Oncogene *25*, 6968–6974.

Yang, F., Camp, D.G., 2nd, Gritsenko, M.A., Luo, Q., Kelly, R.T., Clauss, T.R.W., Brinkley, W.R., Smith, R.D., and Stenoien, D.L. (2007). Identification of a novel mitotic phosphorylation motif associated with protein localization to the mitotic apparatus. J. Cell Sci. *120*, 4060–4070.

Yang, K.-T., Li, S.-K., Chang, C.-C., Tang, C.-J.C., Lin, Y.-N., Lee, S.-C., and Tang, T.K. (2010). Aurora-C kinase deficiency causes cytokinesis failure in meiosis I and production of large polyploid oocytes in mice. Mol. Biol. Cell *21*, 2371–2383.

Yeung, S.-C.J., Gully, C., and Lee, M.-H. (2008). Aurora-B kinase inhibitors for cancer chemotherapy. Mini Rev. Med. Chem. *8*, 1514–1525.

Yue, Z., Carvalho, A., Xu, Z., Yuan, X., Cardinale, S., Ribeiro, S., Lai, F., Ogawa, H., Gudmundsdottir, E., Gassmann, R., et al. (2008). Deconstructing Survivin: comprehensive genetic analysis of Survivin function by conditional knockout in a vertebrate cell line. J. Cell Biol. *183*, 279–296.

Zachariae, W., and Nasmyth, K. (1999). Whose end is destruction: cell division and the anaphase-promoting complex. Genes Dev. *13*, 2039–2058.

Zebrowski, D.C., and Engel, F.B. (2013). The cardiomyocyte cell cycle in hypertrophy, tissue homeostasis, and regeneration. Rev. Physiol. Biochem. Pharmacol. *165*, 67–96.

Zeitlin, S.G., Shelby, R.D., and Sullivan, K.F. (2001). CENP-A is phosphorylated by Aurora B kinase and plays an unexpected role in completion of cytokinesis. J Cell Biol *155*, 1147–1157.

Zhang, T., Dayanandan, B., Rouiller, I., Lawrence, E.J., and Mandato, C.A. (2011). Growth-arrest-specific protein 2 inhibits cell division in Xenopus embryos. PloS One *6*, e24698.

Zhao, W.-M., and Fang, G. (2005). Anillin is a substrate of anaphase-promoting complex/cyclosome (APC/C) that controls spatial contractility of myosin during late cytokinesis. J. Biol. Chem. *280*, 33516–33524.

Zhou, H., Ge, Y., Sun, L., Ma, W., Wu, J., Zhang, X., Hu, X., Eaves, C.J., Wu, D., and Zhao, Y. (2014). Growth arrest specific 2 is up-regulated in chronic myeloid leukemia cells and required for their growth. PloS One *9*, e86195.

Zucman-Rossi, J., Legoix, P., and Thomas, G. (1996). Identification of new members of the Gas2 and Ras families in the 22q12 chromosome region. Genomics *38*, 247–254.

8. Appendix

8.1. List of figures

Figure 1.1: Schematic illustration of the mammalian cell cycle.

Figure 1.2: Composition and function of the DREAM complex in mammalian cells.

Figure 1.3: Overview of the Growth arrest specific 2 (GAS2) protein family.

Figure 3.1: Expression of GAS2L3 is cell cycle regulated.

Figure 3.2: Depletion of GAS2L3 leads to defects in cytokinesis.

Figure 3.3: GAS2L3 interacts with F-actin *in vitro*.

Figure 3.4: GAS2L3 interacts with microtubules *in vitro*.

Figure 3.5: Summary of the data obtained from co-sedimentation assays.

Figure 3.6: GAS2L3 crosslinks microtubules and F-actin *in vitro*.

Figure 3.7: GAS2L3 bundles microtubules *in vitro*.

Figure 3.8: Summary of the *in vitro* binding data.

Figure 3.9: The GAR domain of GAS2L3 is required and sufficient to mediate binding to the chromosomal passenger complex *in vitro*.

Figure 3.10: GAS2L3 interacts with Borealin and Survivin, but not with Aurora B *in vitro*.

Figure 3.11: The GAR domain of GAS2L3 interacts with the C-terminus of Borealin and the N-terminus of Survivin.

Figure 3.12: GAS2L3 interacts with the chromosomal passenger complex.

Figure 3.13: GAS2L3 interacts with the chromosomal passenger complex in cells.

Figure 3.14: GAS2L3 is not a substrate of Aurora B, but is phosphorylated by CDK1.

Figure 3.15: CDK1 phosphorylates GAS2L3 at multiple sites.

Figure 3.16: GAS2L3 depletion slightly influences stability and activity of the chromosomal passenger complex.

Figure 3.17: Depletion of GAS2L3 phenocopies moderate pharmacological inhibition of the chromosomal passenger complex.

Figure 3.18: The GAR domain is necessary for proper localization of GAS2L3 during cytokinesis.

Figure 3.19: The GAR domain of GAS2L3 is necessary for successful completion of cytokinesis.

Figure 3.20: Mass spectrometrical analysis revealed 38 potentially new GAS2L3 interacting proteins.

Figure 3.21: GAS2L3 interacts with cytoskeleton associated proteins and co-chaperones identified by mass spectrometrical analysis.

Figure 3.22: GAS2L3 is ubiquitously expressed in mouse tissues.

Figure 3.23: Long range PCR confirms correct orientation of the insertion cassette in the targeted Gas2l3 allele of embryonic stem cells.

Figure 3.24: Breeding strategy for generation of conditional and knockout alleles of Gas2l3.

Figure 3.25: Breeding strategy for mice harboring a conditional Gas2l3 allele.

Figure 3.26: Breeding strategy for isolation of Gas2l3$^{fl/fl}$ CreER$^{T2\ cre/+}$ mouse embryonic fibroblasts.

Figure 3.27: Gas2l3 expression is lost in Gas2l3$^{fl/fl}$ CreER$^{T2\ cre/+}$ MEFs after hydroxytamoxifen administration.

Figure 3.28: Breeding strategy to generate non-conditional Gas2l3 knockout mice.

Figure 3.29: Loss of Gas2l3 leads to an increase in mortality.

Figure 3.30: Gas2l3 knockout mice are fertile.

Figure 3.31: Expression of Gas2l3 is declining during rat heart development.

8.2. Abbreviations

4-OHT	4-Hydroxytamoxifen
aa	Amino acids
APC/C	Anaphase promoting complex/Cyclosome
APS	Ammonium persulfate
bp	Base pairs
BSA	Bovine serum albumine
CDK	Cyclin dependent kinase
CH	Calponin homology
ChIP	Chromatin immunoprecipitation
Ci	Curie
Co-IP	Co-immunopreciptation
Ctrl.	Control
DMEM	Dulbecco`s modified eagle medium
DMSO	Dimethylsulfoxyde
DNA	Deoxyribonucleic acid
dNTP	Deoxyribonucleotide triphosphate
dpc	days post coitus
DREAM	DP, RB-like, E2F and MuvB complex
dREAM	Drosophila RBF E2F and Myb complex
DRM	DP, RB and MuvB complex
DTT	Dithiothreitol
EDTA	Ethylenediaminetetraacetic acid
F-actin	Actin filaments
FCS	Fetal calf serum
Fig.	Figure
G0, G1, G2	Gap phases
GAPDH	Glyceraldehyde-3-phosphate dehydrogenase
GAS2	Growth arrest specific 2
GST	Glutathione-S-transferase
h	Hours
His	Hexa histidine
HPRT	Hypoxanthine-phosphoribosyltransferase 1
HRP	Horseradish peroxydase
IB	Immunoblot
IF	Immunofluorescence
IgG	Immunoglobulin G
IP	Immunoprecipitation
IPTG	Isopropyl-β-D-1-thiogalactopyranoside
kDa	kiloDalton
LB	Luria Bertani
LINC	LIN complex
M phase	Mitosis and cytokinesis
MEFs	Mouse embryonic fibroblasts
min	Minutes

Mip	Myb-interacting protein
MMB	Myb-MuvB
MTs	Microtubules
NP-40	Nonylphenoxylpolyethoxyl- ethanol
PAGE	Polyacrylamide gel electrophoresis
PBS	Phosphate buffered saline
PCR	Polymerase chain reaction
PFA	Paraformaldehyde
PI	Protease Inhibitor
PIPES	1,4-Piperazinediethanesulfonic acid
PMSF	Phenylmethylsulphonyl fluoride
pRB	Retinoblastoma protein
qPCR	Quantitative polymerase chain reaction
RNA	Ribonucleic acid
RNAi	RNA interference
rpm	Rounds per minute
RT	Reverse transcriptase / Room temperature
S phase	Synthesis phase
SDS	Sodium dodecyl sulfate
shRNA	short hairpin RNA
SILAC	Stable isotope labelling by amino acids in cell culture
siRNA	small interfering RNA
TAE	Tris-acetate-EDTA
TBS	Tris-buffered saline
TBST	Tris buffered saline-Tween
TEMED	N'N'N'N'-tetramethylethylene-diamine
Tris	Tris(hydroxymethyl)aminomethane
WT	Wild type

8.3. Curriculum vitae

Persönliche Angaben

Name:	Marc Fackler
Adresse:	
Geburtsdatum:	
Geburtsort:	
Nationalität:	

Ausbildung

09/2010 – 03/2014   **Dissertation im Labor von Prof. Dr. Stefan Gaubatz**
Institut für Physiologische Chemie
Universität Würzburg
Titel: Biochemical characterization of GAS2L3, a target gene
of the DREAM complex

07/2010   **Diplom-Biologe Univ.**
Universität Würzburg

09/2009 – 06/2010   **Diplomarbeit (extern)**
Medizinische Hochschule Hannover
Titel: Charakterisierung neuer domänenspezifischer
Interaktoren des humanen VASP

10/2007 – 08/2009   **Hauptstudium der Biologie**
Universität Würzburg
Hauptfach: Biochemie
Nebenfächer: Humangenetik & Molekulare Pflanzenphysiologie

10/2004 – 09/2007   **Grundstudium der Biologie**
Universität Ulm

06/2003   **Abitur**
Carl-von-Linde Gymnasium Kempten

8.4. Publications

Wolter, P., Schmitt, K., **Fackler, M.**, Kremling, H., Probst, L., Hauser, S., Gruss, O.J., and Gaubatz, S. (2012). GAS2L3, a target gene of the DREAM complex, is required for proper cytokinesis and genomic stability. J. Cell Sci. *125*, 2393–2406.

Fackler, M., Wolter, P., and Gaubatz, S. (2014). The GAR domain of GAS2L3 mediates binding to the chromosomal passenger complex and is required for localization of GAS2L3 to the constriction zone during abscission. FEBS J. *281*, 2123–2135.

Conference contributions

25.-27.09.2013

Final retreat of the Integrated Graduate College of the SFB Transregio 17, Pommersfelden

Talk: Biochemical and *in vivo* characterization of GAS2L3

10.-13.04.2011

Joint meeting of the SFB Transregio 17 "Ras-dependent pathways in human cancer" and the LOEWE Research Cluster "Tumor and Inflammation", Rothenburg ob der Tauber

Poster: **Fackler, M.**, Schmitt, K., Wolter, P., Gruss, O. and Gaubatz, S.

Characterization of GAS2L3, a novel target gene of the human DREAM complex

06.-08.10.2010

Retreat of the Integrated Graduate College of the SFB Transregio 17, Würzburg

8.5. Eidesstattliche Erklärung

Hiermit erkläre ich an Eides statt, dass ich die vorliegende Dissertation selbständig und ohne Hilfe einer kommerziellen Promotionsberatung verfasst habe und dabei keine anderen als die von mir angegebenen Hilfsmittel und Quellen benutzt habe. Zitate sind als solche gekennzeichnet.

Ich versichere, dass die Regeln der Universität Würzburg über gute wissenschaftliche Praxis eingehalten wurden und dass ich die Gelegenheit zum Promotionsvorhaben nicht von einer Person oder Organisation vermittelt bekommen habe, die gegen Entgelt Betreuer bzw. Betreuerinnen für die Anfertigung von Dissertationen sucht.

Ich erkläre außerdem, dass die vorliegende Dissertation weder in gleicher noch in ähnlicher Form bereits in einem anderen Prüfungsverfahren vorgelegen hat.

Ich habe früher, außer den mit dem Zulassungsantrag urkundlich vorgelegten Graden, keine weiteren akademischen Grade erworben oder zu erwerben versucht.

Würzburg, den

_____

Marc Fackler